HIV-1/HCV co-infection; proteomics and liver fibrosis

Presented by

Carlos Enrique Melendez-Peña

Division of Experimental Medicine

Faculty of Medicine

McGill University

Montreal, Québec, Canada

November 2014

A thesis submitted to McGill University in partial fulfillment of the requirement of the degree of Doctor of Philosophy.

To my Sister,
Ana Melendez,
You are my sister, my best friend,
my number 1 fan and my number 1 support.

Table of Contents

Acknowledgements

I would like to express my gratitude to all those who helped me in the completion of this thesis. I would like to express my deepest appreciation to my co-supervisors Drs Brian Ward and Momar Ndao for their valuable guidance and continued support. They have taught me how to be a better scientist and a better person. I also want to thank my advisory committee, especially Drs Klein and Bernard for the helpful discussions. I would like to thank Drs Vidal and Gatignol for helping me get through a rough time. I am grateful to the Division of Experimental Medicine and McGill University for accepting me to the graduate program and giving me this wonderful opportunity. I am indebted to my lab colleagues from Drs Ward's and Ndao's, and Dr Bernard's labs for providing a stimulating and dynamic environment in which I could learn and grow as scientist. I wish to thank my friends, especially Kaitlin, Katie, Matt and Ben. I could not have made it through this degree without their help, emotional support, camaraderie, entertainment, and good sense of humor. Lastly, and most importantly, I am grateful to my family. Thank you to my parents, Rosa and Daniel. I am thankful to my mother for the upbringing and early attitude she instilled in me. She taught me the value of hard work, honesty and perseverance. To my sister Ana, my brother in law Alex and my two beautiful nephews Nathan and Romain, who supported me, encouraged me, loved me and taught me about the important things in life: I say thank you.

Abstract

Hepatitis C virus **(**HCV) co-infection occurs in ≥ 30% of Human immunodeficiency virus type-1 (HIV-1)-infected patients in developed countries. Compared to HIV-1 alone, co-infection with HCV is associated with: increased HIV-1-related kidney problems, higher prevalence of cardiovascular disease, and increased cognitive-motor impairment. However, liver disease is by far the most serious complication of HIV-1/HCV co-infection. HCV–associated liver damage (including fibrosis, cirrhosis and end of stage liver disease (ESLD)) are all more prevalent and accelerated in HIV-1-infected individuals. Although, liver biopsy remains the gold standard for staging HCV-associated liver disease, this test can result in serious complications and is subject to sampling error. These problems have prompted a search for non-invasive methods for liver fibrosis staging.

To this end, we compared plasma proteome profiles at different stages of fibrosis in HCV mono and HIV-1/HCV co-infected patients using surface-enhanced laser desorption ionization-time-of-flight mass spectrometry (SELDI-TOF MS). This technology offers high-throughput protein profiling of native biological specimens. Using SELDI-TOF MS to develop algorithms for the staging of liver fibrosis in HIV-1/HCV co-infected individuals, we were able to identify serum apolipoprotein A1, haptoglobin and plasminogen as candidate biomarkers for liver fibrosis. In the course of this work, we observed an important heterogeneity in the plasma proteome of co-infected patients. In particular, we were interested in fibrosis progression rates in HIV-1/HCV co-infected patients as assessed by the aspartate aminotransferase (AST)-to-platelet-ratio index (APRI)

according to the sequence of infection with both viruses. We have shown that the sequence of infection has no effect on the percentage of patients who will eventually develop liver fibrosis but that those who are infected with HIV-1 first will progress to liver fibrosis at an accelerated rate.

Résumé

Dans les pays développés, la co-infection avec le virus de l'hépatite C (HCV) se produit dans ≥ 30% des patients infectés par le virus d'immunodéficience humain type-1 (VIH-1). Comparé au VIH-1 seul, la co-infection avec HCV est associée avec une augmentation des problèmes rénaux, une plus grande prévalence des maladies cardiovasculaires et une augmentation des problèmes moteur-cognitifs. Par contre, la complication la plus importante reste les maladies du foie dans les cas de co-infection au VIH-1/HCV. Les problèmes du foie reliés au HCV (incluant la fibrose, la cirrhose et maladies du foie en phase terminal) sont plus répandus et accélérés chez les individus infectés par le VIH-1. Même si la biopsie du foie reste le test standard pour déterminer le niveau de fibrose du foie associé avec le HCV, ce test peut causer des complications et être assujetti à des erreurs d'échantillonnage. De ce fait, la recherche pour des méthodes non-invasives pour évaluer le niveau de fibroses du foie demeure nécessaire.

À cette fin, nous avons comparé le profile protéomique du plasma à diffèrent niveau de fibrose chez des patients HCV mono et VIH-1/VHC co-infectés en utilisant le 'surface-enhanced laser desorption ionization-time-of-flight mass spectrometry' (SELDI-TOF MS) : la Spectrométrie de masse utilisant le laser. Cette technologie nous permet une grande capacité de profilage des protéines d'un spécimen biologique natif. En utilisant SELDI-TOF MS pour développer des algorithmes pour évaluer le niveau de fibrose du foie chez les individus co-infectés par le VIH-1/HCV, nous avons identifié les protéines du sérum apolipoprotéine A1, haptoglobine et plasminogène comme des

biomarqueurs potentiels. Au cours de cette étude, nous avons observé une importante hétérogénéité dans le protéome plasmatique des patients co-infectés. En particulier, nous nous sommes intéressés au taux de progression de fibrose du foie chez les patientes co-infectés par le VIH-1/HCV, en mesurant l'index aspartate aminotransférase (AST) sur plaquette (APRI), en relation avec la séquence d'infection avec les deux virus. Nous avons montré que la séquence d'infection n'a pas d'effet sur le pourcentage de patients qui développeront une fibrose du foie mais par contre les patients qui ont été infectés par le VIH-1 en premier auront une progression plus rapide.

Contribution of authors

The candidate performed the majority of the research presented in this thesis under the supervision of Drs. Brian J. Ward and Momar Ndao with the collaboration of Dr Marina Klein. The core of this thesis concentrates on the bench work performed at the end of the PhD in the lab shared by Drs Ward and Ndao. The work performed during his first 2 years of PhD and under the supervision of Dr. Nicole F. Bernard is presented in Annex I with a brief introduction and conclusion. Finally Annex II is a collection of abstracts presented by the candidate at different national and international conference during his PhD. The majority of the results shown in this thesis are in part from the following manuscripts:

Melendez-Pena C, Ward BJ, Saeed S, Santamaria C, Conway B, Cooper C, Segatto B, Klein MB, Ndao M for the Canadian Co-infection Cohort (CTN222), Proteomic Fingerprinting in HCV mono- and HIV-1/HCV Co-infection reveals Serum Biomarkers for prognostic of Fibrosis, *Manuscript prepared for submission to JID.*

The candidate was the primary researcher designing and completing experiments, analyzing and interpreting data and writing the manuscript for the work presented in Chapter 2. Sahar Saeed was a research associated responsible for the coordination of the study with the help of Bianca Segatto. Cynthia Santamaria performed the matrix-assisted laser desorption/ionization (MALDI)-TOF analysis. This work was performed in collaboration with Dr. Brian Conway, Dr. Curtis Cooper and Dr. Marina Klein who is responsible for the Canadian Co-infection Cohort (CCC).

Carlos Melendez-Pena, Kathleen C. Rollet, Briand J Ward, Momar Ndao, Marina B. Klein, Infection with HIV-1 First does not affect the Rate of Liver Fibrosis Progression in HIV-1/HCV Co-infected Persons. *Manuscript prepared for submission to AIDS as short communication.*

The candidate was the primary researcher designing and completing the analysis and interpreting data and writing the manuscript for the work presented in Chapter 3. Kathleen Rollet contributed to hypothesis design and performed the analysis seeing in Table 7- 10.

Annex I: Carlos Melendez-Pena, Philomena Kamya, Christos M. Tsoukas, Mohamed-Rachid Boulassel, Jean-Pierre Routy, Réjean Thomas, Pierre Côté, Colin Kovacs, Stephen A. Migueles, Mark Connors, Martin Potter, Marianne Harris, Cecile L. Tremblay, Nicole F. Bernard, for the Canadian Cohort of HIV Infected Slow Progressors. Natural Killer cells from HIV infected slow progressors who carry the protective HLA-B*27 allele and inhibitory KIR3DL1 receptors have elevated poly-functional potential compared to Bw6 homozygotes. *Chapter published in HIV Infection in the Era of Highly Active Antiretroviral Treatment and Some of Its Associated Complications (2011), Dr. Elaheh Aghdassi (Ed.), ISBN: 978-953-307-701-7, InTech, DOI: 10.5772/22827.*

The candidate was the primary researcher designing and completing experiments, analyzing and interpreting data and writing the manuscript for the work presented in Annex I. Philomena Kamya contributed in completing

experiments. Drs. Tsoukas, Boulassel, Routy, Thomas, Côté, Kovacs, Migueles, Connors, Potter, Harris, Tremblay help in the recruitment of patients.

Chapter 1: Literature Review

1.1 Epidemiology

1.1.1 The HIV-1 Pandemic

Human immunodeficiency virus type-1 (HIV-1) is the primary cause of acquired immunodeficiency syndrome (AIDS), a slow and deteriorating disease of the human immune and central nervous systems, ultimately leading to premature death.

The Joint United Nations Program on HIV and AIDS and the World Health Organization estimated that between 31 and 36 million people around the world were living with HIV in December 2011. During this same year, ~ 2.5 million people were newly infected with the virus and between 1.5 and 1.9 million people died from the disease including 230,000 children (1). Today, no region of the world can be considered as untouched (2) (Figure 1A). The epicenter of the HIV-1 pandemic remains Sub-Saharan Africa. High rates of infection are still seen in this poor region of the world and the continued rapid spread of HIV-1 in many parts of the continent is alarming. Even though drug injection is one of the most important modes of transmission in Europe and in Central and Southeast Asia, heterosexual transmission still accounts for 85% of all HIV-1 infections (3). HIV-1 has a high level of genomic variability, as evidence by the extensive heterogeneity of groups (M, N and O) and subtypes included within the HIV-1 classification. The HIV-1 group M strain is responsible for 90% of current and new HIV-1 infections and may be further subdivided into subtypes A through J

(4). Two out of five of all new infections are seen in adults younger than 25 years of age (1). Women now make up about 47% of those infected worldwide; rising to almost 70% in Sub-Saharan Africa; with serious implications for mother-to-child transmission. Population prevalence of HIV-1 infection, concurrent sexual relationships, partner change, sexual practices, presence of other sexually transmitted diseases, and population mobility patterns for economic and other reasons further complicate the transmission of HIV-1 (3). HIV-1 infection is a chronic infectious disease that can be treated, but not yet cured. In mid-2013, there are effective means of delaying progression to AIDS and allowing HIV-1-infected people to enjoy a higher quality of life. Over the past 10 years, highly active anti-retroviral therapy (HAART), a combination of three antiretrovirals (ARV)s from at least two drug classes (5), has been highly effective in reducing the number of HIV-1 particles in the blood stream and can increase T-cell counts. The guidelines to treat naïve patients consist of two nucleoside reverse transcriptase inhibitors (NRTIs) in combination with a third active ARV from one of the three drug classes are: 1) non-nucleoside reverse transcriptase inhibitors (NNRTIs) 2) a protease inhibitor (PIs) boosted with ritonavir or 3) an integrase strand transfer inhibitor (INSTI).

The HIV-1 pandemic is undoubtedly the defining public-health crisis of our time.

Figure 1: Worldwide distribution of HIV-1 and HCV infections. A) HIV-1 distribution, modes of transmission, and HIV-1 subtypes. Hsex=heterosexual. MSM=Men who have sex with men. IDU=injection drug users. (modified from UNAIDS 2012 (1)) B) HCV distribution and HCV genotype (Modified WHO 2009 (6)).

A

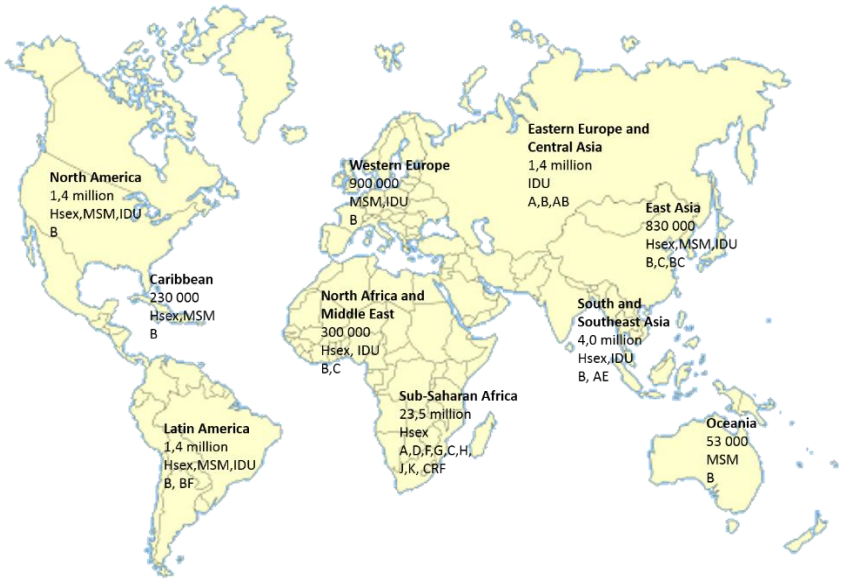
North America
1,4 million
Hsex,MSM,IDU
B
Caribbean
230 000
Hsex,MSM
B
Latin America
1,4 million
Hsex,MSM,IDU
B, BF
Western Europe
900 000
MSM,IDU
B
North Africa and
Middle East
300 000
Hsex, IDU
B,C
Sub-Saharan Africa
23,5 million
Hsex
A,D,F,G,C,H,
J,K, CRF
Eastern Europe and
Central Asia
1,4 million
IDU
A,B,AB
East Asia
830 000
Hsex,MSM,IDU
B,C,BC
South and
Southeast Asia
4,0 million
Hsex,IDU
B, AE
Oceania
53 000
MSM
B

B


North America
3-4 million
Genotype 1
Latin America
12-15 million
Genotype 1 ,2,3
Western Europe
5 million
Genotype 1
Africa
30-40
Genotype 4, 5,1
Eastern Europe and
Central Asia
10 million
Genotype 3,1
East Asia
Genotype 1,6,2
South and
Southeast Asia
Genotype 3,1
Oceania
200 000
Genotype 1,3

FIGURE 1

1.1.2 The HCV Pandemic

At the time that AIDS was still unexplained and HIV-1 was spreading, another blood-borne virus was infecting hundreds of thousands humans around the world and manifested itself slowly, starting with flu-like symptoms and gradually attacking the liver, where it could cause cirrhosis and cancer. This virus was later identified in 1989 as the hepatitis C virus (HCV)(7).

HCV, usually an asymptomatic infection, is present in most parts of the world and has been endemic to human populations for many centuries (Figure 1B). With Egypt having the highest prevalence rate of ~15%[*], the WHO has estimated that 150 million people are infected with HCV worldwide and that up to 4 million people acquire HCV each year, resulting in an overall prevalence of ~3% (6). HCV infection is the commonest cause of liver failure in the United States and a leading killer worldwide with 350 000 related deaths annually (9). HCV can be classified into six genotypes, each with distinctly different geographic distribution, genetic and therapeutic response to treatment. Genotype 1, divided into subtype 1a and 1b, is most prevalent in the Americas and Europe; genotypes 1b and 2 are most commonly found in Japan; genotype 3 is found predominantly in Southeast Asia and India; genotype 4 and 5 are found in Middle East and Africa; and genotype 6 is found in Asia (10, 11). Modern migration is currently playing a major role in genotype distribution patterns. HCV is transmitted through the blood, mainly via transfusions, shared needles and reused

[*] *The anomaly of very high prevalence in socially-conservative Egypt can be explained by well-intentioned (but misguided) attempts to eradicate schistosomiaisis through mass injection campaigns 1980s with extensive re-use of syringes/needles 8. Strickland, G.T. 2006. Liver disease in Egypt: hepatitis C superseded schistosomiasis as a result of iatrogenic and biological factors. *Hepatology* 43:915-922..

medical supplies. Sexual and mother-to-child transmission is much less likely than with HIV-1. In developed nations, most new infections occur in injection-drug users (IDUs), fallow by men who have sex with men (MSM). HCV infections are increasing particularly in older teenagers and young adults (12). For many years, pegylated interferon (pegIFN) plus ribavirin (RBV) have been the 'standard' HCV treatment but the effectiveness of this combination varies widely for different genotypes. This treatment is also very expensive and can last up to 48 weeks in the case of individuals infected with HCV genotype 1. In the last years treatment of HCV has evolved considerably. It began with addition of the protease inhibitors telaprevir and boceprevir to the standard treatment (13) . These have now been replaced with the licensure of sofosbuvir that targets the viral RNA polymerase and has broad efficacy (~80%) against all HCV geneotypes (14).

1.1.3 HIV-1/HCV co-infection transmission risks

Because both viruses share common transmission routes, co-infection with HIV-1 and HCV has emerged as a significant public health concern. Parenteral contact with blood is the primary transmission route among co-infected individuals for both viruses. Individuals who are at the highest risk to acquire both viruses include intravenous drug users, hemophiliacs, and individuals who received blood transfusions prior to 1992. Recipients of blood transfusions prior to 1992 or coagulation factor transfusions prior to 1987 are at a significant risk for HCV and HIV-1 infection (15). Because coagulation factor concentrates were not

heated-inactivated prior to 1987, hemophiliacs who needed these products prior to this date are at particularly high risk for co-infection (16). Hemodialysis patients are also at increased risk of HCV infection, with an incidence ranging from 10 to 65% (17). Although in some studies, sexual exposure may account for up to 20% of HCV infections, other studies have found that sexual exposure to HCV is not a significant route of transmission (15). However, a potential confounding factor in these latter studies is that almost all of the HIV-1/HCV co-infected subjects also had a history of IDU. The percentage of individuals who acquire HCV through vertical transmission is also increased with co-infection in the mother. The incidence of vertical transmission of HCV is 1.7% in HCV mono-infected mothers but increases to 19.4 % in those who are co-infected with HIV-1 (18). The increase in vertical transmission is associated with higher HCV virus titres in the blood of HIV-1/HCV co-infected individuals. Between 50% and 80% of IDUs become infected with HCV within 5 years of beginning injection drug use. As many as 60% of all IDUs become infected within the first year of drug use (15). 50 to 90% of IDUs who acquired HIV-1 infection through injection drug use are co-infected with HCV (19). The population of Canadians who inject drugs is extremely diverse, due in part to factors such as age, gender, culture, geographic location and poly-drug use. Injection drug use has an impact on all of society and is a key issue among the most vulnerable and marginalized individuals in society, such as those with a history of child abuse, mental illnesses, the homeless, street youth, sexually exploited children and inmates of correctional facilities.

1.2 Virology

1.2.1 HIV-1

The inexorable worldwide spread of HIV-1 since the early 1980s indicates that the virus can effectively counteract innate, adapted and intrinsic immunity (20, 21). Despite its modest genome size and small number of genes, HIV-1 excels in taking advantage of host cellular pathways while either neutralizing or hiding from the different components of the immune system (22). HIV-1 is a member of the lentivirus group of retroviruses; its genome is composed of two identical copies of positive-strand RNA encoding *gag*, *pol*, and *env* genes common to all retroviruses (Figure 2 A). Besides these genes, six additional reading frames have been identified (23), providing the virus with several virulence factors.

The virus can enter host cells by both fusion and endocytosis. The surface protein gp120 on the virion binds to its receptor CD4 on the target cell. Conformational changes then occur that increase binding to a number of chemokine receptors. The most commonly used coreceptors are CCR5 and CXCR4. CCR5 facilitates cell entry of the macrophage-tropic, non-syncytium-inducing viral isolates (R5 viruses) while CXCR4 is more relevant for T cell-tropic, syncytium-inducing isolates (X4 viruses) (24). Interestingly, X4 viruses are mainly found in late stages of the disease, it is estimated that 50 % of infected individuals will progress to X4 viruses, whereas R5 viruses mediate both mucosal and intravenous transmission of HIV-1 infection (25). The sequential interplay between gp120, CD4 and chemokine coreceptors triggers a conformational

change in gp41. The release of the HIV-1 viral core into the cell cytoplasm mediated by gp41, a coiled-coil protein with three peptide fusion domains that targets cell membranes and promotes the fusion of the virion (26). Viral uncoating then occurs inside the cell and is increased by the presence of the viral negative factor (Nef) and viral infectivity factor (Vif). The viral 'complex' is now comprised of the diploid RNA genome, $tRNA^{lys}$ primer, matric protein (MA), reverse transcriptase (RT), integrase (IN), nucleocapsid (NC), viral protein R (Vpr) and various host proteins (27) and reverse transcription can start. Vif stabilizes the reverse-transcription complex by inhibiting the effect of the potent antiviral protein APOBEC3G (28). The complex binds to host cell actin microfilaments and, after completion of reverse transcription, a new complex named HIV-1 pre-integration complex (PIC) is formed with the cDNA, IN, MA, RT, Vpr and the high-mobility group DNA-binding proteins. The PIC then leaves the actin microfilaments and moves toward the nucleus using host microtubules as a conduit (29).

Nuclear localization of Vpr is required for the nuclear import of the PIC and viral replication in $CD4^+$ T cells but is dispensable for infection of non-dividing, resting T cells (30, 31). Cellular proteins, the high-mobility group I Y barrier-to-autointergration factor (HMGI(Y) BAF) and the viral IN are required for efficient integration. HIV-1 provirus can integrate at several chromosomal locations and most infected cells harbor more than one provirus (32). Integration can lead to either latent or transcriptionally active forms of infection.

After transcription of the viral genome, more than a dozen HIV-1-specific transcripts are generated (33). The splicing and transport of these viral mRNAs

species must be carefully coordinated to achieved optimal HIV-1 production. In the early phase, some mRNAs are processed co-transcriptionally, double-spliced and are rapidly transported into the cytoplasm while unspliced (9kb) and singly spliced (4kb) transcripts remain in the nucleus. The multiply spliced (2kb) mRNA species encode Nef, Trans-Activator of Transcription (Tat) and Regulator of Expression of Virion Proteins (Rev). The transport of the 4 and 9 kb RNAs to the cytoplasm depends on the presence of a threshold amount of Rev in the nucleus. Rev is a small shuttle protein that binds to a complex RNA stem loop termed the Rev response element (RRE), located in the *env* gene. The nuclear export of the Rev/RRE-containing RNAs is mediated through the CRM1/exportin-1 pathway in the presence of the host factor RAN-GTP (34). In contrast to the RNA transported activities of REV, Nef reshapes the global environment of the infected cell to optimize viral replication by targeting signaling cascades including T cell receptor activation and decreases the expression of CD4 on the cell surface. Nef activates apoptosis in cytotoxic T cells and decreases the expression of major histocompatibility complex I proteins (35). Nef can also block apoptosis within infected host cells, mainly by binding to p53 and inhibiting its function. Other viral proteins also participate to the modification of the general environment of the infected cell. For example, Vpr induces the arrest of proliferating infected cells at G2/M phase of the cell cycle (36). The viral long terminal repeat (LTR) is more active during G2 so this arrest enhances viral gene expression.

Finally, all of the components of the HIV-1 virion are ultimately assembled at the plasma membrane where budding occurs. This process is largely directed by Gag-Pol and Gag polyproteins but is also influenced by Env and

involves the recruitment of two copies of the viral RNA genome as well as Vpr (37). Virion budding occurs through specialized regions in the lipid bilayer yielding virions with cholesterol-rich membranes (so-called lipid rafts). This lipid composition likely favors release, stability and fusion of the progeny virions with the next target cells (38). The final step in the budding reaction necessarily involves a second membrane fusion event for the virus. Virion budding depends critically on a 'late domain' sequence (PTAP) present in the p6 portion of Gag. The viral cycle (Figure 2 B) results in the release of new HIV-1 virus particles into the extracellular milieu. The estimated virion production in untreated infected individuals is 10^{10} virus per day (39).

1.2.1 HCV

HCV is a hepatotropic RNA virus of the genus Hepacivirus in the *Flaviviridae* family. It causes acute and chronic hepatitis only in chimpanzees and humans and has a high propensity for chronicity. HCV is a positive-sense, single-stranded enveloped RNA virus approximately 9600 nucleotides in length. Due to the highly error prone RNA polymerase, HCV also displays remarkable genetic diversity which greatly increases its capacity to mutate under immune or drug pressure (40). The HCV genome has one continuous open reading frame flanked by non-translated regions (NTRs) at the 5' and 3' ends (Figure 3 A). The HCV 5'NTR contains 341 nucleotides located upstream of the coding region and is composed of 4 domains with highly structured RNA elements including numerous stem loops and a pseudoknot (41). The 5' NTR also contains the internal ribosome entry site (IRES), that initiates the cap-independent translation of the

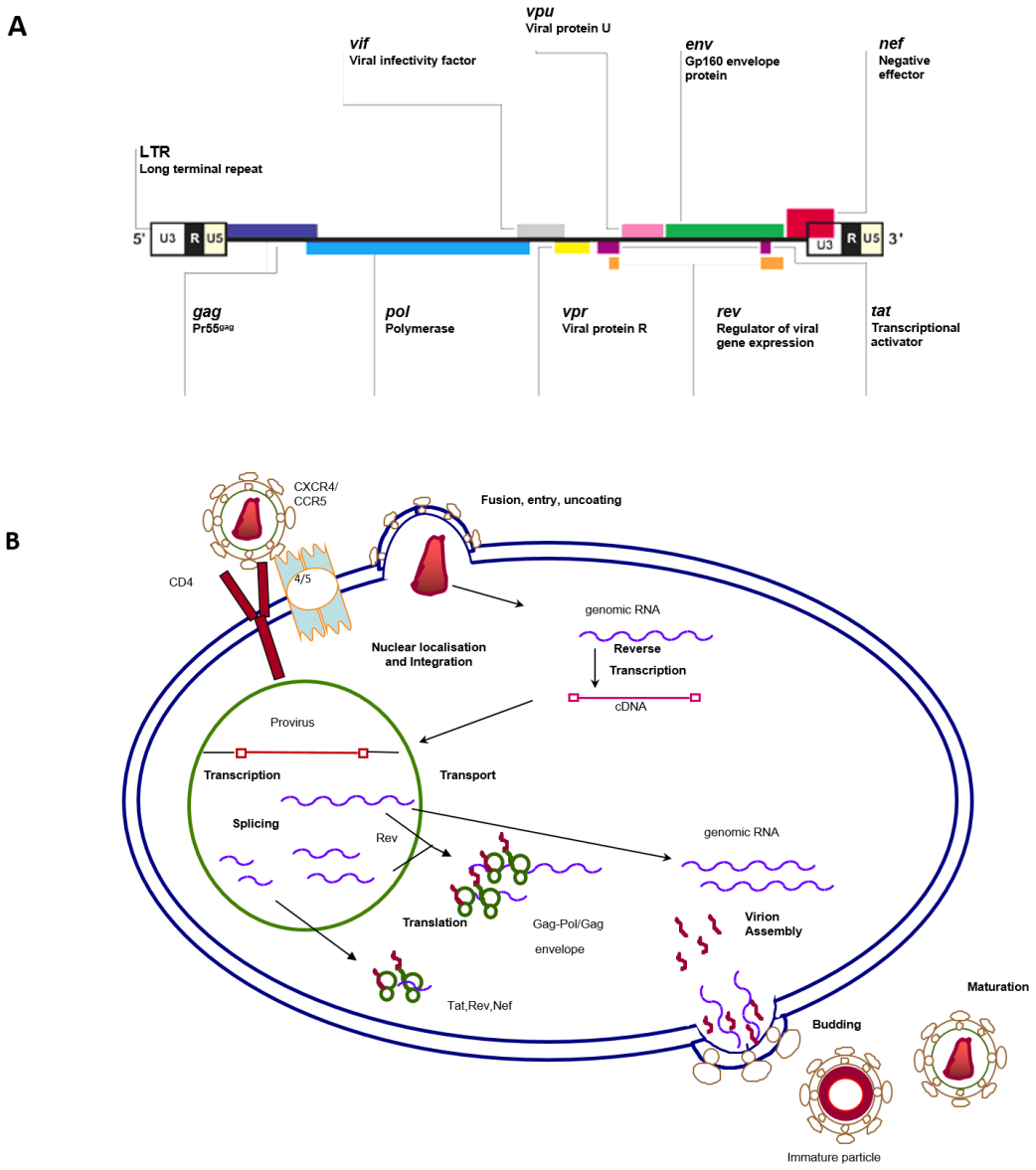

Figure 2: **HIV-1 genome and viral cycle**. A) Overview of the organization of the 9 kilobases genome of the HIV-1 provirus and its 9 genes encoding 15 proteins. *Modified from Sherman et al 2002 (49).* B) Schematic summary of events in the HIV-1 infected cell. Interaction between gp120, CD4 and chemokine receptors (CCR5 and CXCR4) leading to fusion followed by virion uncoating, reverse transcription, nuclear import and integration of the cDNA into the host chromosome. Nuclear export of unspliced and incompletely spliced viral transcript is mediated by the viral protein Rev. Assembly of new virions occurs mainly at the plasma membrane leading to budding and release of new virus particles. *Modified from Gorry et al., 2003 (50).*

HCV genome into a single poly-protein (42) by recruiting both viral and cellular proteins such as eukaryotic initiation factors (eIF) 2 and 3 (43). The HCV poly-protein is cleaved by host and viral proteases into 10 distinct viral proteins (44). Although not all steps are completely understood, HCV enters the host cell by a complex series of interactions including attachment, entry and fusion (Figure 3 B). The initial viral attachment to its receptor/co-receptors may involve the hyper-variable region of HCV E2 (45) with facilitation by heparin sulfate proteoglycans expressed on the hepatocyte surface (46). Following attachment to the entry factors, HCV is internalized into target cells via pH-dependent clathrin-mediated endocytosis (47, 48).

Multiple cellular receptors and entry factors for HCV have been identified, including tetraspanin CD81, scavenger receptor-B1 (SR-B1), and tight-junction proteins claudin-1 (CLDN1) and occludin (OCLN)(43). Following target cell entry, the HCV particle undergoes pH-dependent membrane fusion within an acidic endosomal compartment to release its RNA genome into the cytoplasm (47). The HCV poly-protein is then translated in the rough endoplasmic reticulum (ER) using the positive strand HCV RNA as the template, with translation initiated in a cap-independent manner via the IRES in the 5'NTR. As noted above, HCV translation yields a single poly-protein precursor of approximately 3000 aa in length, that is further processed (NS2, NS3/4A) to generate 10 individual proteins, including core and envelop glycoproteins, E1 and E2, p7, NS2, NS3, NS4A, NS4B, NS5A, and NS5B. In the course of polyprotein processing, the HCV proteins associate with a 'membranous web' that includes double membrane-bound vesicles containing HCV non-structural proteins, HCV

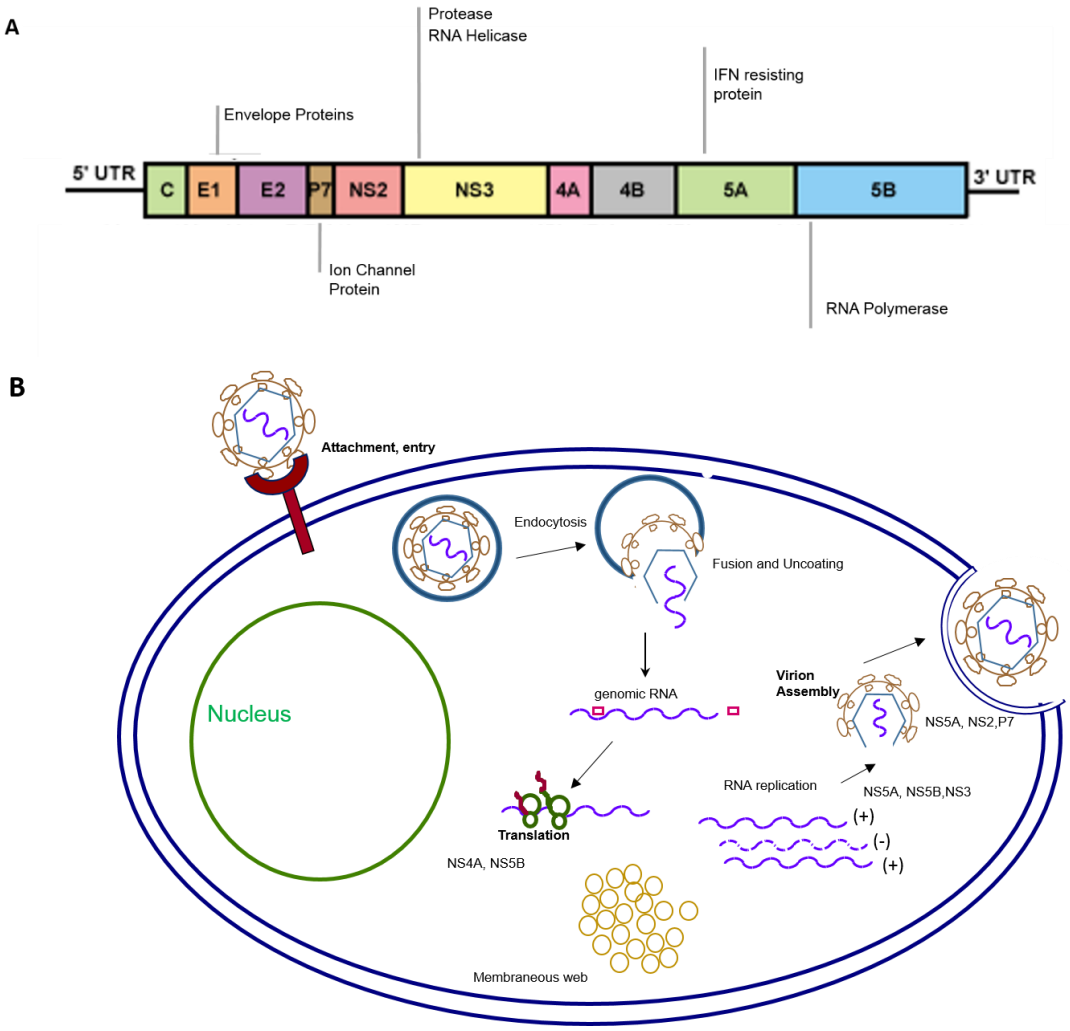

Figure 3: **HCV genome and viral cycle**. A) Overview of the organization of the 9,6 kilobases genome of the HCV genome and its single polyprotein that is cleaved into 10 individuals viral proteins. B) Schematic summary of events in the HCV infected cell. Viral protein E2 interacts with several multiple cellular receptors followed by virion internalization by endocytosis, with pH-dependent fusion and uncoating. Later yhere is polyprotein translation, cleavage and viral RNA processes with the assistance of viral proteins with cellular cofactors. Assembly of new virions and release is closely linked to lipid metabolism. *Modified from Alvisi et al 2011 (44)*

RNA, ER membrane and lipid droplets (51). Viral RNA replication is believed to occur in these webs were the positive-sense; genomic RNA serves as a template for the NS5B RNA-dependent RNA polymerase to generate the negative-strand replicative intermediate, to produce further positive-sense copies of the viral genome. In addition to the host proteins mentioned above, other cellular factors are actively involved in HCV replication, including cyclophilin A and phosphatidylinositol 4 Kinase IIIα (PI4KIIα). Cyclophilin A can modulate RNA-binding capacity of NS5B polymerase and interact with NS5A (52). PI4KIIα is a host lipid kinase that is required for HCV replication. It is recruited to the membranous web by ND5A, where it provides integrity to the membranous viral replication complex (53). The HCV assembly and release process is also not fully understood but appears to be closely linked to lipid metabolism (54). The virion is a lipo-viroparticle. Its lipid composition closely resembles VLDL and LDL with associated apolipoprotein (Apo) E and/or ApoB, which are both essential for the assembly of infectious virions (55, 56). The HCV viral particle includes HCV RNA genome, core and the envelope glycoproteins, E1 and E2 (57). Approximately 10^{12} viral particles are generated daily in a non-treated, chronically HCV-infected patient (58).

1.3 Pathogenesis

1.3.1 HIV-1

During the acute phase of HIV-1 infection, the virus enters lymphocytes and monocytes through the interaction of the HIV-1 viral envelope glycoprotein

gp120, the cell surface CD4 molecule, and the chemokine receptors CCR5 and CXCR4. The CCR5 and CXCR4 receptors are utilized by the virus during different stages of disease and the selective use of each receptor influences HIV-1 pathogenesis. For example, the presence of CXCR4 is associated with accelerated CD4 T cells loss and the progression of disease (59). During acute infection with HIV-1, infected T cells or monocytes migrate from mucosal surfaces where infection typically occurs to regional lymph nodes. Viremia is detectable within 1 to 2 weeks following exposure (60). The initial viremic peak, known as primary HIV-1 infection, is associated with vigorous HIV-1-specific cellular and humoral immune responses. It takes 6 up to 12 weeks before antibodies against the virus are detectable in the infected individuals. These initial responses partially control HIV-1 replication leading to a decrease in HIV-1 RNA in the blood. Approximately 6 months after the onset of HIV-1 infection, the subclinical, chronic phase of the infection is thought to begin. It is defined as a steady state when virion production is roughly equal to immune clearance. At this point, referred to as the 'set point', the level of HIV-1 RNA in peripheral blood varies widely between individuals and has prognostic value in determining the likelihood of progression to AIDS (61). A time at which time $CD4^+$ T cell counts fall below 50 cell/ml and opportunistic infection occurs. The $CD4^+$ T cell depletion that occurs subsequently is thought to be a consequence of increased cellular destruction secondary to apoptosis as opposed to decreased cellular production (62, 63).

1.3.1 HCV

Hepatocytes are the primary target HCV replication in the liver. *In situ* detection of HCV RNA in the liver is significantly correlation with elevated serum HCV RNA levels. HCV RNA can be detected in serum as early as 1 to 3 weeks after exposure and the appearance of anti-HCV antibodies occurs after approximately 2 to 8 weeks (64, 65). Based on current data, HCV itself is not cytopathic, as demonstrated following acute infection in which most individuals are asymptomatic, high HCV RNA levels are observed, and alanine aminotransferase (ALT) levels remain normal (66). In certain individuals, immune responses may likely contribute to HCV pathogenesis through the destruction of HCV-infected as well as uninfected 'by-stander' hepatocytes (67). The cytokines secreted by immune cell, mainly T helper cells, contribute to HCV control stimulating the production of anti-HCV antibodies that facilitate opsonisation, recognition, and phagocytosis of infected cells (68). In addition to their anti-viral activity, these processes can also lead to activation of hepatic stellate cells (HSC) in response to injury, followed by matrix deposition, fibrosis, and eventually cirrhosis (69, 70). However only a portion of HCV infected individuals will eventually develop cirrhosis. Only those who fail to mount adequate $CD8^+$ and $CD4^+$ T cell responses (~50%-80% of patients) will develop chronic HCV infection. Approximately 15 to 20% of these individuals subsequently develop cirrhosis during the next 25 years (71).

1.4 HIV-1/HCV complications

1.4.1 General complications

HIV-1 and HCV are major global causes of morbidity and mortality and due to the shared risk factors of infection, they often are seen in the same host. The ability of each virus to establish persistent infection presents unique challenges to the medical community. In general terms, HCV infection is thought to have only a moderate impact on HIV-1 disease progression, whereas HIV-1 is widely believed to accelerates HCV-related liver disease (72, 73). Even though this thesis is focused on liver fibrosis in co-infected patients, we thought it would be important to mention other complications that can be observed in these patients. One effect of HCV on HIV-1 infection reported in a meta-analysis of 24 observational studies and clinical trials is an increase in HIV-1-related kidney disease risk, including both relatively benign (eg: proteinuria) and serious complications (eg: acute renal failure) compared to HIV-1 mono-infection (74). A large retrospective study of 23,155 HIV-1 infected veterans also found that co-infection was associated with a higher rate of chronic kidney disease (75). In addition, a higher prevalence of cardiovascular disease is observed in co-infection compared with HIV-1 mono-infection. This was demonstrated by a study with 19,424 HIV-1 infected individuals of whom more than a third were co-infected with HCV. Those with co-infection had an increased risk of cerebrovascular disease and a trend toward increased risk of acute myocardial infarction (76). Finally, neurological problems can also be observe in co-infected patients since both HIV-1 and HCV are found in the brain and cerebrospinal fluid of infected

individuals and are known to be implicated in neurocognitive and peripheral neuropathological syndromes (77). Co-infected subjects show significantly greater cognitive-motor impairment compared to HIV-1 mono-infected patients (78) and higher rates of global cognitive impairment, especially in learning and memory (79). However, as mentioned previously, liver disease is the most important complication in co-infected patients. HCV-associated liver disease, including fibrosis, cirrhosis, and ESLD, is accelerated in HIV-1-infected individuals. Progression to cirrhosis is threefold higher in co-infected than HCV mono-infected patients, and approximately 33% progress to cirrhosis in less than 20 years (80).

1.4.2 Liver fibrosis

Fibrosis describes encapsulation or replacement of injured tissue by a collagenous scar. Liver fibrosis results from the perpetuation of the normal wound-healing response, resulting in an abnormal (pathologic) continuation of fibrogenesis (connective tissue production and deposition). Fibrosis progresses at variable rates depending on the cause of liver disease, environmental factors, and host factors (81). Hepatic fibrosis is a dynamic response to the liver injury that results in deposition of extra cellular matrix (ECM) into the space of Disse, the area between the hepatocytes and the hepatic sinusoids in which HSCs reside (82). Cirrhosis is an advanced stage of liver fibrosis that is accompanied by distortion of the hepatic vasculature. Cirrhosis and its associated vascular distortion are traditionally regarded as irreversible. Alcoholic liver disease and

HCV are the most common causes of cirrhosis in developed countries, whereas hepatitis B virus (HBV) is the predominant cause in most parts of Asia and sub-Saharan Africa. Epidemiological studies have identified a number of factors that contribute to the risk of developing cirrhosis. For example, in chronic HCV infection, regular (moderate) alcohol consumption, age older ≥ 50 years, and male gender all increase cirrhosis risk (83, 84). Older age, obesity, insulin resistance or type 2 diabetes, hypertension, and hyperlipidaemia are risk factors in non-alcoholic steatohepatitis (85).

Although recent studies have demonstrated that many different hepatic cells contribute to hepatic fibrogenesis, the principal driver of this process remains the HSC. In their quiescent state, HSCs act as the main reservoir for vitamin A in the liver. However, once activated by cytokines produced in response to cell injury by hepatocytes and Kupffer cells, HSCs create a cytokine microenvironment that promote inflammation, fibrosis, contraction and mitosis (82). Transforming growth factor β1 (TGF- β1) is the best characterized of theses pro-fibrotic cytokines; its activation by HCV through Smad signaling leads to increased production of collagen I and α-smooth muscle actin; 2 main components of ECM (86). TGF- β1 expression is governed through a variety of signal proteins/complexes including nuclear factor kappa-light-chain-enhancer of activated B cells (NF-κB), extracellular signal-regulated kinase (ERK), c-Jun N-terminal kinase (JNK), and p38 mitogen-activated protein kinase (p38MAPK), which tend to be unregulated in the setting of cellular injury (87). Initiation of the hepatic fibrosis cascade is fuelled by a variety of substrates. Reactive oxygen species (ROS) in particular are key contributors to liver injury. They are oxygen-

containing free radicals that cause injury through DNA mutation and oxidation of lipids and proteins. They are produced in diverse liver diseases including viral hepatitis, alcohol-induced and fatty liver disease. De-regulation of the electron transport chain in hepatic mitochondria is the best-known source of ROS in liver injury (88).

1.4.3 Pathogenesis of liver fibrosis in Co-infection

Even though there has being extensive research on HCV immunology in the last two decades, this effort does not compare to the work published on HIV-1 immunology. For purpose of this thesis, we will concentrate only on the aspects of viral immunology that concern liver fibrosis.

HCV infects hepatocytes but does not replicate in T cells or HSCs. Once HCV has entered the hepatocyte, the cellular immune system is the dominant means of limiting viral spread. HIV-1 infects $CD4^+$ T lymphocytes, macrophages, and dendritic cells; in contrast to HCV, HIV-1 does not replicate in human hepatocytes. Although the cognate HIV-1 receptor CD4 is not expressed on hepatocytes or HSCs, the chemokine co-receptors for HIV-1, CCR5 and CXCR4, are expressed on hepatocytes, HSCs, and other resident liver cells. Both HIV-1 itself and the HIV-1 envelope protein gp120 have been demonstrated to induce cell signalling within hepatocytes, HSCs and other immune cells through its interactions with the CCR5 and CXCR4 chemokine receptors (89-91). It has been shown that both HCV mono-infection and HIV-1/HCV co-infection are associated with a significant increase in TGF-β1 expression in the liver and serum

of patients (92, 93). As mentioned above, TGF- β1 is a central mediator of liver fibrogenesis. Both heat-inactivated HIV-1 (HI-HIV) and HIV-1 envelope protein gp120 further augment TGF- β1 expression in HCV infected cells and increase HCV RNA 2-3 fold. This stimulatory effect of HIV-1 on HCV replication is abrogated by neutralizing antibodies directed against TGF- β1, indicating that HIV-1 increases HCV replication in a TGF-β1–dependent manner (93). Liver fibrosis is characterized by excessive accumulation of ECM components, reduction of ECM-removing matrix metalloproteinases (MMPs), and up-regulation of tissue inhibitors of MMPs (TIMPs). HI-HIV increases alpha-1 type I collagen (Col1A1) and TIMP-1 expression and further enhances ROS production in HCV infected cells suggesting that HIV-1 and HCV act synergistically to foster hepatic fibrogenesis as evidenced by the increase in ECM components (89). These data provide further evidence that HIV-1 and HCV, through a variety of mechanisms, act upon hepatocytes and HSCs to increase the production of ROS which in turn, activate the phosphorylation of p38 MAPK, JNK, and ERK. Phosphorylated p38 MAPK, JKN and ERK subsequently induce the phosphorylation of NF-κB. Activated NF-κB is then translocated to the nucleus in order to regulate other genes including increased production of pro-fibrogenic TGF- β1, pro-collagen a1, TIMP-1 and decreased expression of anti-profibrogenic genes such as MMP-3 (87).

Hepatocyte apoptosis is ubiquitous in liver disease with growing evidence that it makes a significant contribution to hepatic fibrogenesis (94). Apoptosis occurs via two intracellular signaling pathways: through the cytosol or the mitochondria. Both pathways are catalyzed by the death inducing signaling

complex (DISC), which is formed after the binding of extracellular ligands (eg, tumor necrosis factor-related apoptosis-inducing ligand (TRAIL)) to cell-membrane death receptors (DR). Although apoptosis has been extensively studied in HIV-1 (95-98) and HCV mono-infection (99-101), considerable attention has recently been paid to apoptotic pathways in HIV-1/HCV co-infection. In fact, when HCV-infected hepatocytes are exposed to HIV-1 *in vitro*, apoptosis is increased in a number of assays with elevated caspase 3/7 activity and expression of TRAIL, TRAIL receptor 1 (DR4) (94). Whether or not increased hepatocyte apoptosis occurs in HIV-1/HCV co-infected individuals is not known but, if it does, it could certainly contribute to the accelerated fibrosis observed in these patients.

In addition to the intra-hepatic mechanisms described above, there is increasing evidence that HIV-1 and HCV promote hepatic fibrosis through augmentation of microbial translocation from the gut to the liver. Recent models of HIV-1 immunopathogenesis have revealed massive depletion of lymphoid tissue associated with the gastrointestinal tract, the largest lymphoid organ, leading to disrupted epithelium and increased microbial translocation. In HIV-1-infected persons, as plasma bacterial lipopolysaccharide (LPS) increases, so does the activation of $CD8^+$ T cells (102). LPS, by itself, can trigger the cascade for hepatic fibrogenesis. It has been shown that LPS binds to TLR4 on the surface of quiescent HSCs leading to both TGF-β1 stimulation through an NF-κB-dependent pathway and Kupffer cell activation, which, in turn, can induce further fibrogenic and inflammatory cytokines (103). These events are dependent on HCV infection since HIV-1 mono-infected individuals do not progress to liver fibrosis. In

support of this hypothesis, in persons with HIV-1/HCV co-infection, advanced liver disease is correlated with higher plasma LPS concentrations (104).

1.4.4 Liver fibrosis diagnosis

Accurate knowledge of the presence and degree of liver fibrosis is essential for predicting prognosis and for planning correct treatment of patients with chronic HCV infection. Liver biopsy is considered the gold standard for the diagnosis of fibrosis, and sequential histological grading of inflammation and staging of fibrosis can assess risk of progression to cirrhosis. However, biopsies are prone to considerable sampling variability in all liver diseases (105, 106). For example, the staging of fibrosis in hepatitis C using the METAVIR system (which is simple and has only five stages, with stage 4 indicating cirrhosis) showed that a third of scores differed by at least one stage when biopsy samples from the left liver lobe were compared with those from the right lobe, with similar results for grading inflammation (107). In addition, correct staging was only achieved for 65 % and 75 % of cases when biopsy samples were 15 mm and 25 mm in length respectively (105) compare to full image analysis of a large surgical section of the liver. Furthermore, a liver biopsy sample is obtained by either a (radiographically-guided) percutaneous, transjugular, or laparoscopical route that can result in an increased risk of bleeding depending of the diameter of the needle. Following biopsy, 2-3% of patients need hospital care for management of complications, of which pain and hypotension are the most prominant. 60% of complications occurred within 2 hours after biopsy, and 96% within 24 hours. The probability of

dying, mainly due to severe bleeding, is 1 in 10,000-12,000, and is higher in subjects with cirrhosis (108). In the last decade, non-invasive methods of assessing liver fibrosis utilizing serum tests and imaging have been developed to reduce the need for biopsy. Several tests are now available for the assessment of liver fibrosis in patients with chronic liver disease. One of these methods is the aspartate aminotransferase (AST) to platelet ratio index (APRI). It is a formula that utilizes measurement of serum AST concentration and platelet count. Its value is determined by the formula AST/(upper limit of normal)/platelet count (10^9/L)X100. APRI is simpler to use than most of the other indices with performance similar to that of the Fibrotest (FT) and the Forns index. APRI is accurate in estimating fibrosis in patients with HCV and with HIV-1/HCV co-infection (109). Others tests that have been developed for the assessment of liver fibrosis in patients of HIV-1 infection, particularly those co-infected with HCV, are FIB-4 and Shasta (110). A recent large study compared several of the non-invasive methods for staging liver fibrosis. The results demonstrated that Hepascore, Fibrometer, and Firbrotest outperformed Shasta, APRI, FIB-4 and the FORNS index in assessing liver fibrosis in HIV-1/HCV co-infected patients (111) (Table 1). A technology that has recently become popular to assess liver fibrosis in HCV infected patients is transient elastography which is based on the assessment of liver stiffness. This method is commonly used in Europe to assess liver fibrosis in a wide variety of liver diseases (112). Shear wave velocity is determined by pulse ultrasound and correlates with liver stiffness. This examination can be limited by morbid obesity, ascites, and small intercostal spaces. Elasticity scans have the ability to sample 1/500 of the liver (81). In a

recent meta-analysis of 35 studies that reports AUC data for severe fibrosis (defined as > stage 3 fibrosis), transient elastography was considered good at differentiating fibrosis stages 0-2 from stage 3-4, with an AUC of 0.89 and no significant difference between studies (113). Although many non-invasive markers have been evaluated in HCV mono-infection, and to a lesser extent in co-infection, none has replaced liver biopsy due to poor overall specificity and lack of sensitivity in the early stages of fibrosis.

1.5 Proteomics

Since the beginning of this millennium, a new field of research based on the detailed analysis of proteins has burst onto the scientific scene with stunning rapidity. Proteins possess unique properties that create an enormous hurdle for methodologies that seek to assign an activity to sets of proteins that may number in the thousands. However with several breakthroughs in biochemical and genetic strategies, cloning and expression technologies, and most importantly the instrumentation of mass spectrometry, such assays have become increasingly common.

1.5.1 Proteomic fingerprinting

Proteomic fingerprinting is a diagnostic concept based on the idea that disease states are sometimes associated with distinctive configurations of proteins (ie: biomarkers) in body fluids. Because the biological complexity of most diseases means that individual biomarkers have limited diagnostic sensitivity and

Table 1: Non-evasive tests used to diagnose liver fibrosis. Aspartate Aminotransferase (AST), Alanine Aminotransferase (ALT), Prothrombin time (PT), Gamma Glutamyl Transferase (GGT), Hyaluronic acid (HA), Apolipoprotein (APO), α2 macroglobulin (A2MG).

Test	Description	Reference
Hepascore	GGT, HA,A2MG, age and gender	Leroy 2007
Fibrometer	HA, PT, Platelets, AST, A2MG, urea and age	Cacoub 2008
Fibrotest	alpha-2 globulin, A2MG, gamma globulin, APO-A1, GGT, and total bilirubin,	Castera 2005, Colletta 2005, Cales 2005, Bourliere 2006, Maor 2006mLeroy 2007
Shasta	HA, albumin, and AST	Cacoub 2008
APRI	AST concentration and platelet count	Castera 2005,Cales 2005, Schneider 2006,Leroy 2007
FIB-4	AST, PLT and ALT	De Ledinghen 2006
FORNS	age, serum concentrations of total cholesterol and GGT and platelet count	Coco 2007

specificity, analysis of combinations of biomarkers offers the possibility of enhanced diagnostic accuracy. Serum is a complex mixture of 'classical' and 'non-classical' proteins. Classical serum proteins are involved in number of processes including proteolysis, inhibition, binding, transport, coagulation, and immune response. Non-classical proteins are not directly tied to any known function within the serum and often originate from cellular leakage or shedding and may simply utilize the bloodstream for transportation en route to their eventual metabolism/removal (114). Serum contains upwards of 10,000 different proteins at any given time that are being actively produced and secreted/released by the body's cells and tissues. A small number (n= 22) of highly abundant serum proteins constitute ~ 99% of the total serum proteome; these include albumin, IgG, transferrin, haptoglobin, fibrinogen, etc (115). High throughput proteomic profiling of serum has been revolutionized by advances in mass spectrometry (MS), such as surface-enhanced laser desorption ionization time of flight (SELDI-TOF) MS (116). This platform has been successfully used as a discovery tool for biomarkers associated with inflammation (117), cancers (116, 118-120) and human infections (121-124).

1.5.2 SELDI-TOF MS

First described in 1993, the SELDI platform has made great progress during the last decade. This technique combines retention chromatography with TOF-MS detection. This approach to protein biomarker discovery is referred as 'top-down' proteomics and describes the analysis of intact proteins. This

approach is well suited to address questions requiring larger number of samples compared to 'bottom-up' platforms that are more suited for basic biological questions with smaller numbers of samples but better resolution. SELDI-TOF MS permits high-throughput analysis of the protein/peptide content of complex biological fluids such as serum, plasma, urine, breast milk, cell lysates and tissue extracts. This system is comprised of three main components: protein chip array, the mass analyzer and data analysis software.

Protein chip arrays are 10 mm wide x 80 mm long aluminium strips with 8 to 16 two-mm 'spots' that constitute the active surface of the chip (Figure 4 A). These spots can either be chemically or biochemically active (e.g. hydrophobic, hydrophilic, ion exchange, immobilized metal or antibodies, receptors, oligonucleotides) (125). Each type of chip has affinity for a subset of specific proteins, implying that different chips will produce different protein spectra from the same sample. In order to maximize proteome coverage in any given experiment, different types of chips are often used on multiple sample fractions.

The sample of interest is spotted on these chips. After binding to the active surface, they are washed with buffers of increasing stringency which wash off low-affinity proteins while high-affinity ones are enriched. In MS analysis, the most common ion sources are electrospray ionization (ESI) and matrix-assisted laser desorption/ionization (MALDI). The former produces a continuous source of ions from a test solution while the latter sublimates and ionizes from a dry, crystalline matrix containing the sample via discontinuous laser pulses (126). SELDI functions on the same principles as MALDI except that the SELDI chip is 'enhanced' by being chemically active allowing for proteins with specific

properties to bind preferentially while MALDI plates are inert. The bound proteins are then co-crystalized on the SELDI chips in the presence of an energy-absorbing matrix (EAM) (α-cyano-4hydroxy cinnamic acid or sinapinic acid) in order to facilitate ionization/desorption (127). Once ionized by a laser of a specific intensity, the ions can be separated according to their mass-to-charge ratio (*m/z*) (Figure 4 B). In a typical experiment, low laser intensities are used (range 1500-2500 nJ) to ionize smaller peptides/proteins (≤ 25 kDa) while higher intensities (range 3500-6000 nJ) are needed to ionize larger peptides proteins (20-200 kDa). The TOF analyzer of the SELDI apparatus is a pulsed analyzer and, as such, is often coupled with a MALDI-like ion source. The sample is 'hit' by a laser pulse of specific energy to generate a burst of gaseous ions under vacuum, a phenomenon not yet fully understood. The laser pulse therefore provides each ion with the same energy. The ions are then accelerated by an electrical potential before entering the electric field-free vacuum region (flight tube). As they enter the flight tube, each ion travels at a velocity corresponding to their *m/z*. At the end of the tube, a detector records the time of flight of each ion, producing the TOF spectrum. The time of flight or drift time (t_d) can be estimated as $t_d = D\sqrt{2qV/m}$ constants calculated for the standard peptides can then be used for mass calibration of the peaks from the experimental samples. Mass calibration provides the experiment with a maximal mass accuracy, facilitates subsequent peak clustering and enables comparison of biomarker candidates from different experimental conditions or across different studies.

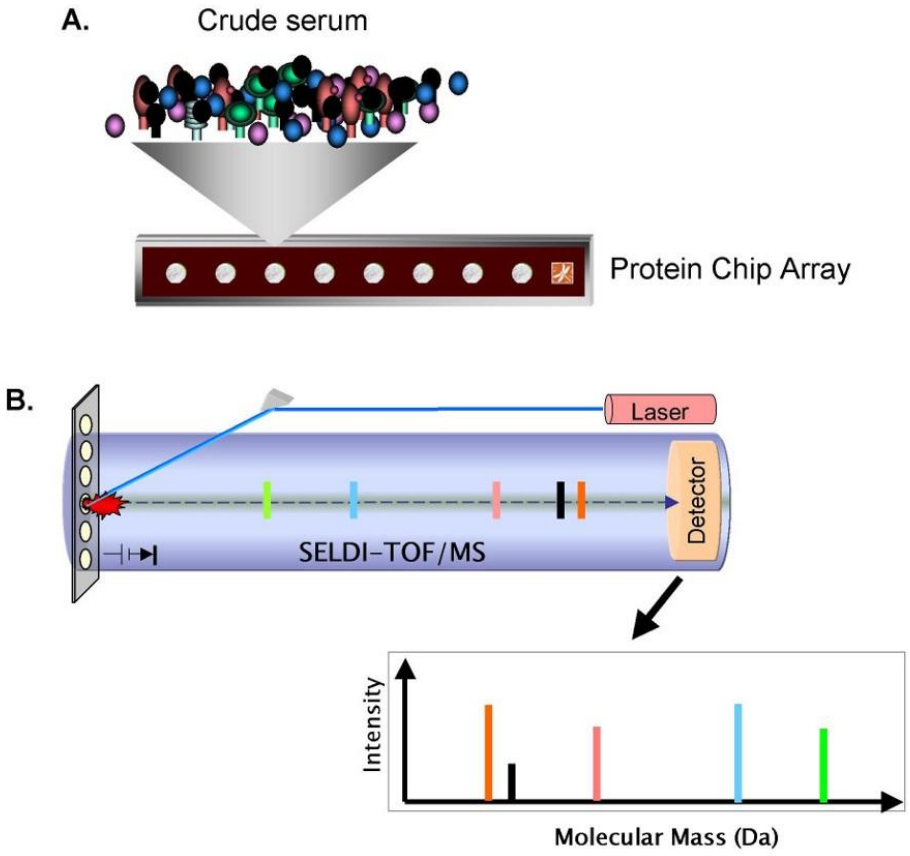

Figure 4: Analysis of biological sample using ProteinChip arrays and SELDI-TOF/MS. A) Crude sample is placed on a ProteinChip array which contains chemically or biologically treated surfaces for specific interaction with proteins of interest. B) Retained proteins are "eluted" from the ProteinChip array by SELDI. Ionized proteins are detected and their mass determined by TOF/MS. *Modified from* *http://www.proteomesci.com/content/4/1/5/figure/F3?highres=y*

Mass spectrometers may not always deliver a flat baseline. To compensate, one can apply a baseline subtraction algorithm to each spectrum that will subtract intensity contributions from the 'noise' in order to calculate more accurate peak intensities. Total in current (TIC) normalization standardizes the intensities of a set of spectra to compensate for any spectrum-spectrum variations due to minor differences in total protein concentration, sample preparation, or data collection. This improves reproducibility and helps the user to identify spectra of poor quality by generating normalizations factors. The normalization process first calculates the TIC by summing up all the peak intensities (area under the curve) across a spectrum. The average TIC from all selected spectra is then calculated and used to generate the normalization coefficient, which will be used in turn to generate the normalization factors for each spectrum to adjust the intensity scales (128).

The main objective of peak clustering is to create a list of all peaks and their corresponding intensities across all spectra. The main parameters for clustering peaks are the sensitivity setting for peaks detections (e.g. signal-to-noise ratio, valet depth, minimum peak threshold percentage) and the mass window setting for cluster completion (peak width or percentage of mass). In the first peak detection step, peaks are identified for each individual mass spectrum. After peak clustering, single mass spectra are reanalyzed, focusing with less strict parameters. Thereby, peaks that are initially missed can be recognized based on the assumption that a peak is likely to exist in a spectrum if it has already been found in many other spectra.

The rapid development of new biomarkers increasingly motivates multi-marker studies to assess the value of different biomarkers for diagnostic predictions. Several different approaches exist for classifier generation (e.g., decision tress, artificial neural networks, and support vector machines), each with their own strengths and weaknesses. One of these analytical approaches is the classification and regression tree (CART) methodology. Software such as ProteinChip Pattern Analysis Software (a.k.a. Biomarker Pattern Software (BPS)) provides users with an easy-to-use interface to perform CART analysis.

CART is a binary recursive partitioning method. This approach is considered 'binary' because parent nodes are always split into exactly two child nodes and recursive because the process can be repeated by treating each child node as a parent. Moreover, the method is non-parametric, making no assumptions about the functional form of the data. It can be used to analyze either categorical (classification) or continuous data (regression). The defining feature is that this approach represents the result in the form of decision trees. The three basic steps of CART involve first the split of the overall study group into two subgroups using the most powerful predicator of the outcome (ie: protein biomarker candidate), then to split the subgroups into two until no further significant splits are found or the subgroups become too small. Once terminal nodes have been achieved (see below), the result are displayed in a binary tree structure that can be subjected to 'tree pruning' if necessary (129).

Many different splitting criteria have been proposed, but all begin by defining the impurity of a node. Impurity functions are symmetrical, concave functions with maximum value at $p_{i/j}=0.5$ and value zero when there is no

impurity (130). In other words, node impurity is minimal when all the variables at the node are of the same category and reaches its maximum when all are equally likely. Impurity functions include but are not limited to Gini, entropy, and minimum error. Regardless of which impurity function is chosen, the splitting criterion selects the split that has the largest difference between the impurities of the parent node and a weighted average of the impurities of the two child nodes. One concern of this recursive splitting method is determining when to stop growing the tree. Usually the user can define what are called *stopping rules* in order to control how large the tree can become. Examples of stopping rules involves defining the minimum number of individuals in the child nodes or in the terminal nodes, or determining the maximum number of levels to which the tree can grow (i.e. the maximum number of independent variable that can define a single terminal done) (130). However, implementing stopping rules may cause some important associations to be missed. Instead, BPS begins by growing a maximal tree, followed by a set of sub-trees derived from it.

Even though we have highlighted some of SELDI-TOF's advantages such as high-throughput, minimal sample volumes and the ability to analyze crude biological samples, it is also important to acknowledge the limitations of this platform. In addition to its high cost (131), SELDI tends to be relatively imprecise in the assignment of molecular mass to any given peak. This 'deficiency' is mainly due the hardware used for analysis and arises to some degree as a compromise to achieve broad dynamic range (116). Another important consideration when using the SELDI technology is the tendency of the software to identify false candidate biomarkers in studies with small numbers of samples (e.g.

< 10). Few candidate biomarkers arising from small studies survive larger-scale validation work (122). Therefore, the use of this technology requires large numbers of samples with appropriate controls to ensure the successful identification of key biomarkers.

1.6 Rational and objectives

We sought to study plasma proteome profiles at different stages of fibrosis in HCV mono- and HIV-1/HCV co-infected patients using SELDI-TOF MS. This approach offers high-throughput protein profiling of native biological specimens. Our hypothesis was that SELDI-TOF MS could be used to develop a diagnostic test that will detect and stage liver fibrosis in HIV-1/HCV co-infected individuals and identify new biomarkers for liver fibrosis. Reliable biomarkers could have significant diagnostic and prognostic value, as well as aid in the evaluation of therapeutic responses. Furthermore, biomarker studies may provide a key to understanding why HCV disease progresses more rapidly in the context of HIV-1. Finally, we also investigated the consequences on liver fibrosis of the sequence of infection in HIV-1/HCV co-infected individuals.

Specific objectives:

1. Determine the plasma proteome of HCV mono and HIV-1/HCV co-infected individuals depending on their stage of liver fibrosis.
2. Develop an algorithm that is capable of staging liver fibrosis in these individuals
3. Identify candidate biomarkers by MALDI-TOF/TOF and confirm by immune assays
4. Assess the effect of acquiring HIV-1 infection prior to HCV infection on the proportion of individuals progressing of liver fibrosis.
5. Assess the effect of acquiring HIV-1 infection prior to HCV infection on accelerated liver fibrosis.

Chapter 2: Materials and Methods

2.1 Study design, setting and population

The Canadian Co-infection Cohort Study [CCC, CIHR Canadian Trials Network (CTN222)] is a prospective multicenter study recruiting HIV-1/HCV co-infected patients at 17 centers across Canada since 2003 with approval by participating research ethics boards and has been described in detail (132). The eligibility criteria are: i) over 16 years of age, ii) documented HIV-1 infection (HIV-1 positive by ELISA with Western blot confirmation), iii) evidence of HCV infection (HCV seropositive by ELISA with recombinant immunoblot assay II or enzyme immunoassay confirmation, or if serological false negative, HCV RNA positive). After informed consent, each participant undergoes an initial evaluation followed by study visits approximately every 6 months. At each visit, sociodemographic and behavioral information are self-reported in questionnaires; medical treatment and new diagnoses are collected by research personnel and laboratory analyses, including AST and platelet count, are performed using a standard protocol. $CD4^+$ T-cell counts and plasma HIV-1 viral loads are measured using standard techniques (133). As of December 2012, 1150 patients were enrolled and followed for a median of 31.8 months. For the proteomics study, patients were selected in the CCC based on the availability of a plasma specimen within one year of liver biopsy. HCV mono-infected persons undergoing liver biopsies were prospectively recruited from 3 sites participating in the CCC and plasma samples were obtained within a year of liver biopsy. A total of 151 individuals were studied, including 68 HCV mono-infected and 83 HIV-1/HCV

co-infected subjects in each of the 4 stages of fibrosis (0-1, 2, 3, 4). The stages can be describe as: 1) portal fibrosis without septa, 2) portal fibrosis with few septa, 3) numerous septa without cirrhosis and 4) cirrhosis. For the progression of fibrosis, a sub-cohort was defined that included all co-infected patients with HCV replication (at least one positive test of plasma HCV RNA RT-PCR (Roche COBAS Amplicor), without significant fibrosis (APRI score <1.5), radiological or histological diagnosis of cirrhosis and/or ESLD at baseline, known or estimated duration of infection for both HIV-1 and HCV and no HCV treatment. HCV treated patients were excluded because treatment can affect the AST and platelet counts, thus influencing the APRI score and those who are cured would be expected to have reduced risk of fibrosis progression. Patients were divided in 3 groups; 1) those infected with HCV before HIV-1 (reference category) 2) those infected with HIV-1 before HCV and 3) those infected with HIV-1 and HCV at the same time (+/- 1 year). An APRI score ≥ 1.5 was used to indicate significant liver fibrosis (equivalent to a score ≥ 2 on the Metavir scale) (134).

2.2 Surface-enhanced laser desorption ionization-time-of-flight mass spectrometry (SELDI-TOF)

One hundred fifty one plasma samples were processed and analyzed by SELDI-TOF as described in (122). Briefly, the samples were fractionated by pH into 6 fractions, using serum fraction kits (Bio-Rad, Hercules,CA) following the manufacturer's instructions. All fractionation, binding and washing was performed using a BioMek 2000 robot (Beckman Coulter, Fullerton, CA) with an integrated microplate shaker (MicroMix; Diagnostic Products Company, Los

Angeles, CA) that holds an array bioprocessor (Bio-Rad). Fractions 1, 3 and 6 were stored at -80°C until analyzed. For quality control purposes, commercial human reference serua from healthy donors (Valley Biomedical, Winchester, VA) and duplicates were included with all test runs. Samples were randomized within and across arrays with blank spots included as negative controls, and applied to three types of ProteinChip arrays: 1) weak cation exchange (CM10), 'immobilizes metal affinity capture' (IMAC30) and hydrophobic/reverse-phase (H50) (Bio-Rad). Arrays were analyzed in a ProteinChip biology system reader series (PCS 4000) using ProteinChip software, version 3.5 (Bio-Rad). Each spot was read at low- and high-energy laser intensities. Analyses were performed in two steps. First, automated peak detection was applied, using cluster features of Biomarker Wizard software. Clusters with P values <0.05 (Mann-Whitney U test) were visually inspected, followed by manual peak relabeling. After relabeling, exact P value for differences in average peak intensity between groups with fibrosis 0-1 and fibrosis 3-4 were calculated (Wilcoxon exact test). Peaks with P values <0.05 and receiver operating characteristic (ROC) values >0.75 or <0.25 were considered as potential biomarkers. Biomarker Pattern Software analysis was applied to the cleaned cluster data. This program uses a supervised pattern classification method (classification and regression tree [CART]) to identify peaks with the greatest contribution to discrimination between groups. Specificity was calculated as the ratio of the number of negative samples correctly classified to the total number of true negative samples. Sensitivity was calculated as the ratio of the number of correctly classified diseased samples to the total number of diseased samples. Accuracy was calculated as the ratio of samples correctly

classified to the total number of samples. Similar analysis was performed to find discriminator peaks between the four stages of fibrosis (F1, F2, F3 and F4).

2.3 Purification of candidate biomarkers and identification by MALDI-TOF/TOF

Two samples that showed the highest intensity in SELDI-TOF analysis for each biomarker were selected as positive samples and two with the lowest intensity were selected as negative controls. Enriched fractions were purified in NuPAGE precast gels (Invitrogen Life Technologies, Carlsbad, CA), stained with colloidal blue-stained (Invitrogen) and bands of interest were excised for in-gel digestion (Roche Applied Science, Indianapolis, IN). Trypsin digests were extracted with 50% formic acid-25% acenotrinitril-15% isopropanol-10% water and vacuum dried. Dried peptide samples were resuspended in 0.1% TFA, sonicated for 10 min and desalted with ZipTip C18 according to the manufacturer's protocol (Millipore Co., Billerica, MA) Samples were eluted from the Ziptip in 4 uL of α-cyano-4-hydroxycinnamic acid (CHCA) matrix (10 mg/mL in 50:50 ACN/0.1% TFA in water). The solution was spotted directly onto a 384-well AB OptiTOF MALDI stainless steel plate (ABSciex, Framingham, MA) and allowed to dry at room temperature.

MALDI data were acquired on a 4800 Plus MALDI TOF/TOF Analyzer (ABSciex) with the 4000 Series Explorer v3.5.3 software. Internal calibration was carried out using des-Arg-1-bradykinin (monoisotopic mass 904.4681), angiotensin I (1296.6853), glu1-fibrinopeptide B (1570.6774),

adrenocorticotropic hormone (ACTH) fragment 1-17 (2093.0867), ACTH fragment 18-39 (2465.1989) and ACTH fragment 7-38 (3657.9294). In the positive-ion reflector mode, MS data were collected over a mass range of 800–4000 Da using a fixed laser intensity of 3000 nj for 1000 shots/spectrum, with a uniformly random spot search pattern. In each MS spectrum, the 20 most abundant MS peaks were selected for MS/MS using an acquisition method that excluded ions with S/N less than 20. The precursor ions with the strongest S/N were acquired first using a 1 kV MS/MS operating mode in which the relative precursor mass window was set at 50 and the metastable suppression enabled. MS/MS acquisition of selected precursors was set to 2000 shots per spectrum with 50 shots per subspectrum using fixed laser intensity of 4200 nj.

Protein identification was performed with ProteinPilot 4.0.8 software using the Paragon algorithm (ABSciex). Peptides present in positive samples but absent in the negative samples were selected. MS/MS data were searched against the most recent UniProtKB/Swiss-Prot database releases of Homo sapiens, HCV and HIV-1. Trypsin was selected as the digestion enzyme. Other search parameters included cysteine alkylation by iodoacetamide, gel-based ID, thorough ID, with ID focus on biological modifications.

2.4 Western blot analysis

Pooled plasma from co-infected individuals for each stage of fibrosis (F1, F2, F3 and F4) were separated in 4-12% Novex NuPAGE Bis-Tris gradient gels (Invitrogen) under reducing conditions. Separated proteins were transferred to

nitrocellulose membranes and confirmed with Ponceau Red staining. Nonspecific sites were blocked with 5 % skim milk in 0.05% PBST (0.05% Tween 20 in PBS) for 1 h at room temperature. Membranes were incubated with either anti-APO-A1 1:1000 (Santa-cruz), anti-Plasminogen 1:1000, anti-Transferrin 1:5000 or anti-Haptoglobin 1:500(Abcam), followed by incubation with either HRP-conjugated anti-mouse IgG or anti rabbit IgG at a 1:20 000 dilution (Amersham Bioscience Co., Piscataway, NJ). The membranes were incubated in SuperSignal West Pico detection solution (Pierce, Rockford, IL) and exposed to X-ray film.

2.5 Statistical Analyses

Descriptive characteristics of participants at first available APRI value by order of HIV-1/HCV acquisition status were compared (Kruskal-Wallis or Pearson's χ^2). All tests were two-tailed and p-values <0.05 were considered to be statistically significant. The Spearman rank correlation test was used to assess the significance of associations between biomarkers and VL or $CD4^+$ T cell counts. A multivariate logistic regression model was constructed to define the primary outcome (APRI $\geq$ 1.5) and adjusted for order of HIV-1/HCV acquisition status, age at HCV infection per 10 year period, female gender, aboriginal ethnicity, MSM, history of IDU and alcohol consumption at first available APRI value, $CD4^+$ count per 100 cells and HIV-1 viral load (log10 copies/mL). We modeled the slope of ln(APRI) over time using generalized estimating equations (GEE) with an identity link function, exchangeable correlation structure, and robust variance estimates to account for the correlation of data contributed by the same patient at multiple visits. A base

GEE model was adjusted for time-invariant variables including order of HIV-1/HCV acquisition status, age at HCV infection per 10 years, female gender, aboriginal ethnicity, MSM, history of IDU and alcohol consumption at first available APRI value and time-dependent variables including HCV duration per 5 years (it is our time variable), CD4 count per 100 cells and HIV-1 viral load (log10 copies/mL). An interaction term between order of HIV-1/HCV acquisition status and time (HCV duration per 5 years) was added to the model to evaluate if there was a difference in the rate of change of ln(APRI) according to the order of HIV-1 & HCV acquisition. For interpretation purposes, all continuous variables were centered at their median with $CD4^+$ cells centered at 200 cells and HIV-1 VL centered at log value of 3. Model fitting was undertaken using the genmod procedure in SAS software version 9.2 (SAS Institute, Cary, NC). To evaluate the rate of progression to liver fibrosis, a survival analysis was carried out on all co-infected patients, censoring was done at the date of the last documented visit while still having no significant fibrosis (APRI < 1.5). A log rank test was used to test the significance of between-groups differences in time of HCV infection to development of fibrosis using Prism software version 5.04 (GraphPad, La Jolla,CA).

Chapter 3: Results

3.1 Proteomic Fingerprinting in HCV mono- and HIV-1/HCV Co-infection reveals Serum Biomarkers for prognostic of Fibrosis

3.1.1 Demographic and clinical characteristics of the study population for proteomics study

As shown in Table 2, we observed a difference in recent alcohol use with 63% in the co-infected acknowledging alcohol use versus 38% in mono-infected groups. A larger proportion of the mono- than co-infected subjects were women (31% vs 16% respectively). There were also significant differences between groups in both age and duration of HCV infection. Co-infected individuals were generally younger (~45.4 years) compared to mono-infected (~49.6 years) and had been HCV-infected for less time, 16.5 years versus 20.7 years. These last differences would be expected with the known accelerated progression of fibrosis in co-infected patients (72, 73). Each group was divided in 4 categories depending on liver biopsy score of the individual; F1 (score 0-1), F2 (score 2), F3 (score 3) and F4 (score 4 and ESLD). There was no difference between groups for any parameter in the mono- and co-infection groups, except for a higher HIV-1 VL in F2 co-infected group compared to the others.

3.1.2 Comparison of SELDI-Spectra in HCV mono-infection

The SELDI-TOF approach was applied to samples from 151 patients. Due to the difference in parameters (age and HCV infection) between HCV mono-infected and HIV-1/HCV co-infected individuals and HAART treatment in the majority of co-infected individuals, spectra of each group were analyzed separately. Most biomarkers programs focus on a single disease and have consider candidate biomarkers to be dichotomous (ie: either positive or negative).

Table 2: Demographic information on the samples in the HCV mono-infection and HIV/HCV co-infection

	Study population (n=151)										
				HCV mono-infection				HIV/HCV co-infection			
	HCV mono (n=68)	Co-infection (n=83)	P value	F1 n=20	F2 n=20	F3 n=20	F4 n=8	F1 n=30	F2 n=19	F3 n=20	F4 n=14
Age (yr)	49.59± 0.941	45.39± 0.879	<0.01	46.95± 1.90	50.25± 2.16	50.95 ± 1.20	51.13 ± 1.63	44.63± 1.69	44.72± 1.76	45.63 ± 1.66	47.93 ±1.81
Duration HCV (yr)	20.75 ± 1.812	16.53± 1.128	<0.05	19.49 ± 3.18	17.49± 3.75	23.64 ± 3.36	25.37± 4.09	14.46 ± 1.83	13.64± 2.11	20.46 ± 2.49	19.58± 2.58
Duration HIV (yr)	-		-	-	-	-	-	11.37 ± 1.15	10.47 ± 1.59	14.69 ± 1.74	12.59 ± 1.57
CD4 count	-		-	-	-	-	-	520.6±47.12	410.8±39.87	501.4±39.37	484.9±65.14
VL	-		-	-	-	-	-	992.7±661	*1880±1498	47.21±1.047	44.07±2.414
Sex											
men	69%	82%	<0.05	60%	70%	75%	63%	88%	78%	84%	64%
women	31%	16%		35%	30%	25%	37%	8%	22%	11%	36%
transgender	0%	2%		5%	0%	5%	0%	4%	0%	5%	0%
Ethnicity											
caucasian	82%	82%	1	75%	80%	75%	100%	81%	83%	79%	86%
other	18%	18%		25%	20%	25%	0%	19%	17%	21%	14%
Alcohol	88%	95%	0.178	55%	65%	65%	75%	100%	83%	100%	100%
Last 6 month	38%	63%	<0.01	40%	35%	40%	25%	74%	56%	63%	58%
Smoking	92%	81%	0.06	90%	90%	80%	100%	78%	78%	74%	92%
Last 6 month	57%	69%	0.16	60%	35%	45%	63%	59%	78%	68%	67%

Values are median (SE) or %, * p<0.05

HCV, hepatitis C virus; HIV, human immunodeficiency virus; VL, Viral Load.

We opted to compare non-fibrotic patients (defined as F1) to more advanced fibrotic patients (F3-F4). Due to the relatively small number of samples in F4 group we pooled F3 and F4 groups for analysis. Using Biomarker Wizard software, fourteen potential biomarkers with significant intensity differences and good AUCs from ROC curve analysis were identified between F1 and F3-4 group (Table 3). Five of these individual biomarkers (4.5-, 9.2-, 18.4-, 27.6- and 84.6-k(m/z)) were down regulated during fibrosis progression, while nine were up-regulated (2.5-, 4.1-, 22.8-, 24.2-, 33.3-, 46.8-, 66.4-, 100.2- and 133-k(m/z)). For example, we observed more than a 5-fold decrease in intensity in the 18.4-k(m/z) biomarker between patients with limited fibrosis (F1) and those in the advanced stages (F3-4). Overall, moderate changes in the levels of biomarkers between F1 and F3-4 groups (1.15 to 2.80 fold) were observed. In addition, we performed an analysis comparing all four groups (F1, F2, F3 and F4). Twelve of the 14 biomarkers had significant intensity differences between the four groups with p values <0.05 while four had p values <0.01 (Figure 5). The cumulative data illustrates how changes in multiple biomarker proteins can be used as 'fingerprints' reflective of a particular disease state.

To select biomarkers with the greatest discriminatory power to distinguish between non-fibrotic (F1) and fibrotic patients (F2-3-4), biomarker pattern software was used to generate random training and test data sets and candidate decision trees. The 4 peaks (4.1-, 24.1-, 100.2- and 133.0- k(m/z)) that served as the main splitters for the trees with the highest individual predictive rates were chosen, and a candidate algorithm was built using these peaks alone. A representative, decision tree that achieved 81% sensitivity and 90% specificity is

Table 3: SELDI-TOF Spectra in HCV mono-infection. Mass (m/z), mean signal intensities, and AUC for selected differentially expressed peptides/proteins between fibrosis 0-1 (F1), fibrosis 2 (F2), fibrosis 3 (F3) and ESLD or fibrosis 4 (F4) patients determined by liver biopsy.

m/z (/1,000)	Fractions and Chemistries	P value (F1 vs F3-4) AUC for ROC Curve (fold F1/F3-4)	Mean signal intensity ± SE				P value
			F1 (n=20)	F2 (n=20)	F3 (n=20)	F4 (n=8)	
2.5	F1 IMAC30	0.003 , 0.76 (2.80)	2.37 ± 1.54	2.76 ± 1.66	7.17 ± 2.68	5.30 ± 2.51	0.008
4.1	F1 CM10, F3-F6 H50	0.001 , 0.91 (2.34)	3.21 ± 1.79	5.90 ± 2.43	7.10 ± 2.66	7.50 ± 1.32	0.005
4.5	F1,F3 CM10-IMAC30	0.001 , 0.22 (-2.40)	10.10 ± 3.18	6.04 ± 2.46	4.45 ± 2.11	3.58 ± 1.57	0.014
9.2	F3 IMAC30, F3 CM10	0.002 , 0.23 (-2.33)	11.72 ± 3.42	7.92 ± 2.81	5.14 ± 2.27	4.78 ± 2.55	0.017
18.4	F1 CM10	0.011 , 0.30 (-5.86)	0.54 ± 0.74	0.04 ± 0.21	0.12 ± 0.34	0.01 ± 0.09	0.052
22.8	F3 CM10	0.016 , 0.70 (1.41)	0.76 ± 0.87	0.83 ± 0.91	0.97 ± 0.99	1.30 ± 0.80	0.043
24.2	F1 CM10	0.048 , 0.68 (2.47)	0.51 ± 0.71	0.73 ± 0.86	1.03 ± 1.02	1.98 ± 0.99	0.013
27.6	F1 CM10	0.013 , 0.30 (-2.31)	0.12 ± 0.35	0.04 ± 0.21	0.05 ± 0.23	0.05 ± 0.26	0.025
33.3	F3 IMAC30	0.013 , 0.70 (1.15)	5.31 ± 2.30	5.35 ± 2.31	6.02 ± 2.45	6.23 ± 1.04	0.067
46.8	F1 CM10	0.004 , 0.74 (1.75)	0.41 ± 0.64	0.49 ± 0.70	0.64 ± 0.80	0.94 ± 0.63	0.022
66.4	F3 IMAC30	0.001 , 0.75 (1.16)	24.62 ± 4.96	26.05 ± 5.10	28.36 ± 5.33	29.34 ± 1.96	0.015
84.6	F6 IMAC30	0.003 , 0.76 (-1.63)	0.10 ± 0.32	0.18 ± 0.42	0.18 ± 0.42	0.14 ± 0.23	0.003
100.2	F3 IMAC30	0.004 , 0.77 (1.51)	0.16 ± 0.41	0.21 ± 0.46	0.24 ± 0.49	0.26 ± 0.29	0.036
133	F3 IMAC30	0.000 , 0.79 (1.21)	2.34 ± 1.53	2.68 ± 1.64	2.79 ± 1.67	2.91 ± 0.51	0.003

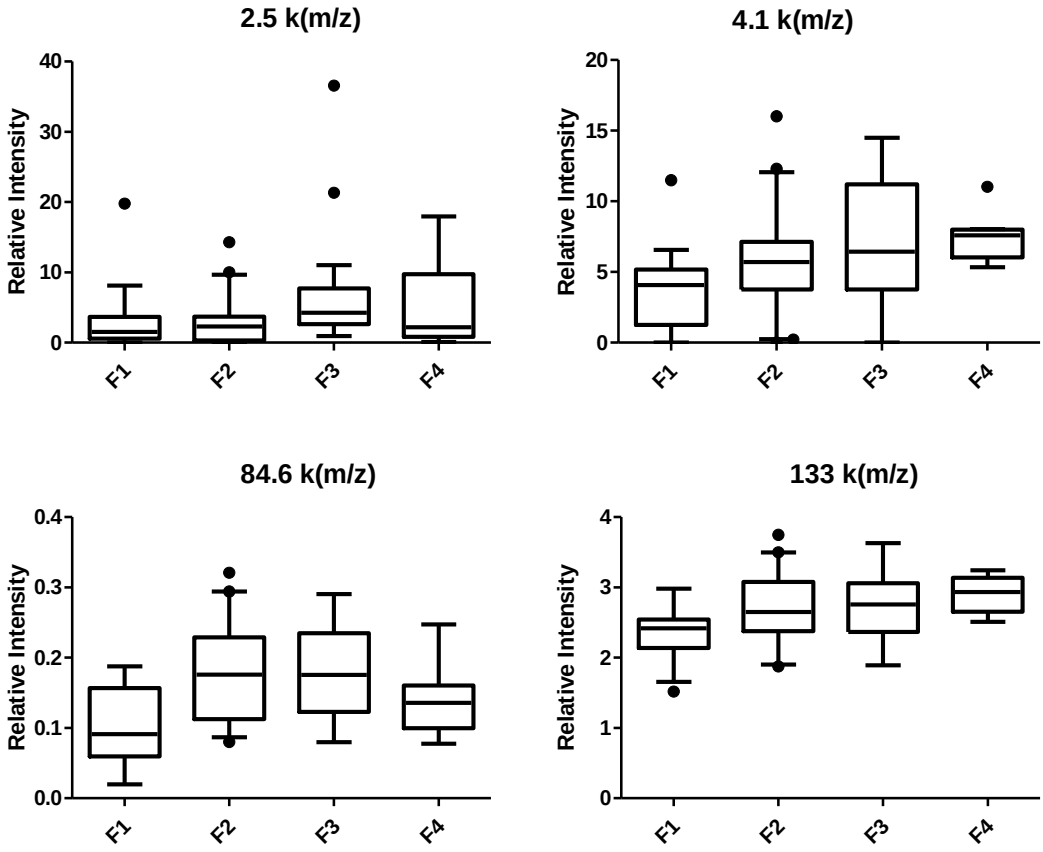

Figure 5: Plasma level of 2.5-, 4.1-, 84.6- and 113 k(m/z) biomarkers in each HCV mono-infection group. Box –whiskers; 10-90 percentile.

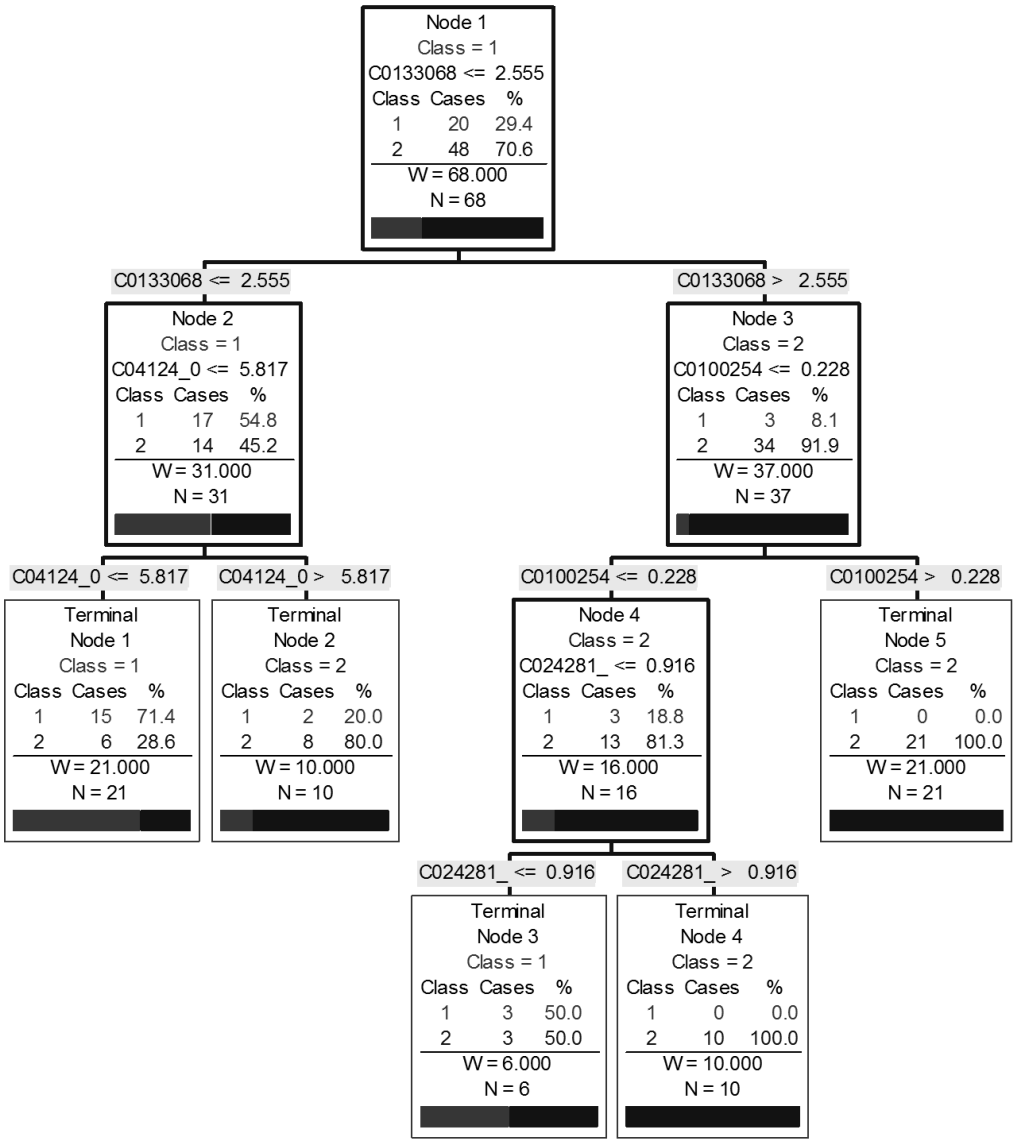

Figure 6: Decision tree to differentiate non-fibrotic individuals (F1) from individuals with significant fibrosis (F2 and above) in HCV mono-infection. Biomarker pattern based on CART analysis was used to generate candidate diagnostic algorithms.

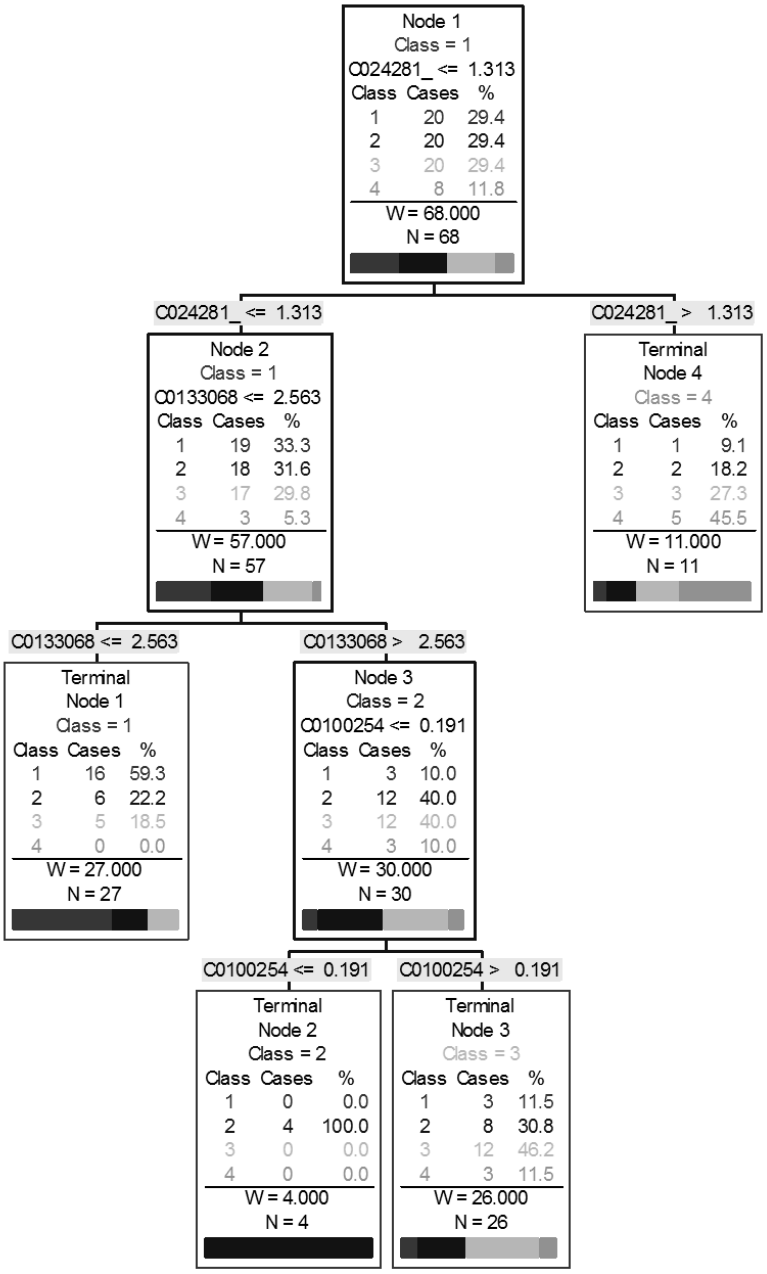

Figure 7: Decision tree to differentiate between the four stages of fibrosis in HCV mono-infection. Biomarker pattern based on CART analysis was used to generate candidate diagnostic algorithm

shown in Figure 6. Using this algorithm we were able to correctly diagnose 57/68 individuals (84%). Application of the same algorithm to co-infected samples obtained an accuracy of 63% (52/83): 72% sensitivity and 47% specificity (data not shown).

Using the same 4 biomarkers to create a new algorithm to differentiate between liver fibrosis stages, we obtained a 3-node decision tree that achieved 54% (35/64) accuracy (Figure 7) and could distinguish non-fibrotic patients with 80% sensitivity and 77% specificity. However, it was not successful to correctly classified most of the patients with stages 2, 3 and 4 of liver fibrosis. These data show that our algorithms can identify patients with significant fibrosis (vs no fibrosis) but are much less accurate in distinguishing among patients with grades F2-F4.

3.1.3 Comparison of SELDI-Spectra in HIV-1/HCV co-infection

Applying a similar approach to spectra obtained in the HIV-1/HCV co-infected individuals, sixteen classifiers with significant intensity difference between F1 and F3-4 (Table 4) were identified. Six of these individual biomarkers were down-regulated during fibrosis progression, while 10 were up-regulated with moderate fold-changes between the two groups (1.3 to 2.6 fold). When we tested the ability of these 16 biomarkers to differentiate patients with regard to their stage of liver fibrosis (F1, F2, F3 and F4), 8 of these 16 biomarkers had significant intensity differences with p values ≤ 0.01. The best four are shown in Figure 8.

Table 4: SELDI-TOF Spectra in HIV-1/HCV co-infection. Mass (m/z), mean signal intensities, and AUC for selected differentially expressed peptides/proteins between fibrosis 0-1 (F1), fibrosis 2 (F2), fibrosis 3 (F3) and ESLD or fibrosis 4 (F4) patients determined by liver biopsy.

m/z (/1,000)	Fractions and Chemistries	P value (F1 vs F3-4) AUC for ROC Curve (fold F1/F3-4)	Mean signal intensity ± SE				P value
			F1 (n=20)	F2 (n=20)	F3 (n=20)	F4 (n=8)	
2.2	F6 CM10	0.002 , 0.73 (1.65)	6.45 ± 2.54	7.19 ± 2.68	9.05 ± 3.01	12.20 ± 2.61	0.008
4.6	F3 IMAC30	0.006 , 0.31 (-2.04)	4.05 ± 2.01	2.68 ± 1.64	2.44 ± 1.56	1.09 ± 1.36	0.010
6.4	F3 H50	0.007 , 0.27 (-2.14)	6.42 ± 3.05	3.75 ± 2.94	3.97 ± 2.45	1.61 ± 1.62	0.002
8.2	F6 CM10	0.007 , 0.27 (-0.58)	3.07 ± 1.83	2.97 ± 1.45	2.04 ± 1.06	1.51 ± 1.01	0.006
8.8	F3 IMAC	0.005 , 0.31 (-1.71)	1.82 ± 1.19	1.59 ± 1.13	1.23 ± 1.38	0.73 ± 0.82	0.013
9.4	F6 H50, F3 IMAC30-CM10	0.002 , 0.29 (-2.55)	11.33 ± 3.37	10.12 ± 3.18	5.84 ± 2.42	2.50 ± 1.68	0.002
13.8	F6-F1 H50,	0.004 , 0.30 (-1.33)	1.80 ± 0.54	1.39 ± 0.67	1.45 ± 0.33	1.14 ± 0.46	0.004
18.4	F1 CM10	0.009 , 0.28 (-2.13)	0.29 ± 1.19	0.46 ± 1.00	0.11 ± 1.00	0.17 ± 0.83	0.021
22.8	F6-F3 CM10	0.010 , 0.67 (1.65)	0.60 ± 0.78	0.82 ± 0.91	0.74 ± 0.86	1.28 ± 1.11	0.014
24.2	F1 CM10	0.018 , 0.71 (1.74)	0.58 ± 0.76	0.85 ± 0.92	0.87 ± 0.93	1.13 ± 0.85	0.071
33.3	F3 CM10-IMAC30	0.004 , 0.71 (1.32)	3.21 ± 1.79	3.91 ± 1.98	4.21 ± 2.05	4.54 ± 1.20	0.015
66.4	F3 IMAC30	0.003 , 0.71 (1.16)	23.88 ± 4.89	24.60 ± 4.96	26.75 ± 5.17	29.25 ± 1.92	0.002
78.8	F6 IMAC30	0.010 , 0.69 (1.54)	0.45 ± 0.67	0.66 ± 0.81	0.61 ± 0.78	0.76 ± 0.64	0.030
133	F3 IMAC30	0.006 , 0.71 (1.14)	2.32 ± 1.52	2.38 ± 1.54	2.69 ± 1.64	2.67 ± 0.74	0.015
162.3	F6 IMAC30	0.004 , 0.71 (1.82)	0.03 ± 0.18	0.05 ± 0.22	0.05 ± 0.21	0.07 ± 0.20	0.005
177.9	F1 IMAC30	0.009 , 0.72 (2.45)	0.01 ± 0.07	0.02 ± 0.15	0.01 ± 0.11	0.01 ± 0.14	0.100

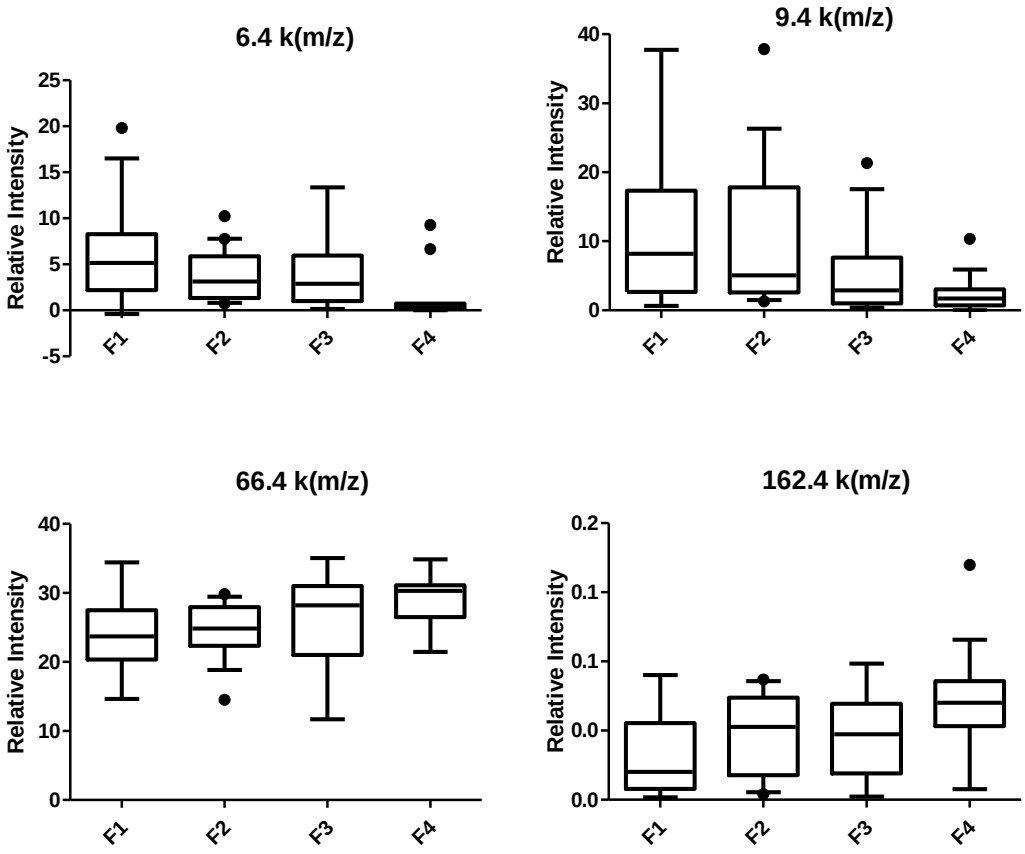

Figure 8: Plasma level of 6.4-, 9.4-, 66.4- and 162.4 k(m/z) biomarkers for each HIV-1/HCV co-infected group. Box –whiskers; 10-90 percentile.

Four biomarkers (8.2-, 8.8-, 13.8- and 22.8- k(m/z)) served as the main splitters for the decision trees with the highest individual predictive rates and were used to build an algorithm. A representative decision tree that achieved 91% sensitivity and 73% specificity is presented in Figure 9. This algorithm was able to correctly diagnosed 77/83 individuals (93%). When the same algorithm was used to diagnose the HCV mono-infected samples, we obtained an accuracy of only 53% (35/64), 50% sensitivity and 55% specificity (data not shown). To evaluate the possible influence of HIV-1 disease progression on these biomarkers, we performed a Spearman rank correlation test and observed no correlation between these biomarkers and markers of HIV-1 progression (VL and CD4 counts), except for the 22.8-kDA and VL (Figure 10). Using the same 4 biomarkers, we created a new algorithm that would allow us to differentiate individuals in their respective fibrotic states (Figure 11). In this exercise, we obtained a decision tree that achieved 59% (49/83) accuracy and was able to correctly classified F4 patients with 80% sensitivity and 76% specificity but failed to diagnose the remaining stages of fibrosis. The biomarkers 22.8-, 24.2-, 33.3-, 66.4- and 133- k(m/z) were also found in mono-infected individuals (Figure 12 A). It was interesting that we observed a good overall correlation between these biomarkers (Figure 12 B). Unfortunately we were not able to obtain a good decision tree using these biomarkers to identify all 151 samples (data not shown). Similar to our findings with the mono-infected subjects, our data shows that our algorithms can quite reliably diagnose patients with significant liver fibrosis (vs no fibrosis) but are not helpful to diagnose the stage of the fibrosis in co-infected individuals.

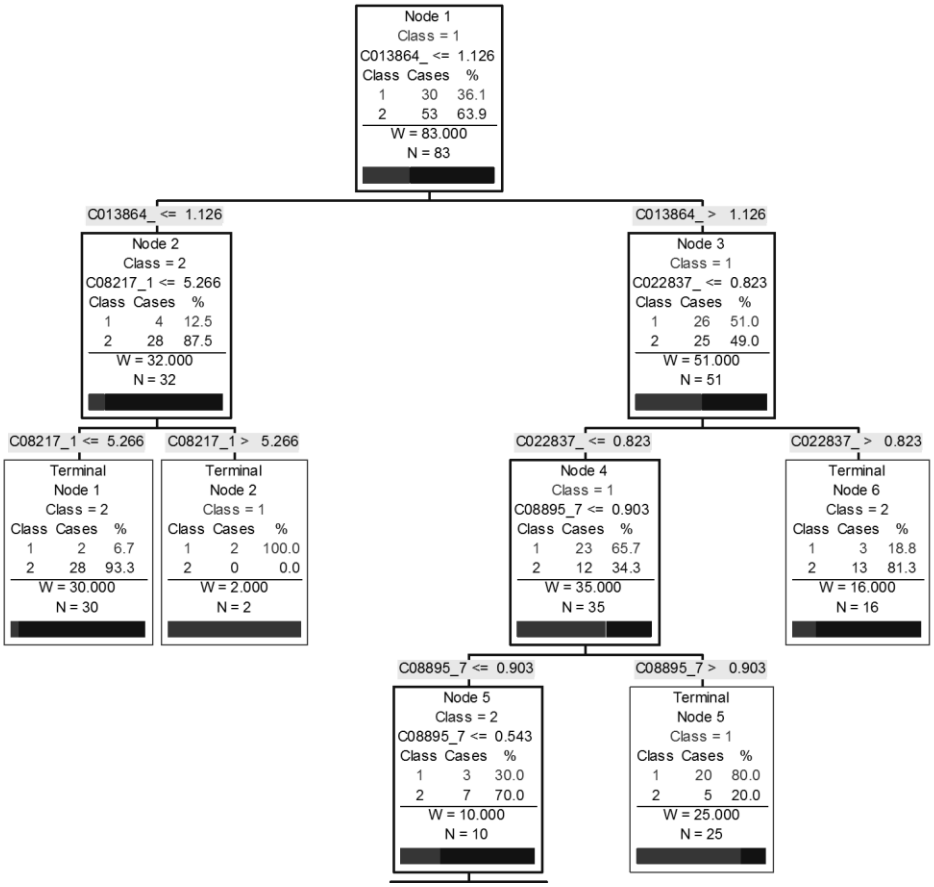

Figure 9: Decision tree to differentiate none fibrotic individuals (F1) to individuals with significant fibrosis (F2 and above) in HIV-1/HCV co-infection. Biomarker pattern based on CART analysis was used to generate candidate diagnostic algorithms

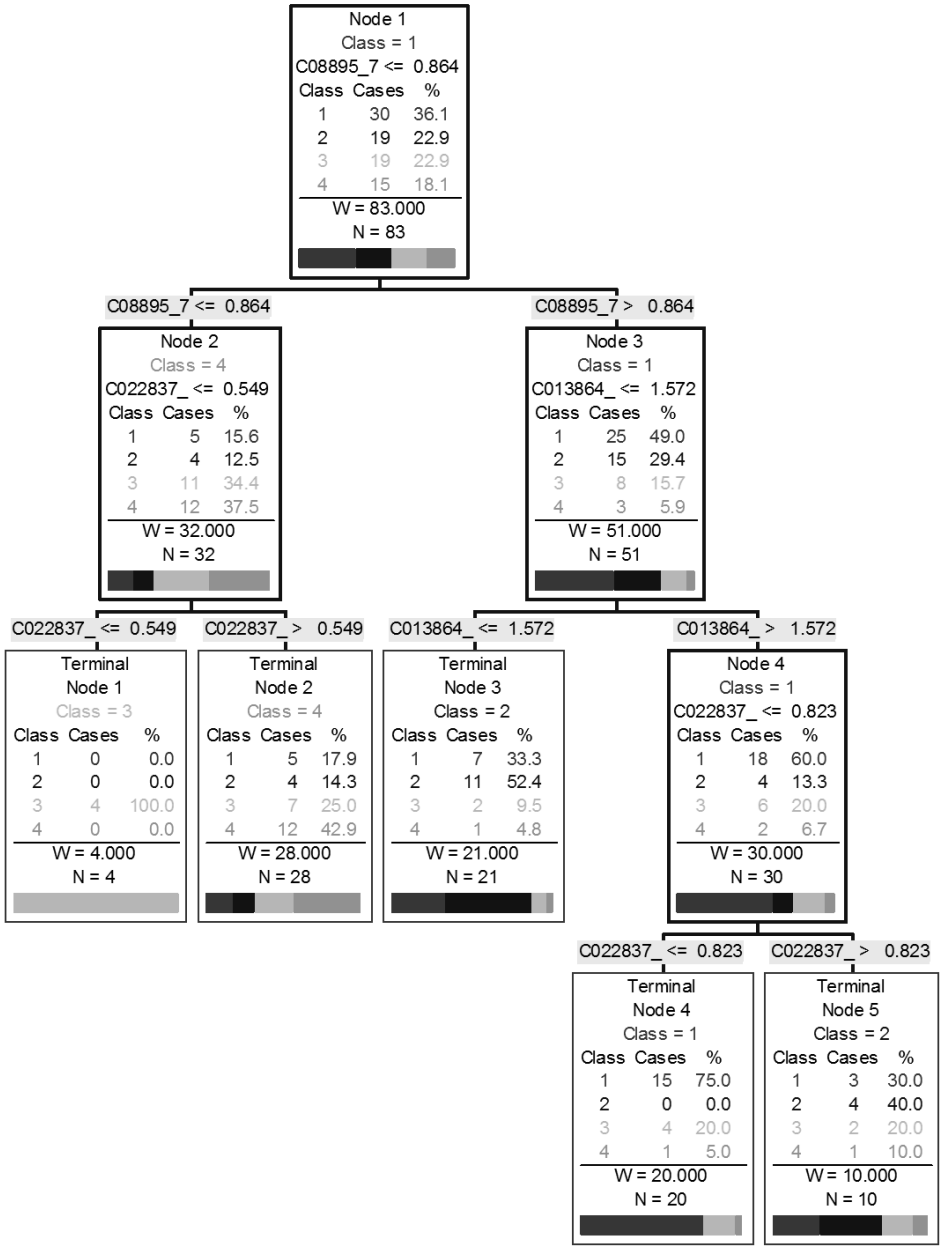

Figure 10: Decision tree to differentiate between the four stages of fibrosis in HIV-1/HCV co-infection. Biomarker pattern based on CART analysis was used to generate candidate diagnostic algorithms.

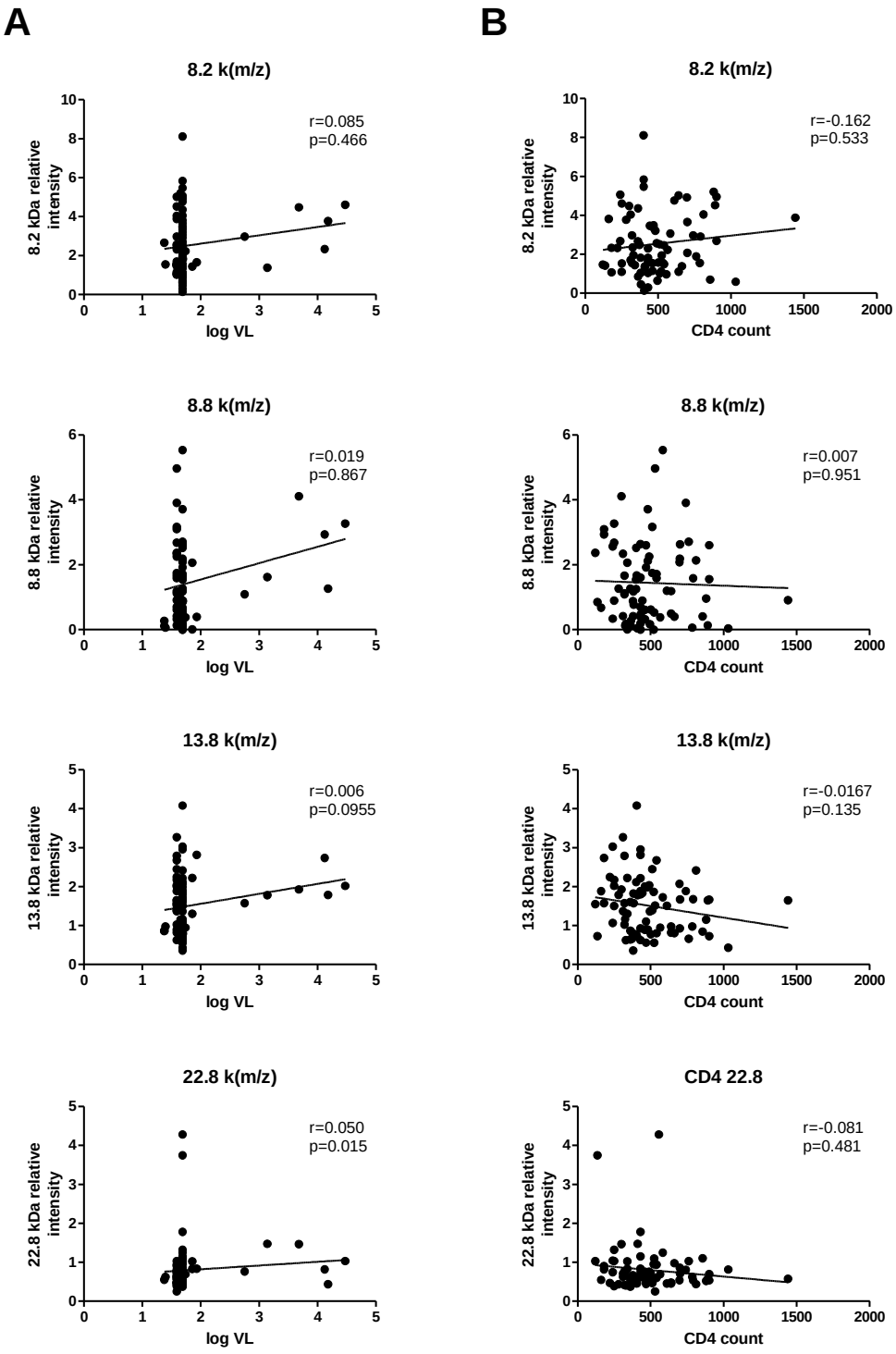

Figure 11: Biomarkers in HIV-1/HCV co-infection do not correlate with VL and CD4 count. Each data point represent results from separate individuals showing the relative intensity of 8.2-, 8.4-, 13.8- and 22.8- k(m/z) and patient VL in A and $CD4^+$ counts in B. A spearman's correlation test was used.

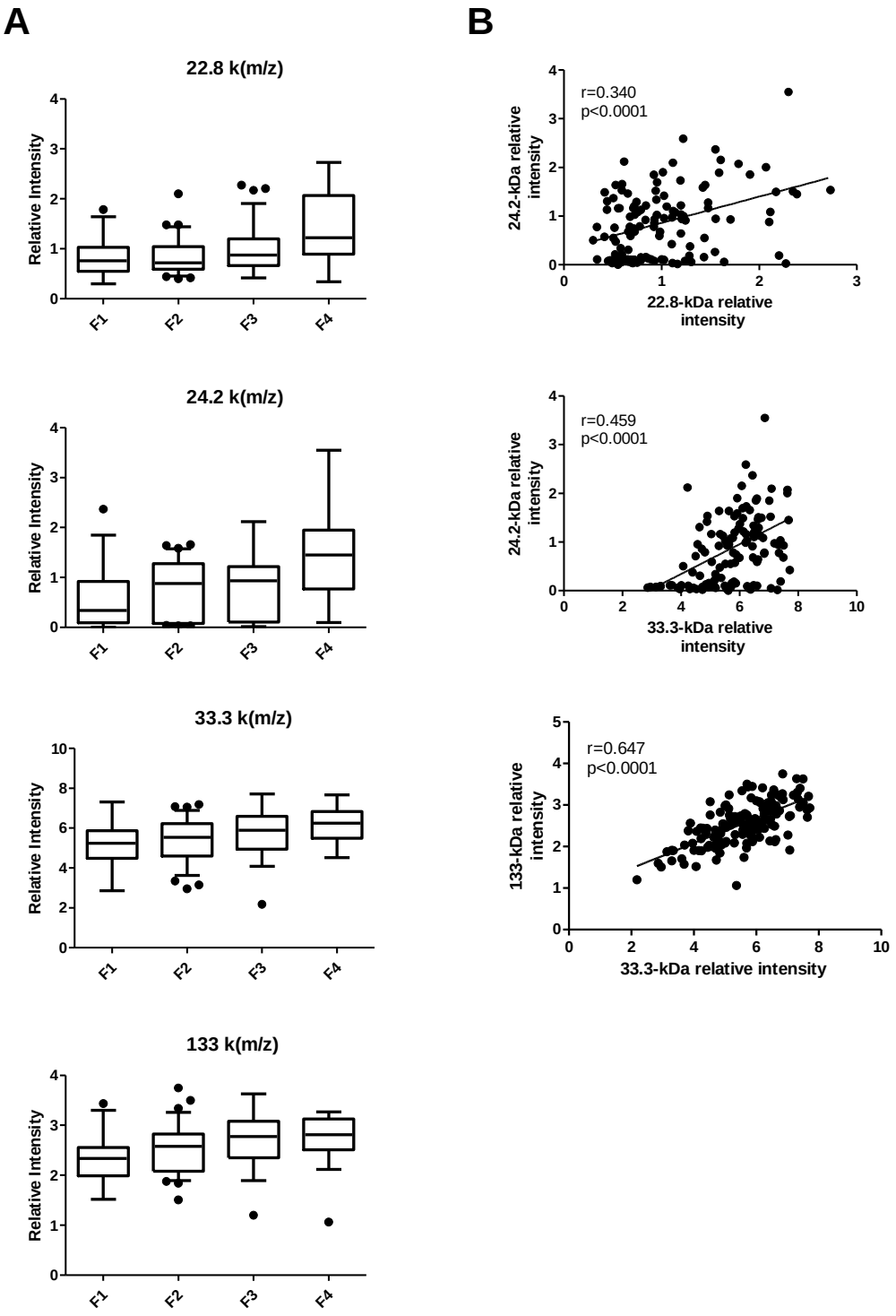

Figure 12: Plasma level of the 22.8-, 24.2-, 33.3- and 133 k (m/z) proteins for each group in all individuals. A) Box –whiskers; 10-90 percentile. B) Correlation between different biomarkers each point represents results from separate individuals. A spearman's correlation was used.

3.1.4 Identification of Biomarkers

Plasma fractionations were run on SDS-Page. Selected bands were cut with their negative control. Samples that demonstrated the highest intensity for each biomarker were selected as positive samples. The two samples with the lowest intensity for each biomarker were selected as negative contols. These biomarkers were identified using matrix- assisted laser desorption/ionization-time-of-flight (MALDI-TOF) MS. Presumptive identifications were based on peptides present in the positive samples and absent in negative samples. Table 5 summarizes the biomarkers identified when comparing positive and negative samples. All candidate biomarkers were of host origin including Ig kappa chain C region (12.6kDa), haptoglobin (46,8kDa) and its alpha chain (18,4kDa), a possible truncated form of apolipoprotein- A1 (22.8 kDa), plasminogen (84.6kDa) and serotransferrin (78.8kDa). We then attempted to confirm the identities of these biomarkers using specific immunoassays. We also performed western blots on pooled samples from co-infected individuals (Figure 13). We observed no change in the levels of serotransferrin in any of the 4 stages of liver fibrosis. On the other hand, we observed steady decreases in levels of haptoglobin, plasminogen and the APO-A1 truncation peptide as the stage of liver fibrosis increased.

3.2 Sequence of HCV and HIV-1 infection in co-infected patients affects fibrosis progression rates

Although this difference was not quantified, we observed a much greater heterogeneity in SELDI spectra from the co-infected samples compared to mono-

Table 5: Sample identification of selected candidate biomarkers. Plasma fractions were run on SDS-PAGE. Selected bands were cut with their negative control. These biomarkers were identified using matrix-assisted laser desorption/ionization-time-of-flight (MALDI-TOF) MS. Presumptive identifications were based on peptides present in the positive samples and absent in negative samples.

m/z (/1,000)	Protein Identity	Predicted Mass (Da)
12.4	Ig kappa chain C region	11,609
18.4	Haptoglobin alpha chain	15,920
22.8	Apolipoprotein- A1	28,081
46.8	Haptoglobin	45,205
78.8	Serotransferrin	77,064
84.6	Plasminogen	90,569

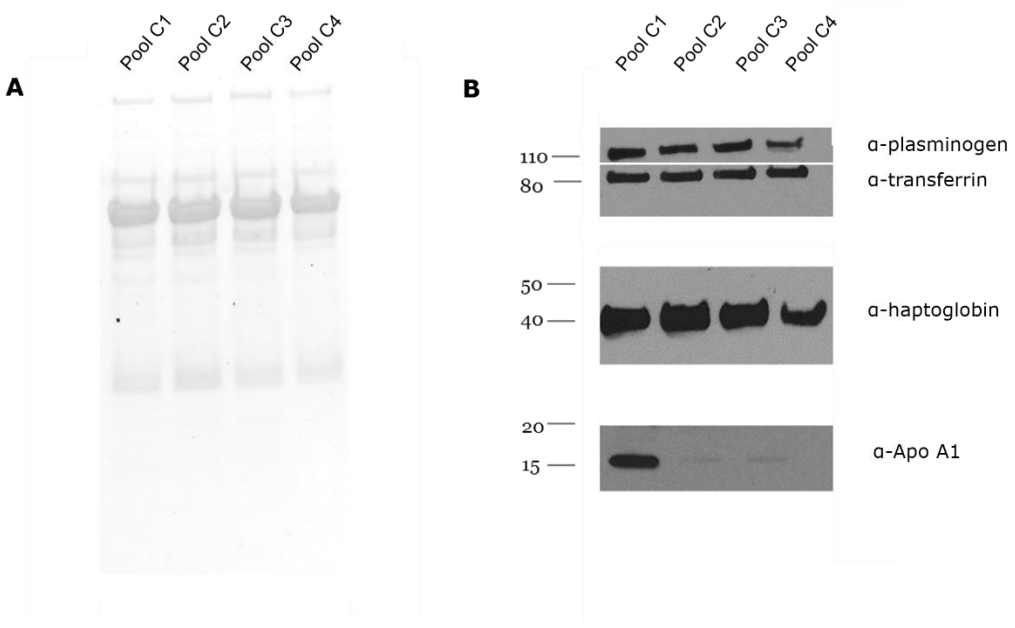

Figure 13: Western blot analysis of plasma pools from co-infected individuals, probed for anti-transferrin, anti-haptoglobin and anti-Apo A1. A) Red Ponceau staining of the nitrocellulose membranes B) Western-blots showing full length plasminogen (~91 kDa) serotransferrin (~80 kDa), full length haptoglobin (~42 kDa) and APO A1 truncation (~17kDa).

infected subjects. Co-infected individuals can differ based on the sequence of infection with the individual viruses. We used clinical data collected as part of the CCC to investigate the effect of the sequence of infection on the pace of liver fibrosis.

3.2.1 Baseline Characteristics of study subjects

The CCC database contained information from 1150 HIV-1/HCV co-infected individuals of whom 930 had at least two visits with available APRI result and information on their social-demographic and clinical characteristic at cohort entry (Table 6). 602 were documented to have been infected with HCV followed by HIV-1 (HCV-prior), 148 were infected with HIV-1 followed by HCV (HIV-prior) and 180 were infected within one year by both viruses (same-time). On average, HCV-prior individuals were infected at a younger age (~20 years old: range 16 to 25) compared to HIV-prior (39 years old: range 30 to 46) or same-time (31 years old: range 23 to 39) individuals. HCV-prior individuals were less educated and had lower income compared to the other groups. We observed comparable alcohol-use between groups, this was in contrast to smoking, where we observed a larger proportion individuals in HCV-prior group who were active smokers. The HCV-prior group was mainly IDUs (98%) with a small proportion of MSM (24%). HIV-prior individuals were mainly MSM (63%) but with a substantial proportion who were also IDU (43%). The most striking difference between groups was the reported mode of transmission of both infections with HCV-prior individuals mostly obtaining both infection by injection of drugs (HCV 71%, HIV-1 64%) and

Table 6: Socio-demographic characteristics of HIV-1/HCV co-infected patients at cohort entry (2003-2012).

	TOTAL (N= 930)	HCV prior (N= 602)	HIV prior (N= 148)	Same time (N= 180)	P-value
Age at HCV infection (Years)	23.0 (17.0, 32.6)	20.0 (16.0, 25.0)	39.3 (30.2, 45.9)	31.0 (23.0, 38.8)	<0.0001
Age (Years)	44.4 (38.9, 49.9)	44.2 (38.9, 49.7)	45.6 (40.7, 51.4)	43.5 (37.9, 49.3)	0.101
Born in Canada	784 (91%)	523 (93%)	116 (86%)	145 (85%)	0.001
Female	229 (25%)	163 (27%)	23 (16%)	43 (24%)	0.014
Aboriginal	139 (15%)	100 (17%)	16 (11%)	23 (13%)	0.143
Greater than high school education	242 (26%)	**103 (17%)**	**77 (52%)**	62 (34%)	<0.0001
Gross monthly income >$1500	219 (24%)	**90 (15%)**	**80 (54%)**	49 (27%)	<0.0001
Heterosexual	241 (26%)	501 (83%)	58 (39%)	130 (72%)	<0.0001
Ever MSM	290 (31%)	**142 (24%)**	**93 (63%)**	55 (31%)	<0.0001
Ever IDU	756 (81%)	**590 (98%)**	**63 (43%)**	103 (57%)	<0.0001
Active IDU	343 (37%)	279 (46%)	25 (17%)	39 (22%)	<0.0001
Ever consumed alcohol	838 (92%)	544 (92%)	129 (90%)	165 (93%)	0.68
Current alcohol consumption	493 (53%)	310 (51%)	82 (55%)	101 (56%)	0.452
Current alcohol abuse*	145 (29%)	107 (35%)	16 (20%)	22 (13%)	0.005
Ever smoked	848 (91%)	583 (97%)	111 (76%)	154 (86%)	<0.0001
Current smoking	717 (78%)	530 (88%)	70 (48%)	117 (65%)	<0.0001
History of transfusion	263 (29%)	154 (26%)	52 (35%)	57 (32%)	0.041
Reported mode of HIV transmission					<0.0001
IDU	472 (51%)	**390 (65%)**	**18 (12%)**	64 (36%)	
Sex	306 (33%)	**136 (23%)**	**97 (66%)**	73 (41%)	
Blood	51 (6%)	9 (2%)	20 (14%)	22 (12%)	
Other	40 (4%)	29 (5%)	5 (3%)	6 (3%)	
Don't know	56 (6%)	34 (6%)	8 (5%)	14 (8%)	
Reported mode of HCV transmission					<0.0001
IDU	518 (57%)	**415 (71%)**	**33 (22%)**	70 (40%)	
Sex	143 (16%)	**49 (8%)**	**46 (31%)**	48 (27%)	
Blood	69 (8%)	26 (4%)	19 (13%)	24 (14%)	
Other	52 (6%)	28 (5%)	15 (10%)	9 (5%)	
Don't know	129 (14%)	70 (12%)	34 (23%)	25 (14%)	

Values are n (%) or median (Q1, Q3)

HCV, hepatitis C virus; HIV, human immunodeficiency virus; IDU, injection drug use; MSM, men having sex with m

*** Percentage based on number of patients on patient currently comsuming alcohol.**

Table 7. Clinical characteristics of HIV-1/HCV co-infected patients at cohort entry (2003-2012).

	TOTAL (N= 930)	HCV prior (N= 602)	HIV prior (N= 148)	Same time (N= 180)	P-value
Duration HIV (Years)	11.1 (6.0, 16.5)	9.7 (4.6, 14.2)	15.6 (10.1, 22.0)	12.1 (6.9, 19.4)	<0.0001
Duration HCV (Years)	18.3 (10.2, 25.1)	21.9 (15.0, 29.2)	5.8 (2.5, 13.2)	12.4 (7.1, 19.1)	<0.0001
CD4 count (cells/µL)	380.0 (245.0, 550.0)	370.0 (229.5, 540.0)	450.0 (300.0, 599.0)	358.5 (260.0, 558.2)	0.002
HIV viral load (log_{10} copies/mL)	1.7 (1.7, 3.0)	1.7 (1.7, 3.5)	1.7 (1.6, 2.3)	1.7 (1.7, 2.9)	0.206
Undetectable HIV viral load (≤50 copies/mL)	550 (60%)	340 (58%)	96 (66%)	114 (64%)	0.139
On cART	748 (80%)	471 (78%)	131 (89%)	146 (81%)	0.018
APRI	0.7 (0.4, 1.4)	0.7 (0.4, 1.4)	0.7 (0.4, 1.4)	0.7 (0.5, 1.5)	0.657
ln (APRI)	-0.3 (-0.9, 0.3)	-0.4 (-0.9, 0.3)	-0.3 (-0.9, 0.3)	-0.3 (-0.8, 0.4)	0.657
APRI ≥1.5	214 (24%)	133 (23%)	35 (24%)	46 (27%)	0.491
APRI ≥2.0	145 (16%)	92 (16%)	25 (17%)	28 (16%)	0.88
AST (U/L)	49.0 (33.0, 78.0)	47.0 (33.0, 75.0)	54.0 (33.8, 75.3)	51.5 (34.8, 88.3)	0.19
Platelets (x 10⁹/L)	202.0 (157.0, 247.0)	201.0 (155.0, 247.0)	206.0 (161.0, 245.5)	199.0 (160.5, 244.5)	0.737
History of ESLD diagnosis	91 (10%)	58 (10%)	16 (11%)	17 (9%)	0.903
HCV genotype					<0.001
1	583 (74%)	359 (73%)	107 (79%)	117 (75%)	
2	37 (5%)	21 (4%)	9 (7%)	7 (4%)	
3	142 (18%)	106 (22%)	14 (10%)	22 (14%)	
4	22 (3%)	6 (1%)	5 (4%)	11 (7%)	
Hepatitis A	71 (10%)	45 (10%)	14 (12%)	12 (9%)	0.619
Hepatitis B (hbsag)	34 (4%)	22 (4%)	4 (3%)	8 (4%)	0.736
History of AIDS diagnosis	272 (30%)	170 (29%)	49 (33%)	53 (30%)	0.533

Values are n (%) or median (

HCV, hepatitis C virus; HIV, human immunodeficiency virus; APRI, aspartate aminotrasferase to platelet r

cART, current antiretroviral therapy; AIDS, acquired immunodeficiency syndrom; ESLD, end-stage liver di

AST, aspartate aminotransferase; BMI, body mass index.

HIV-prior individuals through sexual transmission (HCV 28%, HIV-1 58%). In the HIV-prior group, 25% of patients contracted HCV via injection of drugs and 23 did not know. In the same-time group, roughly the same proportions contracted HIV-1 via sexual transmission or injection of drugs (~37%) though, the majority 40% contracted HCV via IDU.

We observed a significant difference in the duration of the infections at cohort entry between the groups (Table 7). HIV-prior individuals were infected with HIV-1 on average for 15.6 years when they entered the cohort compared to 9.7 years in the HCV-prior group. The duration of HCV infection was also longer in the HCV-prior group (21.9 years) compared to 5.8 years for the HIV-prior group. At cohort entry, HCV-prior individuals had lower $CD4^+$ counts compared to HIV-prior, but similar and very low viral loads. We observed no significant difference in history of AIDS diagnosis and the proportion of individuals progressing to liver disease was comparable between all groups (24% with APRI≥1.5, 16 % APRI≥2.0 and 10% ESLD).

3.2.2 Sequence of infection was not a predictor of rate of developing fibrosis

We performed logistic regression to assess the predicators of liver fibrosis defined as APRI≥1.5 (Table 8). In our analysis, the order of acquisition of the two viral infections was not predictive of fibrosis outcome. In univariate analysis we observed that the variables MSM, lower $CD4^+$ count (per 100 cells) and HIV-1 duration (per 5 years) at cohort entry were all significantly associated with APRI≥1.5. In multivariate analysis however, only HCV duration and lower $CD4^+$ count were predicative of liver fibrosis. Older age and longer HCV duration were

Table 8. Predictors of liver fibrosis for HIV-1/HCV co-infected patients at baseline (N= 930)

	Univariate			Multivariate 1 (outcome= APRI≥1.5)		
Independent Variables at cohort en	Unadjusted OR*	95% confidence interval	p-value	Adjusted OR*	95% confidence interval	p-value
Age at HCV infection (per 10 years)	0.959	(0.852, 1.080)	0.49	1.106	(0.919, 1.332)	0.286
Age (Years)	1.012	(0.996, 1.027)	0.143			
Female gender	1.022	(0.753, 1.386)	0.891	0.96	(0.672, 1.371)	0.821
Aboriginal ethnicity	1.079	(0.747, 1.558)	0.685	1.104	(0.743, 1.640)	0.625
Heterosexual	1.121	(0.829, 1.517)	0.458			
Ever MSM	0.726	(0.543, 0.969)	0.03	0.745	(0.529, 1.047)	0.09
Ever IDU	0.91	(0.650, 1.275)	0.585	0.783	(0.500, 1.225)	0.283
Ever consumed alcohol	1.272	(0.770, 2.104)	0.348	1.235	(0.725, 2.105)	0.437
Ever smoked	0.995	(0.624, 1.586)	0.983			
Order of HIV/HCV acquisition						
HCV first	ref	ref	ref	ref	ref	ref
HIV first	0.799	(0.548, 1.163)	0.241	0.945	(0.553, 1.617)	0.837
HCV & HIV at the same time	1.11	(0.792, 1.556)	0.545	1.194	(0.785, 1.814)	0.407
Duration HCV (per 5 years)	1.061	(0.998, 1.129)	0.058	1.11	(1.007, 1.225)	0.036
Duration HIV (per 5 years)	1.097	(1.001, 1.201)	0.048			
Baseline CD4 count (per 100 cells/µl	0.889	(0.841, 0.940)	<0.0001	0.904	(0.853, 0.958)	0.001
HIV viral load (log_{10} copies/mL)	1.044	(0.935, 1.166)	0.442	1.05	(0.931, 1.184)	0.43
Undetectable HIV viral load (≤50 cc	0.889	(0.678, 1.166)	0.395			
On cART	0.908	(0.653, 1.263)	0.568			
AST (U/L)	1.041	(1.035, 1.048)	<0.0001			
Platelets (x 10⁹/L)	0.985	(0.983, 0.988)	<0.0001			
History of ESLD diagnosis	4.775	(2.950, 7.729)	<0.0001			
Hepatitis A	1.433	(0.875, 2.346)	0.153			
Hepatitis B (hbsag)	0.835	(0.408, 1.709)	0.622			
History of AIDS diagnosis	1.09	(0.817, 1.456)	0.557			

*** Odds Ratio**

HCV, hepatitis C virus; HIV, huma

APRI, aspartate aminotrasferase to platelet ratio; AST, aspa

IDU, injection drug use; MSM, men having sex with men; cAI

ESLD, end-stage liver disease.

Table 9: Association between ln APRI and order of HIV-1-HCV acquisition in HIV-1/HCV co-infected patients (N= 724)

Independent Variables	Adjusted estimates*	95% CI	p-value
Intercept	-0.224	(-0.5651, 0.1170)	0.198
Time= HCV duration (per 5 years)	**0.094**	**(0.0537, 0.1335)**	**<0.0001**
Age at HCV infection (per 10	**0.093**	**(0.0123, 0.1733)**	**0.024**
Female gender	-0.016	(-0.1679, 0.1367)	0.841
Aboriginal ethnicity	0.033	(-0.1415, 0.2068)	0.713
MSM ever	-0.052	(-0.1957, 0.0924)	0.482
IDU ever	-0.161	(-0.3707, 0.0491)	0.133
Alcohol consumption ever	0.195	(-0.0486, 0.4379)	0.117
Log10 (HIVRNA) -centered at	**0.05**	**(0.0199, 0.0802)**	**0.001**
CD4_t (per 100 cells) -centered at	**-0.02**	**(-0.0366, -0.0032)**	**0.019**
Order of HIV/HCV acquisition			
HCV first	ref	ref	ref
HIV first	0.006	(-0.3642, 0.3762)	0.975
HIV & HCV at the same time	0.086	(-0.2711, 0.4426)	0.638
Time*Order of HIV/HCV aquisition			
*Time*HCV first*	ref	ref	ref
*Time*HIV first*	0.039	(-0.0848, 0.1625)	0.538
*Time*HIV & HCV at the same*	-0.006	(-0.1034, 0.0918)	0.907

*** GEE parameter estimates**

CI, confidence interval; HCV, hepatitis C virus; HIV, human immunodeficiency virus

also found to be predicators of APRI ≥2.0 and ESLD (data not shown). It is important to note that these factors might not be predictive of subsequent fibrosis as the outcome excluded APRI≥1.5 at study entry. Exploratory plots of lnAPRI by years of HCV infection suggested no relationship between sequence of infection and fibrosis (Table 9). The differences in lnAPRI with HIV-prior and same-time versus those with HCV-prior were 0.006 and 0.086 respectively, which did not reach statistical significance. In addition our GEE model demonstrated that age at HCV infection per 10 years, level of HIV-1 VL (log 10), and $CD4^+$ count all had independent effects on fibrosis.

3.2.3 Sequence of infection is a predictor of accelerated fibrosis

We wished to evaluate if sequence of infection had any effect on the kinetics of liver fibrosis progression. Using survival analysis, we observed a negative influence of acquiring HIV-1 infection prior to (HIV-prior) or within a year of HCV infection (same-time) leading to more rapid progression to liver fibrosis (relative hazard (RH) =0.09-0.31) (Figure 14 A). In table 7 we observed that HIV-prior individuals are HCV infected later in life than HCV-prior individuals. To explore the possible effect of the age at infection, we assessed the progression of individuals HCV infected between 25-40 years of age. We observed a similar influence of sequence of infection to progression to fibrosis (RH=0.32-0.35) (Figure 14 B). We also observed that HCV-prior individuals enter the cohort at a later time of their HCV infection compared to the other

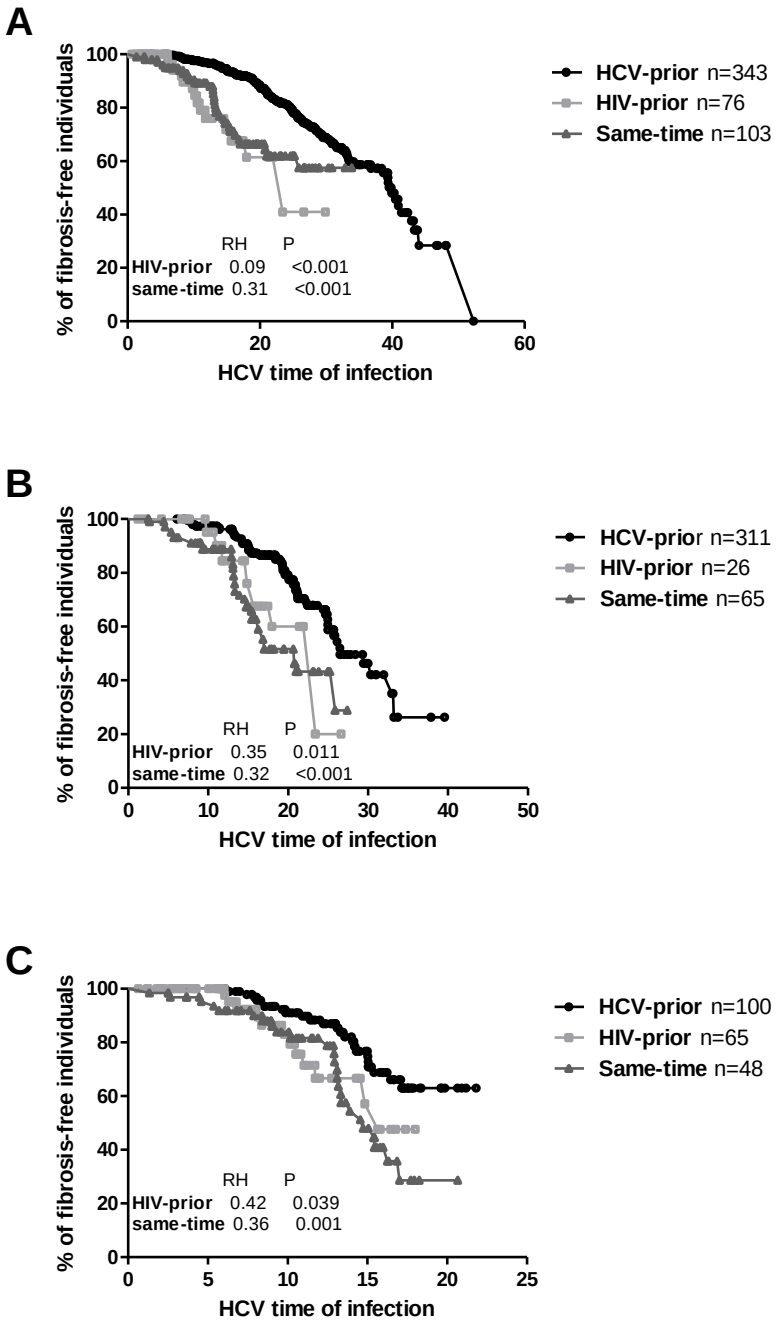

Figure 14: Effect of sequence of infection on progression to liver fibrosis. Kaplan-Meir survival analyses comparing the effects of the sequence of infection on progression to liver fibrosis in the cohort (A), in patients infected with HCV between 25-40 years old (B) and in patients that were HCV infected for less than 15 years before entry the cohort(C). Relative hazard (HR) and significance (P) are given for cox model analyses.

groups. To determine if the time of entry influenced the observed trend, we assessed the progression of individuals that entered the cohort with less than 15 years of HCV infection (ie: the average of our cohorts). Once again, we observed a similar influence of the sequence of infection (RH=0.36-0.42) (Figure 14 C). These data demonstrate that individuals infected with HCV during acute or chronic HIV-1 infection progress more rapidly to liver fibrosis then those that acquire HIV-1 infection when chronically-infected with HCV.

Chapter 4: General Discussion

HIV-1/HCV co-infection affects more than 30% of HIV-1-infected patients in developed countries (135). Co-infection with the two viruses is associated with accelerated liver disease, including fibrosis and both cirrhosis and end of ESLD are accelerated in HIV-1-infected individuals (136). To date, new biomarkers for fibrosis have been sought primarily by using differential two-dimensional gel separations of tissues or serum together with mass spectrometry (MS) for protein identification (137, 138). Proteomic analysis of plasma or serum derived from HCV infected subjects is an emerging technique for the identification of biomarkers indicative of disease progression and severity (139, 140). Use of MS proteomic profiling approaches like SELDI-TOF allow greater sample throughput and the ability to examine both low and high mass proteins that have been difficult to assess effectively with other methods. Using plasma samples from clinically defined patients of fibrosis progression by biopsy, we have obtained results that support the potential use of SELDI-TOF profiling as a surveillance tool to follow disease progression. Ideally, specimens should be obtained from patients who are well matched for as many variables as possible. Since we observed significant differences between the HCV mono-infected and HIV-1/HCV co-infected individuals in sex, age and alcohol use, we decided to analyze each group separately. However, the age difference between mono and co-infected patients was interesting in itself. Co-infected individuals were younger and were HCV infected for a shorter duration than mono-infected

patients. These differences are in concordance with the known accelerated progression to fibrosis in co-infected patients (72, 73).

4.1 Biomarkers of liver fibrosis

Using SELDI-TOF MS, we observed changes in the level of 14 plasma proteins/peptides in mono-infection and 16 in co-infection during the progression of liver fibrosis. Five of these biomarkers were detected in both mono- and co-infected individuals. We were able to obtain good decision trees with accuracy between 84% -93% to identify non-fibrotic patients compared to individuals with significant fibrosis in mono (91% sensitivity; 73% specificity) and co-infection (81% sensitivity; 91% specificity). It is important to note that some ‘of the ‘misclassified’ patients in our algorithm could be due to the low reliability of the biopsy-assigned disease stage categorization. In support of this possibility, four of the nine mono-infection patients ‘misclassified’ by our SELDI biomarkers had APRI values that did not correlate with their biopsy score. The same was true for five of eight SELDI ‘misclassified’ subjects with co-infection. Unfortunately we were not able to generate a good algorithm that could accurately diagnose all patients (mono- and co-infected). This could be due to the biological discrepancies between the infections. Even though we observed the same phenotype (liver fibrosis), it is possible that the actual liver disease and its progression are different in the two populations. Several studies have reported that co-infected individual progress more rapidly to ESLD than mono infected individuals (15, 80, 136, 141). Therefore, it is possible that biomarkers we observed in co-infection are, in fact, markers for accelerated fibrosis. It is

important to note that most of the biomarkers used in the algorithm in HIV-1/HCV co-infection, with the exception of one (22.8-kDa), did not correlate with markers of HIV-1 diseases progression (VL or $CD4^+$ counts). Consequently, these biomarkers are probably related to liver fibrosis. While several non-invasive models utilize tests that are not routinely available, some groups have incorporated routine tests and laboratory data (109) into their models. We tried to improve our algorithms by adding APRI values without success (data not shown). However, it might be interesting to evaluate the potential of other clinical (e.g.: Age, Body Mass Index) or laboratory data (e.g.: HCV RNA, ferritin, serum IgG, INR) to improve the accuracy of our diagnostic algorithms.

In the emerging field of MS-based protein profiling of body fluids, the profile itself can be used to diagnose disease. Using such profiles does not depend on identification of the proteins in the discriminating peaks. However, protein identification is still possible, and adds biological relevance to the findings .We were able to identify some of the biomarkers we discovered using MALDI-TOF and others were confirmed by Western blot. All of these biomarkers were of host origin including Ig kappa chain C region (12.6kDa), haptoglobin (46,8kDa) and its alpha chain (18,4kDa), a possible truncated form of apolipoprotein- A1 (APO-A1) (22.8 kDa) and plasminogen (84.6kDa). It is interesting that two of these proteins, APO-A1 and haptoglobin, are currently used to stage liver fibrosis in the Fibrotest protocol. Looking at other proteins used in Fibrotest , some could be responsible for the unidentified clusters. For example, alpha-2-macroglobulin has a molecular weight of 185 kDa but can produced polypeptide chains of 125,85

and 62 kDa. GGT is a 61 kDa protein and gamma-globulin produces bands in routine electrophoresis of 155-160 kDa, 55-60 kDa and 25-28 kDa.

APO-A1 is a protein that has a role in lipid metabolism and is trapped on extracellular matrices (142). Its serum concentration has long been associated with the presence of liver fibrosis (143). Haptoglobin, an acute phase protein characterized by considerable genetic polymorphism, has been negatively associated with fibrosis (144). The decrease of haptoglobin during fibrosis could be explained by the different roles of hepatocyte growth factor and TGF-β1 in fibrogenesis. Transduction of the hepatocyte growth factor gene suppresses production of TGF-β1 and reduces synthesis of haptoglobin (145). Louagie *et al* also demonstrated that one of the haptoglobin genotypes (*hp 1-1*) is overrepresented in HCV infected individuals. Hp 1-1 is biologically the most effective genotype in binding free hemoglobin and suppressing inflammatory response associated with free hemoglobin. The haptoglobin molecule contains 2 types of polypeptide chains: α (light; α1, 8.9 kDa, α2, 16 kDa) and β (heavy, 40 kDa). Hp 1-1 consists of an α1β dimer, which is the smallest haptoglobin and has a molecular weight of ~86 kd (146). Even though our SELDI-TOF data did not show a decrease of haptoglobin β chain, it was interesting to observe that several clusters (8.8-, 9.2- and 9.4-kDa) close to the molecular weight of the α1 chain negatively correlated with liver fibrosis. Furthermore, we observed a negative correlation with liver fibrosis and the cluster of 84.6-kDa. Even though this cluster was identified by MALDI-TOF and confirmed by Western blot to be plasminogen, it was interesting to notice its negative correlation with liver fibrosis (Figure 14). At the current time, we cannot exclude the possibility that this peak

cluster represents haptoglobin. Plasminogen is a released zymogen of plasmin. Plasmin is a serine protease that acts to dissolve fibrin blood clots. Plasminogen deficient mice have a major defect in hepatic tissue remodeling (147). Plasminogen and haptoglobin both have the potential to be important biomarkers for liver fibrosis. One way to directly assess whether the 84.6 kDa cluster is haptoglobin or plasminogen would be to use a SELDI-TOF immunocapture assay. In this assay, chips are coated with a specific antibody (e.g.: anti-plasminogen or anti-haptoglobin), and pools of plasma representative of the different stages of fibrosis could be tested to observe which antibody results in a change in the 84.6-kDa cluster insensitivity.

Even though we were not able to identify any novel biomarkers in this study, our assays did identify several established markers of liver fibrosis, thus providing validation of our method. Since we were able to fully identify only five of the candidate 25 biomarker peaks/clusters discovered by SELDI, it would clearly be interesting to identify the proteins underlying the remaining clusters. While it is possible that some of these candidate biomarkers will prove to be truncations of the five full-length proteins already defined, there is a very good chance that new biomarkers will be detected among these 25 peak clusters.

In our experiment, we used fractionation to reduce the complexity of the tested samples. One advantage of this method is that it keeps the complete proteome of the biological sample intact. In our case, it also meant that we did not exclude the high-abundance proteins; a decision that was supported by our discovery of several powerful biomarkers among these proteins. However, the presence of the high abundance proteins was undoubtedly a disadvantage when

we were trying to determine the identity of other, less abundant biomarkers by MALDI-TOF. High abundance proteins are well-known to hinder the detection of the low abundance proteins on the SELDI-TOF platform (148). In the past, we have overcome this obstacle by adding a step of IgG depletion using protein A resin and/or purification by reverse-phase chromatography between the fractionation and MALDI-TOF steps (122). Another option would be to replace SDS-PAGE by a 2-dimensional gel to separate proteins not only by their mass but also by their isoelectric point. Methods exist to reduce or eliminate high abundance proteins from serum to increase the relative concentrations of low abundance proteins. The Ig-Y technology is specifically designed to remove a number of the most common serum proteins using IgY antibodies covalently conjugated to polymeric microbeads. For example, the IgY-12™ kit from Beckman Coulter removes Albumin, IgG, Transferrin, Fibrinogen, IgA, α2-macroglobulin, IgM, α1-antitrypsin, haptoglobin, orosomucoid, APO-A1 and APO-A2. Since the polyclonal IgYs are of avian origin, the Fc region of the antibody does not bind mammalian complement factors, rheumatoid factor, IgM, Fc receptor and protein A or G. This method has been used with SELDI-TOF to identify low abundance serum biomarkers (149). ProteoMiner™ uses an alternate technology based on the interaction of complex proteins with a large, highly diverse library of hexapeptides bound to chromatographic supports where saturated proteins are washed during the procedure. This method has been successfully coupled to 2-D Fluorescence Difference Gel Electrophoresis (2-D DIGE) to study serum proteome (150). A final approach that can be used to identify lower-abundance proteins is 2D DIGE, a variant of two-dimensional gel

electrophoresis, that can be used to compare and accurately quantitate two different samples. In future work, these methods could be used in tandem with MALDI-TOF to profile the remaining 25 clusters and identify additional candidate biomarkers of liver fibrosis. No doubt, identifying viral or immune biomarkers would strength our algorithms.

Regardless of the identification of the individual biomarkers in our study, our data demonstrates the existence of specific 'protein fingerprints' between the different stages of fibrosis. However, the clusters of biomarker peaks that were indicative of progression of fibrosis were not identical in mono- and co-infection. At the outset of our work, we would predicted that most of the clusters found in the subjects with mono-infection to be present in those with co-infection as well. As mentioned previously, this was not the case and only 5 clusters were present in both conditions. It is possible that some of the protein clusters found in mono-infection are protein truncations that did not reach statistical significance in co-infection or were hard to isolate due to the increased number of clusters present in the co-infection samples. Nevertheless, it is important to note that none of the clusters, except for 22.8 k(m/z), detected in co-infection correlated with HIV-1 disease progression (ie: correlations with VL or $CD4^+$ count). It is also possible that the unique co-infection clusters correlate with other HIV-1 complications that can influence liver fibrosis such as chronic immune activation. It would be interesting to explore possible relationships between the clusters we found with known biomarkers of immune activation such as CXCL9, CXCL10 or sCD14 (151). It would also be interesting to investigate if these clusters relate to HIV-induced lymphoid fibrosis (152), particularly in the gut. It is important to

emphasize that, even though we have detected biomarkers that can be used to stage liver fibrosis in mono- and co-infected individuals, we cannot affirm that these biomarkers are specific for HCV-induced fibrosis. In order to establish specificity, we will need to validate our algorithms with non-HCV liver anomalies such as alcoholic liver disease, hepatitis B-induced fibrosis or HCC. It is very likely that several of our candidate biomarkers are 'general' markers for liver damage since most are liver-derived and some have already being found in liver infection (122). Future studies should also take in account that genetic factors have being shown to correlate with fibrosis (153).

Although collection biases were difficult to control since archived samples were used for our work, we still observed a good correlation in intensity between biomarkers. We also found increased levels of certain biomarkers and decreased levels in others. This leads us to believe that differences in storage time of archived samples was not a factor in our analysis. In addition, unlike previous studies, we wanted to evaluate the progression of a disease and not a dichotomous 'positive' or 'negative' outcome. As expected, we did not observe either the absence or presence of specific biomarkers/peaks but rather a gradual difference in plasma levels of certain peptides/proteins at the different stages of liver fibrosis. Of course, we still need to take in consideration that our reference point was the biopsy test done within one year of sample collection and that biopsies are subjected to sampling error and inter-observe variability

Although we have demonstrated that SELDI-TOF technology can be used to identify biomarkers useful for staging liver fibrosis, we believe that this platform might be better suited for proteomics research rather than diagnostic test

development. The quantitative accuracy of virtually all MS platforms remains questionable and the mass accuracy of the SELDI-TOF platform is (by design) among the worst. Improved accuracy might be achieved by adding internal controls or identifying a protein that remains unchanged during the disease progression. These approaches would permit an index to be established and subsequently used within the diagnostic algorithm(s). Nevertheless, SELDI-TOF is an excellent tool to observe qualitative changes in protein levels during infection or disease. Such changes can give valuable clues to explain the biological causes of disease progression or understand host-pathogen interaction. Such information helped to determine the protective effect of soluble TLR2 in mother to child HIV-1 transmission through breast feeding (154) and the ability of the Chagas parasite to cleave APO-A1 and HDL for its own benefit (155). In our case, it would be interesting to use this technology, not only to study biomarkers of liver fibrosis, but also to detect biomarkers of accelerated liver fibrosis which is observed in a large proportion of HIV-1/HCV co-infected individuals.

4.2 Accelerated liver fibrosis in co-infected patients

Compared to mono-infected subjects, co-infected individuals have not only an increased rate of cirrhosis but also an accelerated progression to liver disease. While studying protein fingerprinting, we observed a much greater heterogeneity of the proteome in co-infected individuals than in mono-infected patients. We wondered if this variability might be due to the different possible sequences of infection in the co-infected individuals. An individual can become co-infected by first contracting HIV-1 and then HCV, or by contracting HCV and

then HIV-1 or both viruses simultaneously. To study the effect of the sequence of infection in progression to liver fibrosis, we analyzed clinical information in the Canadian co-infected cohort of 1150 individuals.

At cohort entry, we observed an average of 18.7 years of HCV infection and a progression in liver fibrosis (APRI $\geq$1.5) in 23% of patients. These observations are in agreement with current literature, which has shown a more rapid progression of liver fibrosis in co-infected individuals than mono-infected (156, 157). In our study, we detected no difference in the percentage of patients developing liver fibrosis, regardless of the sequence of infection. Factors that appeared to be associated with an increase of liver fibrosis were MSM, lower $CD4^+$ counts, and longer HCV duration. An unexpected finding in our work was the lack of association between IDU and more rapid progression to fibrosis. One plausible explanation for this observation is that this population is likely to die before developing fibrosis. IDUs are at much higher risk of morbidity and mortality than the general population (158). Even in HCV mono-infected groups, IDUs are at increased risk of premature mortality due to their lifestyle (159). Accidental drug overdose is the leading cause of death in IDUs and HIV-1-positive IDUs and AIDS-related death follows in close second (160, 161). Unfortunately the mortality rate in our cohort has not yet been studied. It would be interesting to see if our cohort has similar premature mortality even though we did not observe an effect of the sequence of infection on rate of liver fibrosis. Furthermore, it was interesting to observe a similar rate of patients with liver fibrosis or ESLD in HIV-prior and same-time groups compared to HCV-prior at cohort entry, even though there was a significant difference in duration of HCV

infection (7.2 years and 12.6 to 22.1 years). This observation raises the question if the sequence of infection might correlate with an accelerated liver fibrosis.

To assess the potential effect of the infection sequence on liver fibrosis progression, we performed a Kaplan-Meier survival analysis (Figure 14). We observed that HIV-prior and same-time individuals progressed more rapidly than HCV-prior. However, due to significant differences in both the HCV time of infection and the total HCV duration at time of cohort entry, we performed two sub-sequent analyses. First, we analyzed individuals infected between the age of 25-40 years and a second analysis focused on individuals who had less than 15 years of HCV infection at cohort entry. In both cases, we observed an accelerated progression to liver fibrosis in HIV-prior and same-time. As previously mentioned, we cannot exclude that the HCV-prior group contained a disproportionate number of IDU patients who could have died before entry into the cohort. To confirm the accelerated progression observed in HIV-prior and same-time groups, it would be interested to perform the same analysis using HCV mono-infected individuals as control. We believe that HCV-prior and mono-infected patients would have a similar liver fibrosis progression and only HIV-prior and same-time would show an accelerated progression compared to mono-infected patients. In fact, preliminary analysis performed in our lab with a restricted number of patients (less than 20 per group) demonstrated the tendency that HCV-prior individuals have similar liver fibrosis progression to HCV mono-infected individuals. It would also be interesting to evaluate the fibrosis progression of co-infected individuals before and after co-infection. If our data are correct, we would observe no significant increase in fibrosis rate in HCV mono-

infected individuals after contracting HIV-1 and the progression would be much slower that the rate of progression HIV-1 mono-infected individuals following HCV infection. A potential limitation of this study was the use of APRI as a surrogate marker for liver fibrosis. Both AST and platelets can be subject to variations due to factors other than liver disease. It would be interesting to confirm our findings with other methods to classify the stage of hepatic fibrosis such as liver biopsies or Fibroscan.

It is possible that the accelerated fibrosis observed in our cohort was due to the immune environment of patients with HIV-1/HCV co-infection. HIV-1 infects cells of the immune system; such infection is characterized by the gradual loss of $CD4^+$ T cells and a progressive immune deficiency that first leads to opportunistic infections, and ultimately death. Since most of the individuals were on ART, the major effect in HIV-prior individuals is probably due to the burden caused to the immune system by the chronic HIV-1 infection and note the viral replication itself. During chronic HIV-1 infection, T-cell exhaustion is observed mainly due to effector T cells that become progressively less functional over time in the face of continued antigenic load, despite preservation of the cognate antigen. Cross-sectional studies have shown a correlation between low levels of T cells and functionality, and persistence of HCV infection (162, 163). In addition, others have reported that HIV-1 infection deregulates NK cell subset distribution such that there is a reduction in the frequency of $CD56^+CD16^+$ NK cells with cytolytic activity with an associated increase in the frequency of an anergic $CD56^-$ $CD16^+$ cells (164, 165). NK cells are important innate effectors of antiviral defenses. NK cells constitute a significant proportion of liver-infiltrating

lymphocytes during HCV infection (166), they promote virus-specific adaptive responses (167) and can develop memory-like features (168). The consequences of chronic HIV-1 infection may therefore result not only in an increase of HCV persistence but can also result in increased HCV levels in the liver, therefore promoting hepatic fibrosis. In the case of same-time group we have to consider that a majority of these individuals are infected by a second virus during the acute phase of their first infection. In the case of HIV-1 acute infection the host immune system is targeted, we observe in individuals very low CD4 counts but also high VL. In addition, i*n vitro* studies have shown that HIV-1 enhances HCV replication (169, 170).

In summary, we have shown that sequence of infection can affect the rate of progression of liver fibrosis. People infected with HIV-1 first are at higher risk to develop accelerated fibrosis. More intensive HCV screening of HIV-1-infected individuals is therefore warranted.

4.3 Conclusion

Using SELDI-TOF, we observed 14 protein biomarker peaks associated with mono HCV-infection and 16 associated with HIV-1/HCV co-infection with an overlap of only five. For both disease conditions, we were able to create decision trees capable of distinguished between healthy patients and individuals with significant fibrosis with high sensitivity and good specificity. Although the first biomarkers identified at the protein level have been previously described, this approach clearly has the potential to discover new biomarkers correlated with liver fibrosis and its progression. We demonstrated that sequence of infection

does not affect the percentage of patients who progress to liver fibrosis but can promote accelerated liver fibrosis. Using this approach, we believe that biomarkers correlated with accelerated liver fibrosis can be discovered by comparing HIV-prior or same-time individuals to HCV mono-infected individuals. In our cohort, less than 30% of the individuals progressed to fibrosis. Another interesting exploration would be to use a retrospective approach and identify biomarkers that distinguish people who will progress to fibrosis. Once identified, such biomarkers may help to target and treat co-infected individuals most at risk for rapid fibrosis progression. These new insights into the mechanisms of HIV-1/HCV pathogenesis causing accelerated liver fibrosis could lead to new therapeutic strategies designed to prevent or delay the process. Although HIV-1 remains a disease that can only be controlled, new therapeutic approaches raise the possibility that most individuals infected with HCV can be cured. It will also be of considerable importance to determine whether or not mono-HCV and/or co-infected subjects continue to experience liver fibrosis following HCV cure. Biomarkers of fibrosis in these different conditions will undoubtedly continue to be of interest.

Chapter 5: Contribution of Original Knowledge

This thesis studied the use of SELDI-TOF technology to develop diagnostic tests to assess liver fibrosis in HCV mono and HIV-1/HCV co-infected patients. It also addressed the effect of HIV-1 infection prior to HCV infection on liver fibrosis in co-infected individuals. The main contribution of this work to original knowledge are as follows:

- Characterization of plasma proteome in HCV mono and HIV-1/HCV co-infection individuals.
- Levels of 14 proteins/peptides change depending on the stage of liver fibrosis in HCV mono-infected individuals.
- Levels of 16 proteins/peptides change depending on the stage of liver fibrosis in HIV-1/HCV co-infected individuals.
- Levels of 5 proteins/peptides change depending on the stage of liver fibrosis in both HCV mono and HIV-1/HCV infected individuals.
- Created an algorithm using SELDI-TOF data that can differentiate between healthy patients and those with liver fibrosis.
- Determined that the sequence of infection in HIV-1/HCV co-infected individuals has no effect on the percentage of patients who will progress to liver fibrosis. However, MSM are more likely to progress to liver fibrosis compare to IDUs.

- Demonstrate that the sequence of infection in HIV-1/HCV co-infected individuals has an effect on accelerated liver fibrosis with individuals infected, with HIV-1 first progressing more rapidly than HCV first.

References

1. UNAIDS. 2012. 2012 report on the global AID epidemic.
2. Inciardi, J.A., and Williams, M.L. 2005. Editor's introduction: the global epidemiology of HIV and AIDS. *AIDS Care* 17 Suppl 1:S1-8.
3. Hayes, R., and Weiss, H. 2006. Epidemiology. Understanding HIV epidemic trends in Africa. *Science* 311:620-621.
4. Quinones-Mateu, M.E., Gao, Y., Ball, S.C., Marozsan, A.J., Abraha, A., and Arts, E.J. 2002. In vitro intersubtype recombinants of human immunodeficiency virus type 1: comparison to recent and circulating in vivo recombinant forms. *J Virol* 76:9600-9613.
5. Hammer, S.M., Squires, K.E., Hughes, M.D., Grimes, J.M., Demeter, L.M., Currier, J.S., Eron, J.J., Jr., Feinberg, J.E., Balfour, H.H., Jr., Deyton, L.R., et al. 1997. A controlled trial of two nucleoside analogues plus indinavir in persons with human immunodeficiency virus infection and CD4 cell counts of 200 per cubic millimeter or less. AIDS Clinical Trials Group 320 Study Team. *N Engl J Med* 337:725-733.
6. Houghton, M. 2009. The long and winding road leading to the identification of the hepatitis C virus. *J Hepatol* 51:939-948.
7. Organisation, W.H. Revised July 2012. Hepatitis C Fact Sheet.
8. Strickland, G.T. 2006. Liver disease in Egypt: hepatitis C superseded schistosomiasis as a result of iatrogenic and biological factors. *Hepatology* 43:915-922.
9. Brown, R.S. 2005. Hepatitis C and liver transplantation. *Nature* 436:973-978.
10. Freeman, A.J., Marinos, G., Ffrench, R.A., and Lloyd, A.R. 2001. Immunopathogenesis of hepatitis C virus infection. *Immunol Cell Biol* 79:515-536.
11. Negro, F., and Alberti, A. 2011. The global health burden of hepatitis C virus infection. *Liver Int* 31 Suppl 2:1-3.
12. Gravitz, L. 2011. Introduction: a smouldering public-health crisis. *Nature* 474:S2-4.
13. Gonzalez, S.A., and Talal, A.H. 2003. Hepatitis C virus in human immunodeficiency virus-infected individuals: an emerging comorbidity with significant implications. *Semin Liver Dis* 23:149-166.
14. Rockstroh, J.K., Spengler, U., Sudhop, T., Ewig, S., Theisen, A., Hammerstein, U., Bierhoff, E., Fischer, H.P., Oldenburg, J., Brackmann, H.H., et al. 1996. Immunosuppression may lead to progression of hepatitis C virus-associated liver disease in hemophiliacs coinfected with HIV. *Am J Gastroenterol* 91:2563-2568.
15. Pol, S., Vallet-Pichard, A., Fontaine, H., and Lebray, P. 2002. HCV infection and hemodialysis. *Semin Nephrol* 22:331-339.
16. Yeung, L.T., King, S.M., and Roberts, E.A. 2001. Mother-to-infant transmission of hepatitis C virus. *Hepatology* 34:223-229.
17. Sulkowski, M.S., Mast, E.E., Seeff, L.B., and Thomas, D.L. 2000. Hepatitis C virus infection as an opportunistic disease in persons infected with human immunodeficiency virus. *Clin Infect Dis* 30 Suppl 1:S77-84.

18. Mahalingam, S., Meanger, J., Foster, P.S., and Lidbury, B.A. 2002. The viral manipulation of the host cellular and immune environments to enhance propagation and survival: a focus on RNA viruses. *J Leukoc Biol* 72:429-439.
19. Bieniasz, P.D. 2004. Intrinsic immunity: a front-line defense against viral attack. *Nat Immunol* 5:1109-1115.
20. Nabel, G.J. 2001. Challenges and opportunities for development of an AIDS vaccine. *Nature* 410:1002-1007.
21. Joshi, S., and Joshi, R.L. 1996. Molecular biology of human immunodeficiency virus type-1. *Transfus Sci* 17:351-378.
22. Doms, R.W., and Trono, D. 2000. The plasma membrane as a combat zone in the HIV battlefield. *Genes Dev* 14:2677-2688.
23. Scarlatti, G., Tresoldi, E., Bjorndal, A., Fredriksson, R., Colognesi, C., Deng, H.K., Malnati, M.S., Plebani, A., Siccardi, A.G., Littman, D.R., et al. 1997. In vivo evolution of HIV-1 co-receptor usage and sensitivity to chemokine-mediated suppression. *Nat Med* 3:1259-1265.
24. Chan, D.C., and Kim, P.S. 1998. HIV entry and its inhibition. *Cell* 93:681-684.
25. Karageorgos, L., Li, P., and Burrell, C. 1993. Characterization of HIV replication complexes early after cell-to-cell infection. *AIDS Res Hum Retroviruses* 9:817-823.
26. Malim, M.H. 2006. Natural resistance to HIV infection: The Vif-APOBEC interaction. *C R Biol* 329:871-875.
27. McDonald, D., Vodicka, M.A., Lucero, G., Svitkina, T.M., Borisy, G.G., Emerman, M., and Hope, T.J. 2002. Visualization of the intracellular behavior of HIV in living cells. *J Cell Biol* 159:441-452.
28. Eckstein, D.A., Sherman, M.P., Penn, M.L., Chin, P.S., De Noronha, C.M., Greene, W.C., and Goldsmith, M.A. 2001. HIV-1 Vpr enhances viral burden by facilitating infection of tissue macrophages but not nondividing CD4+ T cells. *J Exp Med* 194:1407-1419.
29. Iijima, S., Nitahara-Kasahara, Y., Kimata, K., Zhong Zhuang, W., Kamata, M., Isogai, M., Miwa, M., Tsunetsugu-Yokota, Y., and Aida, Y. 2004. Nuclear localization of Vpr is crucial for the efficient replication of HIV-1 in primary CD4+ T cells. *Virology* 327:249-261.
30. Purcell, D.F., and Martin, M.A. 1993. Alternative splicing of human immunodeficiency virus type 1 mRNA modulates viral protein expression, replication, and infectivity. *J Virol* 67:6365-6378.
31. Cullen, B.R. 1998. Retroviruses as model systems for the study of nuclear RNA export pathways. *Virology* 249:203-210.
32. Collins, K.L., Chen, B.K., Kalams, S.A., Walker, B.D., and Baltimore, D. 1998. HIV-1 Nef protein protects infected primary cells against killing by cytotoxic T lymphocytes. *Nature* 391:397-401.
33. Jowett, J.B., Planelles, V., Poon, B., Shah, N.P., Chen, M.L., and Chen, I.S. 1995. The human immunodeficiency virus type 1 vpr gene arrests infected T cells in the G2 + M phase of the cell cycle. *J Virol* 69:6304-6313.

34. Freed, E.O. 1998. HIV-1 gag proteins: diverse functions in the virus life cycle. *Virology* 251:1-15.
35. Campbell, S.M., Crowe, S.M., and Mak, J. 2001. Lipid rafts and HIV-1: from viral entry to assembly of progeny virions. *J Clin Virol* 22:217-227.
36. Perelson, A.S., Neumann, A.U., Markowitz, M., Leonard, J.M., and Ho, D.D. 1996. HIV-1 dynamics in vivo: virion clearance rate, infected cell life-span, and viral generation time. *Science* 271:1582-1586.
37. Sherman, M.P., and Greene, W.C. 2002. Slipping through the door: HIV entry into the nucleus. *Microbes Infect* 4:67-73.
38. Gorry, P.R., Ong, C., Thorpe, J., Bannwarth, S., Thompson, K.A., Gatignol, A., Vesselingh, S.L., and Purcell, D.F. 2003. Astrocyte infection by HIV-1: mechanisms of restricted virus replication, and role in the pathogenesis of HIV-1-associated dementia. *Curr HIV Res* 1:463-473.
39. De Francesco, R., and Migliaccio, G. 2005. Challenges and successes in developing new therapies for hepatitis C. *Nature* 436:953-960.
40. Wang, C., Le, S.Y., Ali, N., and Siddiqui, A. 1995. An RNA pseudoknot is an essential structural element of the internal ribosome entry site located within the hepatitis C virus 5' noncoding region. *RNA* 1:526-537.
41. Honda, M., Ping, L.H., Rijnbrand, R.C., Amphlett, E., Clarke, B., Rowlands, D., and Lemon, S.M. 1996. Structural requirements for initiation of translation by internal ribosome entry within genome-length hepatitis C virus RNA. *Virology* 222:31-42.
42. Kim, C.W., and Chang, K.M. 2013. Hepatitis C virus: virology and life cycle. *Clin Mol Hepatol* 19:17-25.
43. Alvisi, G., Madan, V., and Bartenschlager, R. 2011. Hepatitis C virus and host cell lipids: an intimate connection. *RNA Biol* 8:258-269.
44. Flint, M., and McKeating, J.A. 2000. The role of the hepatitis C virus glycoproteins in infection. *Rev Med Virol* 10:101-117.
45. Albecka, A., Belouzard, S., Op de Beeck, A., Descamps, V., Goueslain, L., Bertrand-Michel, J., Terce, F., Duverlie, G., Rouille, Y., and Dubuisson, J. 2012. Role of low-density lipoprotein receptor in the hepatitis C virus life cycle. *Hepatology* 55:998-1007.
46. Tscherne, D.M., Jones, C.T., Evans, M.J., Lindenbach, B.D., McKeating, J.A., and Rice, C.M. 2006. Time- and temperature-dependent activation of hepatitis C virus for low-pH-triggered entry. *J Virol* 80:1734-1741.
47. Blanchard, E., Belouzard, S., Goueslain, L., Wakita, T., Dubuisson, J., Wychowski, C., and Rouille, Y. 2006. Hepatitis C virus entry depends on clathrin-mediated endocytosis. *J Virol* 80:6964-6972.
48. Gosert, R., Egger, D., Lohmann, V., Bartenschlager, R., Blum, H.E., Bienz, K., and Moradpour, D. 2003. Identification of the hepatitis C virus RNA replication complex in Huh-7 cells harboring subgenomic replicons. *J Virol* 77:5487-5492.
49. Foster, T.L., Gallay, P., Stonehouse, N.J., and Harris, M. 2011. Cyclophilin A interacts with domain II of hepatitis C virus NS5A and stimulates RNA binding in an isomerase-dependent manner. *J Virol* 85:7460-7464.

50. Reiss, S., Rebhan, I., Backes, P., Romero-Brey, I., Erfle, H., Matula, P., Kaderali, L., Poenisch, M., Blankenburg, H., Hiet, M.S., et al. 2011. Recruitment and activation of a lipid kinase by hepatitis C virus NS5A is essential for integrity of the membranous replication compartment. *Cell Host Microbe* 9:32-45.
51. Targett-Adams, P., Boulant, S., Douglas, M.W., and McLauchlan, J. 2010. Lipid metabolism and HCV infection. *Viruses* 2:1195-1217.
52. Chang, K.S., Jiang, J., Cai, Z., and Luo, G. 2007. Human apolipoprotein e is required for infectivity and production of hepatitis C virus in cell culture. *J Virol* 81:13783-13793.
53. Merz, A., Long, G., Hiet, M.S., Brugger, B., Chlanda, P., Andre, P., Wieland, F., Krijnse-Locker, J., and Bartenschlager, R. 2011. Biochemical and morphological properties of hepatitis C virus particles and determination of their lipidome. *J Biol Chem* 286:3018-3032.
54. Bartenschlager, R., Penin, F., Lohmann, V., and Andre, P. 2011. Assembly of infectious hepatitis C virus particles. *Trends Microbiol* 19:95-103.
55. Neumann, A.U., Lam, N.P., Dahari, H., Gretch, D.R., Wiley, T.E., Layden, T.J., and Perelson, A.S. 1998. Hepatitis C viral dynamics in vivo and the antiviral efficacy of interferon-alpha therapy. *Science* 282:103-107.
56. Dragic, T. 2001. An overview of the determinants of CCR5 and CXCR4 co-receptor function. *J Gen Virol* 82:1807-1814.
57. Clark, S.J., Saag, M.S., Decker, W.D., Campbell-Hill, S., Roberson, J.L., Veldkamp, P.J., Kappes, J.C., Hahn, B.H., and Shaw, G.M. 1991. High titers of cytopathic virus in plasma of patients with symptomatic primary HIV-1 infection. *N Engl J Med* 324:954-960.
58. Mellors, J.W., Rinaldo, C.R., Jr., Gupta, P., White, R.M., Todd, J.A., and Kingsley, L.A. 1996. Prognosis in HIV-1 infection predicted by the quantity of virus in plasma. *Science* 272:1167-1170.
59. Mohri, H., Perelson, A.S., Tung, K., Ribeiro, R.M., Ramratnam, B., Markowitz, M., Kost, R., Hurley, A., Weinberger, L., Cesar, D., et al. 2001. Increased turnover of T lymphocytes in HIV-1 infection and its reduction by antiretroviral therapy. *J Exp Med* 194:1277-1287.
60. Badley, A.D., Pilon, A.A., Landay, A., and Lynch, D.H. 2000. Mechanisms of HIV-associated lymphocyte apoptosis. *Blood* 96:2951-2964.
61. Garson, J.A., Tuke, P.W., Makris, M., Briggs, M., Machin, S.J., Preston, F.E., and Tedder, R.S. 1990. Demonstration of viraemia patterns in haemophiliacs treated with hepatitis-C-virus-contaminated factor VIII concentrates. *Lancet* 336:1022-1025.
62. Tremolada, F., Casarin, C., Tagger, A., Ribero, M.L., Realdi, G., Alberti, A., and Ruol, A. 1991. Antibody to hepatitis C virus in post-transfusion hepatitis. *Ann Intern Med* 114:277-281.
63. Thimme, R., Oldach, D., Chang, K.M., Steiger, C., Ray, S.C., and Chisari, F.V. 2001. Determinants of viral clearance and persistence during acute hepatitis C virus infection. *J Exp Med* 194:1395-1406.

64. Jacobson Brown, P.M., and Neuman, M.G. 2001. Immunopathogenesis of hepatitis C viral infection: Th1/Th2 responses and the role of cytokines. *Clin Biochem* 34:167-171.
65. London, C.A., Perez, V.L., and Abbas, A.K. 1999. Functional characteristics and survival requirements of memory CD4+ T lymphocytes in vivo. *J Immunol* 162:766-773.
66. Brown, M.G., Dokun, A.O., Heusel, J.W., Smith, H.R., Beckman, D.L., Blattenberger, E.A., Dubbelde, C.E., Stone, L.R., Scalzo, A.A., and Yokoyama, W.M. 2001. Vital involvement of a natural killer cell activation receptor in resistance to viral infection. *Science* 292:934-937.
67. Iredale, J.P. 2001. Hepatic stellate cell behavior during resolution of liver injury. *Semin Liver Dis* 21:427-436.
68. Seeff, L.B., Hollinger, F.B., Alter, H.J., Wright, E.C., Cain, C.M., Buskell, Z.J., Ishak, K.G., Iber, F.L., Toro, D., Samanta, A., et al. 2001. Long-term mortality and morbidity of transfusion-associated non-A, non-B, and type C hepatitis: A National Heart, Lung, and Blood Institute collaborative study. *Hepatology* 33:455-463.
69. Kim, A.Y., and Chung, R.T. 2009. Coinfection with HIV-1 and HCV--a one-two punch. *Gastroenterology* 137:795-814.
70. Pascual-Pareja, J.F., Caminoa, A., Larrauri, C., Gonzalez-Garcia, J., Montes, M.L., Diez, J., Grande, M., and Arribas, J.R. 2009. HAART is associated with lower hepatic necroinflammatory activity in HIV-hepatitis C virus-coinfected patients with CD4 cell count of more than 350 cells/microl at the time of liver biopsy. *AIDS* 23:971-975.
71. Wyatt, C.M., Malvestutto, C., Coca, S.G., Klotman, P.E., and Parikh, C.R. 2008. The impact of hepatitis C virus coinfection on HIV-related kidney disease: a systematic review and meta-analysis. *AIDS* 22:1799-1807.
72. Fischer, M.J., Wyatt, C.M., Gordon, K., Gibert, C.L., Brown, S.T., Rimland, D., Rodriguez-Barradas, M.C., Justice, A.C., Parikh, C.R., and Team, V.P. 2010. Hepatitis C and the risk of kidney disease and mortality in veterans with HIV. *J Acquir Immune Defic Syndr* 53:222-226.
73. Bedimo, R., Westfall, A.O., Mugavero, M., Drechsler, H., Khanna, N., and Saag, M. 2010. Hepatitis C virus coinfection and the risk of cardiovascular disease among HIV-infected patients. *HIV Med* 11:462-468.
74. Letendre, S., Paulino, A.D., Rockenstein, E., Adame, A., Crews, L., Cherner, M., Heaton, R., Ellis, R., Everall, I.P., Grant, I., et al. 2007. Pathogenesis of hepatitis C virus coinfection in the brains of patients infected with HIV. *J Infect Dis* 196:361-370.
75. Aronow, H.A., Weston, A.J., Pezeshki, B.B., and Lazarus, T.S. 2008. Effects of coinfection with HIV and hepatitis C virus on the nervous system. *AIDS Read* 18:43-48.
76. Hinkin, C.H., Castellon, S.A., Levine, A.J., Barclay, T.R., and Singer, E.J. 2008. Neurocognition in individuals co-infected with HIV and hepatitis C. *J Addict Dis* 27:11-17.
77. Graham, C.S., Baden, L.R., Yu, E., Mrus, J.M., Carnie, J., Heeren, T., and Koziel, M.J. 2001. Influence of human immunodeficiency virus infection

on the course of hepatitis C virus infection: a meta-analysis. *Clin Infect Dis* 33:562-569.
78. Schuppan, D., and Afdhal, N.H. 2008. Liver cirrhosis. *Lancet* 371:838-851.
79. Hernandez-Gea, V., and Friedman, S.L. 2011. Pathogenesis of liver fibrosis. *Annu Rev Pathol* 6:425-456.
80. Poynard, T., Bedossa, P., and Opolon, P. 1997. Natural history of liver fibrosis progression in patients with chronic hepatitis C. The OBSVIRC, METAVIR, CLINIVIR, and DOSVIRC groups. *Lancet* 349:825-832.
81. Bellentani, S., Pozzato, G., Saccoccio, G., Crovatto, M., Croce, L.S., Mazzoran, L., Masutti, F., Cristianini, G., and Tiribelli, C. 1999. Clinical course and risk factors of hepatitis C virus related liver disease in the general population: report from the Dionysos study. *Gut* 44:874-880.
82. Farrell, G.C., and Larter, C.Z. 2006. Nonalcoholic fatty liver disease: from steatosis to cirrhosis. *Hepatology* 43:S99-S112.
83. Friedman, S.L. 2008. Mechanisms of hepatic fibrogenesis. *Gastroenterology* 134:1655-1669.
84. Lin, W., Tsai, W.L., Shao, R.X., Wu, G., Peng, L.F., Barlow, L.L., Chung, W.J., Zhang, L., Zhao, H., Jang, J.Y., et al. 2010. Hepatitis C virus regulates transforming growth factor beta1 production through the generation of reactive oxygen species in a nuclear factor kappaB-dependent manner. *Gastroenterology* 138:2509-2518, 2518 e2501.
85. Choi, J. 2012. Oxidative stress, endogenous antioxidants, alcohol, and hepatitis C: pathogenic interactions and therapeutic considerations. *Free Radic Biol Med* 52:1135-1150.
86. Lin, W., Wu, G., Li, S., Weinberg, E.M., Kumthip, K., Peng, L.F., Mendez-Navarro, J., Chen, W.C., Jilg, N., Zhao, H., et al. 2011. HIV and HCV cooperatively promote hepatic fibrogenesis via induction of reactive oxygen species and NFkappaB. *J Biol Chem* 286:2665-2674.
87. Bruno, R., Galastri, S., Sacchi, P., Cima, S., Caligiuri, A., DeFranco, R., Milani, S., Gessani, S., Fantuzzi, L., Liotta, F., et al. 2010. gp120 modulates the biology of human hepatic stellate cells: a link between HIV infection and liver fibrogenesis. *Gut* 59:513-520.
88. Hong, F., Tuyama, A., Lee, T.F., Loke, J., Agarwal, R., Cheng, X., Garg, A., Fiel, M.I., Schwartz, M., Walewski, J., et al. 2009. Hepatic stellate cells express functional CXCR4: role in stromal cell-derived factor-1alpha-mediated stellate cell activation. *Hepatology* 49:2055-2067.
89. Rotman, Y., and Liang, T.J. 2009. Coinfection with hepatitis C virus and human immunodeficiency virus: virological, immunological, and clinical outcomes. *J Virol* 83:7366-7374.
90. Lin, W., Weinberg, E.M., Tai, A.W., Peng, L.F., Brockman, M.A., Kim, K.A., Kim, S.S., Borges, C.B., Shao, R.X., and Chung, R.T. 2008. HIV increases HCV replication in a TGF-beta1-dependent manner. *Gastroenterology* 134:803-811.
91. Jang, J.Y., Shao, R.X., Lin, W., Weinberg, E., Chung, W.J., Tsai, W.L., Zhao, H., Goto, K., Zhang, L., Mendez-Navarro, J., et al. 2011. HIV

infection increases HCV-induced hepatocyte apoptosis. *J Hepatol* 54:612-620.

92. Laurent-Crawford, A.G., Krust, B., Riviere, Y., Desgranges, C., Muller, S., Kieny, M.P., Dauguet, C., and Hovanessian, A.G. 1993. Membrane expression of HIV envelope glycoproteins triggers apoptosis in CD4 cells. *AIDS Res Hum Retroviruses* 9:761-773.
93. Estaquier, J., Idziorek, T., de Bels, F., Barre-Sinoussi, F., Hurtrel, B., Aubertin, A.M., Venet, A., Mehtali, M., Muchmore, E., Michel, P., et al. 1994. Programmed cell death and AIDS: significance of T-cell apoptosis in pathogenic and nonpathogenic primate lentiviral infections. *Proc Natl Acad Sci U S A* 91:9431-9435.
94. Finkel, T.H., Tudor-Williams, G., Banda, N.K., Cotton, M.F., Curiel, T., Monks, C., Baba, T.W., Ruprecht, R.M., and Kupfer, A. 1995. Apoptosis occurs predominantly in bystander cells and not in productively infected cells of HIV- and SIV-infected lymph nodes. *Nat Med* 1:129-134.
95. Biard-Piechaczyk, M., Robert-Hebmann, V., Roland, J., Coudronniere, N., and Devaux, C. 1999. Role of CXCR4 in HIV-1-induced apoptosis of cells with a CD4+, CXCR4+ phenotype. *Immunol Lett* 70:1-3.
96. Fischer, R., Baumert, T., and Blum, H.E. 2007. Hepatitis C virus infection and apoptosis. *World J Gastroenterol* 13:4865-4872.
97. Zhu, H., Dong, H., Eksioglu, E., Hemming, A., Cao, M., Crawford, J.M., Nelson, D.R., and Liu, C. 2007. Hepatitis C virus triggers apoptosis of a newly developed hepatoma cell line through antiviral defense system. *Gastroenterology* 133:1649-1659.
98. Lan, L., Gorke, S., Rau, S.J., Zeisel, M.B., Hildt, E., Himmelsbach, K., Carvajal-Yepes, M., Huber, R., Wakita, T., Schmitt-Graeff, A., et al. 2008. Hepatitis C virus infection sensitizes human hepatocytes to TRAIL-induced apoptosis in a caspase 9-dependent manner. *J Immunol* 181:4926-4935.
99. Brenchley, J.M., Price, D.A., Schacker, T.W., Asher, T.E., Silvestri, G., Rao, S., Kazzaz, Z., Bornstein, E., Lambotte, O., Altmann, D., et al. 2006. Microbial translocation is a cause of systemic immune activation in chronic HIV infection. *Nat Med* 12:1365-1371.
100. Seki, E., De Minicis, S., Osterreicher, C.H., Kluwe, J., Osawa, Y., Brenner, D.A., and Schwabe, R.F. 2007. TLR4 enhances TGF-beta signaling and hepatic fibrosis. *Nat Med* 13:1324-1332.
101. Balagopal, A., Philp, F.H., Astemborski, J., Block, T.M., Mehta, A., Long, R., Kirk, G.D., Mehta, S.H., Cox, A.L., Thomas, D.L., et al. 2008. Human immunodeficiency virus-related microbial translocation and progression of hepatitis C. *Gastroenterology* 135:226-233.
102. Bedossa, P., Dargere, D., and Paradis, V. 2003. Sampling variability of liver fibrosis in chronic hepatitis C. *Hepatology* 38:1449-1457.
103. Ratziu, V., Charlotte, F., Heurtier, A., Gombert, S., Giral, P., Bruckert, E., Grimaldi, A., Capron, F., Poynard, T., and Group, L.S. 2005. Sampling variability of liver biopsy in nonalcoholic fatty liver disease. *Gastroenterology* 128:1898-1906.

104. Regev, A., Berho, M., Jeffers, L.J., Milikowski, C., Molina, E.G., Pyrsopoulos, N.T., Feng, Z.Z., Reddy, K.R., and Schiff, E.R. 2002. Sampling error and intraobserver variation in liver biopsy in patients with chronic HCV infection. *Am J Gastroenterol* 97:2614-2618.
105. Bravo, A.A., Sheth, S.G., and Chopra, S. 2001. Liver biopsy. *N Engl J Med* 344:495-500.
106. Smith, J.O., and Sterling, R.K. 2009. Systematic review: non-invasive methods of fibrosis analysis in chronic hepatitis C. *Aliment Pharmacol Ther* 30:557-576.
107. Curry, M.P. 2013. HIV and hepatitis C virus: special concerns for patients with cirrhosis. *J Infect Dis* 207 Suppl 1:S40-44.
108. Cales, P., Halfon, P., Batisse, D., Carrat, F., Perre, P., Penaranda, G., Guyader, D., d'Alteroche, L., Fouchard-Hubert, I., Michelet, C., et al. 2010. Comparison of liver fibrosis blood tests developed for HCV with new specific tests in HIV/HCV co-infection. *J Hepatol* 53:238-244.
109. Afdhal, N.H. 2012. Fibroscan (transient elastography) for the measurement of liver fibrosis. *Gastroenterol Hepatol (N Y)* 8:605-607.
110. Friedrich-Rust, M., Ong, M.F., Martens, S., Sarrazin, C., Bojunga, J., Zeuzem, S., and Herrmann, E. 2008. Performance of transient elastography for the staging of liver fibrosis: a meta-analysis. *Gastroenterology* 134:960-974.
111. Jacobs, J.M., Adkins, J.N., Qian, W.J., Liu, T., Shen, Y., Camp, D.G., 2nd, and Smith, R.D. 2005. Utilizing human blood plasma for proteomic biomarker discovery. *J Proteome Res* 4:1073-1085.
112. Van Duyne, R., Guendel, I., Kehn-Hall, K., Easley, R., Klase, Z., Liu, C., Young, M., and Kashanchi, F. 2010. The identification of unique serum proteins of HIV-1 latently infected long-term non-progressor patients. *AIDS Res Ther* 7:21.
113. Issaq, H.J., Veenstra, T.D., Conrads, T.P., and Felschow, D. 2002. The SELDI-TOF MS approach to proteomics: protein profiling and biomarker identification. *Biochem Biophys Res Commun* 292:587-592.
114. Xiao, Z., Prieto, D., Conrads, T.P., Veenstra, T.D., and Issaq, H.J. 2005. Proteomic patterns: their potential for disease diagnosis. *Mol Cell Endocrinol* 230:95-106.
115. McLerran, D., Grizzle, W.E., Feng, Z., Bigbee, W.L., Banez, L.L., Cazares, L.H., Chan, D.W., Diaz, J., Izbicka, E., Kagan, J., et al. 2008. Analytical validation of serum proteomic profiling for diagnosis of prostate cancer: sources of sample bias. *Clin Chem* 54:44-52.
116. Adam, B.L., Qu, Y., Davis, J.W., Ward, M.D., Clements, M.A., Cazares, L.H., Semmes, O.J., Schellhammer, P.F., Yasui, Y., Feng, Z., et al. 2002. Serum protein fingerprinting coupled with a pattern-matching algorithm distinguishes prostate cancer from benign prostate hyperplasia and healthy men. *Cancer Res* 62:3609-3614.
117. Petricoin, E.F., Ardekani, A.M., Hitt, B.A., Levine, P.J., Fusaro, V.A., Steinberg, S.M., Mills, G.B., Simone, C., Fishman, D.A., Kohn, E.C., et al. 2002. Use of proteomic patterns in serum to identify ovarian cancer. *Lancet* 359:572-577.

118. Yip, T.T., Chan, J.W., Cho, W.C., Wang, Z., Kwan, T.L., Law, S.C., Tsang, D.N., Chan, J.K., Lee, K.C., Cheng, W.W., et al. 2005. Protein chip array profiling analysis in patients with severe acute respiratory syndrome identified serum amyloid a protein as a biomarker potentially useful in monitoring the extent of pneumonia. *Clin Chem* 51:47-55.
119. Ndao, M., Spithill, T.W., Caffrey, R., Li, H., Podust, V.N., Perichon, R., Santamaria, C., Ache, A., Duncan, M., Powell, M.R., et al. 2010. Identification of novel diagnostic serum biomarkers for Chagas' disease in asymptomatic subjects by mass spectrometric profiling. *J Clin Microbiol* 48:1139-1149.
120. Papadopoulos, M.C., Abel, P.M., Agranoff, D., Stich, A., Tarelli, E., Bell, B.A., Planche, T., Loosemore, A., Saadoun, S., Wilkins, P., et al. 2004. A novel and accurate diagnostic test for human African trypanosomiasis. *Lancet* 363:1358-1363.
121. Agranoff, D., Fernandez-Reyes, D., Papadopoulos, M.C., Rojas, S.A., Herbster, M., Loosemore, A., Tarelli, E., Sheldon, J., Schwenk, A., Pollok, R., et al. 2006. Identification of diagnostic markers for tuberculosis by proteomic fingerprinting of serum. *Lancet* 368:1012-1021.
122. Reddy, G., and Dalmasso, E.A. 2003. SELDI ProteinChip(R) Array Technology: Protein-Based Predictive Medicine and Drug Discovery Applications. *J Biomed Biotechnol* 2003:237-241.
123. Aebersold, R., and Mann, M. 2003. Mass spectrometry-based proteomics. *Nature* 422:198-207.
124. Kiehntopf, M., Siegmund, R., and Deufel, T. 2007. Use of SELDI-TOF mass spectrometry for identification of new biomarkers: potential and limitations. *Clin Chem Lab Med* 45:1435-1449.
125. R, M. 2007. *Mass spectromety data nalysis in proteomics*: Humanan Press.
126. W.C. Wiley, I.H.M. 1955. *Time-of-Flight Mass Spectrometer with Improved Resolution*.
127. Reiner Westermeier, T.N., Hans-Rudolf Hopker. 2008. *Proteomics in Practice; A Guide to Successful Experimental Design*.
128. 2004. *Ciphergen Express Software 3.0 Operational Manual* Ciphergen Biosystems INC.
129. Muller, R., and Mockel, M. 2008. Logistic regression and CART in the analysis of multimarker studies. *Clin Chim Acta* 394:1-6.
130. Lemon, S.C., Roy, J., Clark, M.A., Friedmann, P.D., and Rakowski, W. 2003. Classification and regression tree analysis in public health: methodological review and comparison with logistic regression. *Ann Behav Med* 26:172-181.
131. Ndao, M., Rainczuk, A., Rioux, M.C., Spithill, T.W., and Ward, B.J. 2010. Is SELDI-TOF a valid tool for diagnostic biomarkers? *Trends Parasitol* 26:561-567.
132. Klein, M.B., Saeed, S., Yang, H., Cohen, J., Conway, B., Cooper, C., Cote, P., Cox, J., Gill, J., Haase, D., et al. 2010. Cohort profile: the Canadian HIV-hepatitis C co-infection cohort study. *Int J Epidemiol* 39:1162-1169.

133. Murphy, D.G., Cote, L., Fauvel, M., Rene, P., and Vincelette, J. 2000. Multicenter comparison of Roche COBAS AMPLICOR MONITOR version 1.5, Organon Teknika NucliSens QT with Extractor, and Bayer Quantiplex version 3.0 for quantification of human immunodeficiency virus type 1 RNA in plasma. *J Clin Microbiol* 38:4034-4041.
134. Wai, C.T., Greenson, J.K., Fontana, R.J., Kalbfleisch, J.D., Marrero, J.A., Conjeevaram, H.S., and Lok, A.S. 2003. A simple noninvasive index can predict both significant fibrosis and cirrhosis in patients with chronic hepatitis C. *Hepatology* 38:518-526.
135. Highleyman, L. 2007. New approaches to HIV prevention. *BETA* 19:29-38.
136. Operskalski, E.A., and Kovacs, A. 2011. HIV/HCV co-infection: pathogenesis, clinical complications, treatment, and new therapeutic technologies. *Curr HIV/AIDS Rep* 8:12-22.
137. Kim, J., Kim, S.H., Lee, S.U., Ha, G.H., Kang, D.G., Ha, N.Y., Ahn, J.S., Cho, H.Y., Kang, S.J., Lee, Y.J., et al. 2002. Proteome analysis of human liver tumor tissue by two-dimensional gel electrophoresis and matrix assisted laser desorption/ionization-mass spectrometry for identification of disease-related proteins. *Electrophoresis* 23:4142-4156.
138. Comunale, M.A., Mattu, T.S., Lowman, M.A., Evans, A.A., London, W.T., Semmes, O.J., Ward, M., Drake, R., Romano, P.R., Steel, L.F., et al. 2004. Comparative proteomic analysis of de-N-glycosylated serum from hepatitis B carriers reveals polypeptides that correlate with disease status. *Proteomics* 4:826-838.
139. Schwegler, E.E., Cazares, L., Steel, L.F., Adam, B.L., Johnson, D.A., Semmes, O.J., Block, T.M., Marrero, J.A., and Drake, R.R. 2005. SELDI-TOF MS profiling of serum for detection of the progression of chronic hepatitis C to hepatocellular carcinoma. *Hepatology* 41:634-642.
140. Poon, T.C., Yip, T.T., Chan, A.T., Yip, C., Yip, V., Mok, T.S., Lee, C.C., Leung, T.W., Ho, S.K., and Johnson, P.J. 2003. Comprehensive proteomic profiling identifies serum proteomic signatures for detection of hepatocellular carcinoma and its subtypes. *Clin Chem* 49:752-760.
141. Soto, B., Sanchez-Quijano, A., Rodrigo, L., del Olmo, J.A., Garcia-Bengoechea, M., Hernandez-Quero, J., Rey, C., Abad, M.A., Rodriguez, M., Sales Gilabert, M., et al. 1997. Human immunodeficiency virus infection modifies the natural history of chronic parenterally-acquired hepatitis C with an unusually rapid progression to cirrhosis. *J Hepatol* 26:1-5.
142. Paradis, V., Mathurin, P., Ratziu, V., Poynard, T., and Bedossa, P. 1996. Binding of apolipoprotein A-I and acetaldehyde-modified apolipoprotein A-I to liver extracellular matrix. *Hepatology* 23:1232-1238.
143. Poynard, T., Aubert, A., Bedossa, P., Abella, A., Naveau, S., Paraf, F., and Chaput, J.C. 1991. A simple biological index for detection of alcoholic liver disease in drinkers. *Gastroenterology* 100:1397-1402.
144. Louagie, H.K., Brouwer, J.T., Delanghe, J.R., De Buyzere, M.L., and Leroux-Roels, G.G. 1996. Haptoglobin polymorphism and chronic hepatitis C. *J Hepatol* 25:10-14.

145. Edwards, A.M., Lucas, C.M., and Baddams, H.M. 1987. Modulation of gamma-glutamyltranspeptidase in normal rat hepatocytes in culture by cell density, epidermal growth factor and agents which alter cell differentiation. *Carcinogenesis* 8:1837-1842.
146. Sadrzadeh, S.M., and Bozorgmehr, J. 2004. Haptoglobin phenotypes in health and disorders. *Am J Clin Pathol* 121 Suppl:S97-104.
147. Bezerra, J.A., Bugge, T.H., Melin-Aldana, H., Sabla, G., Kombrinck, K.W., Witte, D.P., and Degen, J.L. 1999. Plasminogen deficiency leads to impaired remodeling after a toxic injury to the liver. *Proc Natl Acad Sci U S A* 96:15143-15148.
148. Roche, S., Tiers, L., Provansal, M., Piva, M.T., and Lehmann, S. 2006. Interest of major serum protein removal for Surface-Enhanced Laser Desorption/Ionization - Time Of Flight (SELDI-TOF) proteomic blood profiling. *Proteome Sci* 4:20.
149. Liang, C., Tan, G.S., and Chung, M.C. 2012. 2D DIGE analysis of serum after fractionation by ProteoMiner beads. *Methods Mol Biol* 854:181-194.
150. Kamat, A., Misra, V., Cassol, E., Ancuta, P., Yan, Z., Li, C., Morgello, S., and Gabuzda, D. 2012. A plasma biomarker signature of immune activation in HIV patients on antiretroviral therapy. *PLoS One* 7:e30881.
151. Zeng, M., Smith, A.J., Wietgrefe, S.W., Southern, P.J., Schacker, T.W., Reilly, C.S., Estes, J.D., Burton, G.F., Silvestri, G., Lifson, J.D., et al. 2011. Cumulative mechanisms of lymphoid tissue fibrosis and T cell depletion in HIV-1 and SIV infections. *J Clin Invest* 121:998-1008.
152. Weber, S.N., and Lammert, F. 2011. Genetics of liver injury and fibrosis. *Alcohol Clin Exp Res* 35:800-803.
153. Henrick, B.M., Nag, K., Yao, X.D., Drannik, A.G., Aldrovandi, G.M., and Rosenthal, K.L. 2012. Milk matters: soluble Toll-like receptor 2 (sTLR2) in breast milk significantly inhibits HIV-1 infection and inflammation. *PLoS One* 7:e40138.
154. Sulkowski, M.S., Mehta, S.H., Torbenson, M.S., Higgins, Y., Brinkley, S.C., de Oca, R.M., Moore, R.D., Afdhal, N.H., and Thomas, D.L. 2007. Rapid fibrosis progression among HIV/hepatitis C virus-co-infected adults. *AIDS* 21:2209-2216.
155. Macias, J., Berenguer, J., Japon, M.A., Giron, J.A., Rivero, A., Lopez-Cortes, L.F., Moreno, A., Gonzalez-Serrano, M., Iribarren, J.A., Ortega, E., et al. 2009. Fast fibrosis progression between repeated liver biopsies in patients coinfected with human immunodeficiency virus/hepatitis C virus. *Hepatology* 50:1056-1063.
156. Hulse, G.K., English, D.R., Milne, E., and Holman, C.D. 1999. The quantification of mortality resulting from the regular use of illicit opiates. *Addiction* 94:221-229.
157. Cox, A.L., Netski, D.M., Mosbruger, T., Sherman, S.G., Strathdee, S., Ompad, D., Vlahov, D., Chien, D., Shyamala, V., Ray, S.C., et al. 2005. Prospective evaluation of community-acquired acute-phase hepatitis C virus infection. *Clin Infect Dis* 40:951-958.
158. Stoove, M.A., Dietze, P.M., Aitken, C.K., and Jolley, D. 2008. Mortality among injecting drug users in Melbourne: a 16-year follow-up of the

Victorian Injecting Cohort Study (VICS). *Drug Alcohol Depend* 96:281-285.
159. Grady, B., van den Berg, C., van der Helm, J., Schinkel, J., Coutinho, R., Krol, A., and Prins, M. 2011. No impact of hepatitis C virus infection on mortality among drug users during the first decade after seroconversion. *Clin Gastroenterol Hepatol* 9:786-792 e781.
160. Lauer, G.M., Barnes, E., Lucas, M., Timm, J., Ouchi, K., Kim, A.Y., Day, C.L., Robbins, G.K., Casson, D.R., Reiser, M., et al. 2004. High resolution analysis of cellular immune responses in resolved and persistent hepatitis C virus infection. *Gastroenterology* 127:924-936.
161. Wedemeyer, H., He, X.S., Nascimbeni, M., Davis, A.R., Greenberg, H.B., Hoofnagle, J.H., Liang, T.J., Alter, H., and Rehermann, B. 2002. Impaired effector function of hepatitis C virus-specific CD8+ T cells in chronic hepatitis C virus infection. *J Immunol* 169:3447-3458.
162. Mavilio, D., Lombardo, G., Benjamin, J., Kim, D., Follman, D., Marcenaro, E., O'Shea, M.A., Kinter, A., Kovacs, C., Moretta, A., et al. 2005. Characterization of CD56-/CD16+ natural killer (NK) cells: a highly dysfunctional NK subset expanded in HIV-infected viremic individuals. *Proc Natl Acad Sci U S A* 102:2886-2891.
163. Tarazona, R., Casado, J.G., Delarosa, O., Torre-Cisneros, J., Villanueva, J.L., Sanchez, B., Galiani, M.D., Gonzalez, R., Solana, R., and Pena, J. 2002. Selective depletion of CD56(dim) NK cell subsets and maintenance of CD56(bright) NK cells in treatment-naive HIV-1-seropositive individuals. *J Clin Immunol* 22:176-183.
164. Durante-Mangoni, E., Wang, R., Shaulov, A., He, Q., Nasser, I., Afdhal, N., Koziel, M.J., and Exley, M.A. 2004. Hepatic CD1d expression in hepatitis C virus infection and recognition by resident proinflammatory CD1d-reactive T cells. *J Immunol* 173:2159-2166.
165. Lanier, L.L. 2005. NK cell recognition. *Annu Rev Immunol* 23:225-274.
166. Sun, J.C., Beilke, J.N., and Lanier, L.L. 2009. Adaptive immune features of natural killer cells. *Nature* 457:557-561.
167. Qu, J., Zhang, Q., Li, Y., Liu, W., Chen, L., Zhu, Y., and Wu, J. 2012. The Tat protein of human immunodeficiency virus-1 enhances hepatitis C virus replication through interferon gamma-inducible protein-10. *BMC Immunol* 13:15.
168. Zhang, X., Daucher, M., Baeza, J., Kim, C.W., Russell, R., and Kottilil, S. 2012. Human immunodeficiency virus enhances hepatitis C virus replication by differential regulation of IFN and TGF family genes. *J Med Virol* 84:1344-1352.

Annex I: Natural Killer cells from HIV infected slow progressors who carry the protective HLA-B*27 allele and inhibitory KIR3DL1 receptors have elevated poly-functional potential compared to Bw6 homozygotes.

1. Preface

Natural Killer (NK) cells are a subset of lymphoid cells and are mediators of the innate immune defense against viruses and tumors cells. NK cells have the ability to spontaneously kill tumor and virally infected target cells *in vitro*. Several studies have correlated the frequency of NK cells or NK cell activity to reduced susceptibility of certain individuals to HIV-1 infection and with the control of initial plasma viremia in the simian immunodeficiency virus model. Epidemiological studies have implicated the carriage of certain combined genotypes of the Killer Immunoglobulin-like Receptor (KIR) KIR3DL1 locus and the Major Histocompatibility Complex (MHC) HLA-B locus with slower progression to AIDS and lower viral load. Dr Bernard's lab is interested in the interaction between the NK cell receptors KIRs and their ligand. One research project is to assess the KIR/HLA combinations and their correlation with HIV-1 protection. To investigate the subject Dr Bernard has access to a cohort of HIV-1 infected Slow Progressors. We were able to show that *HLA-B*27* had a higher impact on educating NK cells for functional potential than most other *Bw4* or *Bw6* alleles, as was shown for *HLA-B*57*.

2-Introduction

NK cells are a key component of the innate immune system, which can act early in defences against virally infected and tumor cells (1-3). They have the capacity to secrete proinflammatory cytokines and lyse their targets without prior antigen sensitization (4). They are also involved in regulation of the adaptive immune response through their interaction with dendritic cells (DCs)(5, 6).

Activation of NK cells is regulated through the integration of signals from a number of activating and inhibitory receptors(7). Many of the inhibitory receptors use major histocompatibility complex (MHC) class I or class I-like proteins as their ligands(7). The interaction between inhibitory NK receptors and their ligands during NK cell development is important in educating these cells for subsequent function and for avoiding reactivity to normal cells expressing self MHC class I (8, 9). In humans one large family of NK receptors are encoded by the Killer Immunoglobulin-like Receptors (KIR) region that maps to chromosome 19q13.4 (7). The most polymorphic locus among the KIR region genes is *KIR3DL1*, which encodes both inhibitory KIR3DL1 (3DL1) and activating KIR3DS1 (3DS1) alleles (10). *3DL1* alleles can be further classified according to their expression levels on the cell surface into high (**h*), low/intermediate (**l*) and null (**004*) (not cell surface expressed) alleles (10-13). Genotypes homozygous for 3DL1 can be divided into 2 groups: **h/*y*, where **y* can be either another **h* allele or **004* with no **l* alleles, and **l/*x*, where **x* can be an **l*, **x* or **004* allele (14). 3DL1 receptors recognize a subset of MHC class I HLA-B molecules known as Bw4 alleles. HLA-Bw4 differ from the remaining HLA-Bw6 alleles at this locus, which do not interact with 3DL1, in the amino acids present between

positions 77 and 83 of the HLA heavy chain (9). Bw4 allotypes with isoleucine at position 80 (Bw4*80I) have been reported to be better ligands for many of the 3DL1 alleles (15). However, there is evidence that Bw4 alleles with threonine at position 80 (Bw4*80T), particularly HLA-B*2705, interact strongly with certain 3DL1 alleles (16).

Epidemiological studies have reported that several *KIR/HLA* combinations are associated with slower progression to AIDS and suppression of viral load (VL) (14). Compared to *Bw6* homozygotes (hmz) the *3DL1/HLA-B* combination having the most potent influence on slowing time to AIDS and VL control is *3DL1*h/*y* with *HLA-B*57* (**h/*y+B*57*)(14). Previous work from our group showed that NK cells from individuals carrying this genotype combination demonstrated higher functional potential than those from carriers of either the NK receptor genotype or *HLA-B*57* alone or from *Bw6 hmz* (17). In these studies functional potential was defined as the percent contribution of NK cells secreting interferon-γ (IFNγ) and tumor necrosis factor-α (TNF-α) and expressing CD107a, a marker of degranulation to the total response to stimulation with the HLA devoid K562 cell line. Furthermore, NK cells from carriers of **h/*y+B*57* had higher functional potential than carriers of *3DL1*h/*y* with other *Bw4* alleles(17). HLA-B*57 is an HLA allele considered to be protective in the context of HIV infection(18-21). While the protective effect conferred by HLA-B*57 is mediated at least in part through $CD8^+$ T cell recognition of HIV epitopes restricted by this allele, epidemiological studies and our results support the possibility that HLA-

B*57's protective effect may also be mediated through its ability to educate NK cells for superior functional potential (14, 20, 22-24).

Murine models have shown using single MHC class I transgenic mice that MHC class I alleles can differ from each other in the potency of their NK education signals, which directly translates into activation potency upon encountering cells lacking that MHC ligand (25). Since NK cells from **h/*y+B*57* carriers had higher functional potential than carriers of *3DL1*h/*y* with other *Bw4* alleles, HLA-B*57 may be an example in humans of an MHC class I allele with an NK education potency that is superior to that of most other HLA-Bw4 alleles. HLA-B*27 is another allele considered to be protective in the context of HIV infection (26-29). Like HLA-B*57, its protective effect is mediated at least in part through immune pressure exerted by $CD8^+$ T cells (30-33). In this report we questioned whether HLA-B*27, like HLA-B*57, could also act as a ligand for 3DL1 NK receptors that was superior to other HLA-Bw4 alleles in terms of its ability to educate NK cells for functional potential. *HLA-B*27* is found at a higher frequency among the approximately 5% of HIV infected individuals that we have classified as Slow Progressors (SP) compared with HIV infected individuals exhibiting a typical rate of disease progression or uninfected subjects (18, 21) SP are defined by either exhibiting spontaneous control of viremia or maintaining CD4 counts >400 cells/mm3 for at least 7 years (34, 35). In order to determine whether HLA-B*27, like HLA-B*57, could educate NK cells from *3DL1* hmz individuals for superior functional potential we compared the functional potential of NK cells from *3DL1 hmz+B*27* (*3DL1+B*27*) carriers with that from *3DL1*

hmz who were Bw6 hmz (*3DL1+Bw6*) or who expressed at least 1 Bw4 allele other than B*57 or B*27 (*3DL1+Bw4*). NK cells from *3DL1+B*27* carriers had a significantly higher functional potential than those from *3DL1+Bw6*. When the functional potential of NK cells from carriers of the 3DL1 NK receptor /HLA-B ligand pairs *h/*y+B*57, 3DL1+B*27 and 3DL1+Bw4 were compared we observed decreasing levels in the functional potential where NK cells responded to missing self with a *h/*y+B*57 > 3DL1+B*27 > 3DL1+Bw4 hierarchy.

3-Materials and Methods

3.1 Study population

A total of 51 HIV-infected SP were studied. Forty four were from the Canadian Cohort of HIV Infected Slow Progressors and 7 were from a cohort followed at the National Institutes of Allergy and Infectious Diseases (NIAID) (36). The term SP was used here to define treatment naïve HIV infected subjects who maintained absolute CD4 counts above 400 cells/mm^3 for more than 7 years or who were followed for at least 1 year with VL <3000 copies/ml of plasma. Information on CD4 and CD8 T cell counts VL and duration of infection at time of testing, 3DL1 genotype and HLA-B allotype of the study population is provided in Table 1. All individuals in the study populations are *3DL1 hmz* to eliminate the possible confounding effect on NK function of expressing the activating 3DS1 receptor, which is an allele at this locus (11, 14, 37). The study population is classified into 4 groups: group 1 (n=12) carry the *3DL1+B*27* genotype, group 2 (n=13) are

3DL1+Bw4, group 3 (n=14) are *3DL1+Bw6* and group 4 (n=12) are **h/*y+B*57*. Informed consent was obtained from all study subjects and research conformed to the ethical guidelines of the authors' institutions.

3.2 MHC and KIR typing

All subjects were typed for MHC class I alleles by sequence-based typing using kits from Atria Genetics (South San Francisco, CA) and Assign software to interpret sequence information for allele typing (Conexio Genetics, Perth, Australia) as previously described (17). *HLA-Bw6 hmz* subjects lacked any HLA-Bw4 alleles at the *HLA-A* or *B* locus. *3DL1/S1* genotyping was performed using two sets of primers specific for the *3DL1* and *3DS1* alleles at the 3DL1 locus as previously described (37). Subjects were subsequently *3DL1* allotyped by identifying single nucleotide polymorphisms (SNP) corresponding to high frequency *3DL1* alleles as previously described (17). In our study we categorized *3DL1*005, *006, *007, *053, *054* as **l* alleles, *3DL1*001, *002, *008, *009, *015, *020* as **h* alleles and **004* as a null allele.

Subjects ID	gender [1]	Age [2]	Time infected [2]	Group [3]	*HLA-B1*	*HLA-B2*	*KIR* genotype [4]	CD4 [5]	CD8 [5]	VL [6]
1001	M	59	2.9	1	B15:01	B27:05	*h/*y	760	900	1.7
1002	M	59	14.6	1	B15:01	B27:05	*h/*y	788	2498	4.12
1003	M	61	23.5	1	B27:02	B67:01	*h/*y	670	1050	4.7
1004	M	49	20.2	1a	B27:05	B57:01	*h/*y	830	1700	3.91
1005	M	37	2.5	1	B27:05	B40:02	*h/*y	1040	1090	1.7
1006	M	40	3.7	1	B14:02	B27:05	*h/*y	820	570	1.7

1007	M	71	5.2	1	B27:03	B51:01	*l/*x	590	114	1.7
1008	F	31	1.2	1a	B27:05	B57:01	*l/*x	489	672	1.7
1009	F	59	13.2	1	B27:03	B49:01	*l/*x	692	627	1.7
1010	M	38	2.3	1	B15:01	B27:05	*l/*x	396	936	1.7
1011	M	63	25.0	1	B27:05	B51:01	*h/*y	340	748	1.7
1012	M	41	6.4	1	B07:02	B27:05	3DL1 hmz	710	970	3.25
2001	M	35	6.5	2	B15:02	B51:02	*l/*x	500	NA	3.24
2002	F	36	15.9	2	B49:01	B58:02	*h/*y	270	510	3.35
2003	M	15	8.0	2	B38:01	B51:01	*h/*y	596	1614	2.08
2004	M	45	16.2	2	B07:02	B51:01	*h/*y	440	350	3.54
2005	F	46	14.7	2	B07:02	B38:01	*l/*x	720	720	1.7
2006	M	47	17.0	2	B39:01	B35:01	*h/*y	546	572	5.21
2007	M	46	0.5	2	B53:01	B58:01	*l/*x	870	550	1.7
2008	M	49	7.3	2	B44:03	B53:01	*l/*x	360	1610	2.8
2009	F	40	2.8	2	B07:02	B13:01	*h/*y	1487	712	3.76
2010	F	50	6.9	2	B15:03	B44:02	*h/*y	590	1650	3.73
2011	F	44	22.2	2	B44:02	B52:02	*h/*y	420	1180	3.15
2012	F	32	5.1	2	B14:02	B44:03	*l/*x	715	384	1.7
2013	F	36	6.3	2	B49:01	B53:01	*h/*y	535	793	2.43
3001	M	34	3.0	3	B07:02	B14:02	*l/*x	680	890	2.85
3002	M	40	14.4	3	B14:02	B15:01	*h/*y	343	804	1.7
3003	M	40	4.7	3	B14:02	B14:02	*h/*y	350	730	3.41
3004	M	40	3.4	3	B07:02	B07:02	*h/*y	985	605	3.3
3005	M	46	5.6	3	B15:10	B41:01	*l/*x	530	390	1.7
3006	F	42	4.0	3	B07:05	B35:01	*l/*x	919	1557	1.7
3007	F	57	3.1	3	B07:02	B42:01	*l/*x	636	663	1.7
3008	M	53	4.1	3	B07:02	B14:02	*h/*y	447	455	3.3
3009	M	29	4.2	3	B07:02	B14:02	3DL1 hmz	516	788	2.89
3010	F	61	14.3	3	B07:02	B18:01	*l/*x	810	1050	1.7
3011	F	39	6.6	3	B42:01	B45:01	*h/*y	620	408	2.69
3012	M	39	9.9	3	B14:02	B40:06	*h/*y	720	1820	2.59
3013	M	46	7.0	3	B07:02	B07:05	3DL1 hmz	970	1210	1.94
3014	M	62	17.5	3	B14:01	B81:01	*h/*y	650	2110	4.46

4001	F	39	3.0	4	B57	B7	*h/*y	1443	895	1.7
4002	F	55	23.8	4	B57	B57	*h/*y	277	385	1.7
4003	M	58	20.5	4	B57	B15	*h/*y	883	590	1.7
4004	M	41	11.2	4	B40:01	B57:01	*h/*y	1200	860	1.7
4005	M	61	11.0	4	B40:02	B57:01	*h/*y	770	990	3.9
4006	M	45	14.9	4	B07:02	B57:01	*h/*y	650	1460	4.21
4007	F	39	2.6	4	B35:01	B57:01	*h/*y	530	NA	1.7
4008	M	24	2.0	4	B07:02	B57:01	*h/*y	680	880	3.1
4009	M	49	10.0	4	B57	B13	*h/*y	955	881	1.7
4010	M	58	18.0	4	B57	B44	*h/*y	1329	1243	1.7
4011	M	46	21.0	4	B57	B81	*h/*y	1362	1055	1.7
4012	M	36	7.0	4	B57	B52	*h/*y	780	739	1.7

Table 1. Study population characteristics. [1] M=male/ F=female, [2] in years, [3] 1= 3DL1+B*27; 2=3DL1+Bw4; 3=3DL1+Bw5; 4=*h/*y+B*57. The 2 subjects with the 1a designation carry both a B*27 and B*57 allele, [4] the individuals classified as 3DL1 hmz have not been allotyped for KIR3DL1 alleles, [5] cells/mm^3, [6] VL= $\log_{10}$ viral load copies/ml plasma.

3.3 Cells

Peripheral blood mononuclear cells (PBMC) were isolated by density gradient centrifugation (Ficoll-Paque Pharmacia Upsala, Sweden) from whole blood obtained by venipuncture into tubes containing EDTA anti-coagulant or by leukaphersis as previously described (38). Cells were cryopreserved in 10% DMSO (Sigma-Aldrich, St. Louis, MO) with 90% fetal bovine serum (FBS, Wisent, St. Bruno, Quebec, Canada).

3.3 NK cell functional potential

Cryopreserved PBMC were thawed and resuspended at 10^6 cells/ml in RPMI 1640 (Wisent) that contained 10% FBS (Wisent), 2mM L-glutamine and 50 IU penicillin and 50µg/ml streptomycin (Wisent). Brefeldin A (at 5µg/ml, Sigma-Aldrich), Monensin (at 6µg/ml, Golgi-Stop; BD Biosciences, Mississauga, Ontario, Canada) and anti-CD107a–FITC mAb (BD Biosciences) were added to the cells. One million PBMCs were stimulated with media alone or HLA devoid K562 cells (American Type Culture Collection Manassas, VA) at a PBMC to K562 cell ratio of 5:1 or with 1.25µg/ml phorbol 12-myristate 13-acetate (PMA); 0.25µg/ml ionomycin, (Sigma-Aldrich) as a positive control for 6 hours at 37ºC in a humidified 5% CO_2 incubator. All stimulation data shown is from cells that generated a positive result in the PMA and ionomycin stimulation condition.

Cells were stained for viability using the Aqua LIVE/DEAD® fixable dead cell stain kit (Invitrogen, Burlington, Ontario, Canada) following manufacturer's instructions. Cells were then stained for cell surface markers with anti-CD56-APC, anti-CD16-Pacific Blue (BD Biosciences), anti-CD3-ECD and CD158e-PE (ie: Z27-PE, Beckman Coulter, Mississauga, Ontario, Canada) for 30 min. After washing with phosphate buffered saline (PBS) containing 1% FBS (Wisent), cells were fixed and permeabilized using the Fix and Perm Kit (Invitrogen) and stained for intracellular cytokines using anti-IFN-γ-Alexa 700 and anti-TNF-α-PE-Cy7 (BD Biosciences). Cells were washed and fixed with 1% paraformaldehyde solution (Fisher Scientific, Ottawa Ontario, Canada) and kept in the dark at 4ºC until acquisition.

3.5 Flow cytometry analysis

Between 400,000 and 500,000 events were acquired per sample using an LSRII flow cytometer (BD Biosciences). Analysis for NK cell activation was performed using FlowJo software version 9.1 (Tree Star, San Carlos, CA). The functional profiles of stimulated NK cells were determined using a gating strategy where NK cells were defined as $CD3^{-}CD56^{+/-}CD16^{+/-}$. Boolean gating was used to identify seven NK cell functional profiles, i.e. tri-functional NK cells ($CD107a^{+}$ IFN-γ^{+} TNF-α^{+}), bi-functional NK cells (any combination of two of these functions) and mono-functional NK cells (any single one of these functions). All results for the frequency of individual functional subsets were background corrected by subtracting the frequency of positive NK cells in the unstimulated subset. Corrected results were used to generate the percent contribution of each functional subset to the total NK cells response to K562. Results reported as subset frequency or percent contribution of a subset to the total K562 response showed a high level of correlation with each other (17).

3.6 Statistical analysis

GraphPad Instat 3.05 and GraphPad Prism 5.04 were used for statistical analyses and graphical presentations. A Kruskal-Wallis test was used to assess the significance of between group differences in age, duration of infection at the time point tested, CD4 counts, CD8 counts and VL. Mann-Whitney *U* tests were used

to test the significance of between group differences in the percent contribution of an NK cell functional subset to the total NK cell response. A Spearman correlation test was used to test the significance of the trend towards declining tri-functional potential with 3DL1/HLA-B genotype combinations. A *p* value of <0.05 was considered significant.

4. Results

4.1 Study population

Table 2 provides information on the average and standard deviation for age, duration of infection, CD4 count, CD8 count and log_{10}VL at the time point tested for NK functional potential for SP classified as *3DL1+B*27*, *3DL1+Bw4*, *3DL1+Bw6* and **h/*y+B*57* described in Table 1. No between-group differences were seen for any of these parameters (Krukal-Wallis test).

	3DL1+B*27 **(n=12)**	***3DL1+Bw4*** **(n=13)**	***3DL1+Bw6*** **(n=14)**	****h/*y+B*57*** **(n=12)**
Age[1]	50.7 ± 12.8[3]	40.1 ± 9.5	44.9 ± 10.0	45.9 ± 11.0
Duration of infection[1]	10.1 ± 8.9	10.0 ± 6.5	7.2 ± 4.8	12.1 ± 7.6
CD4[2]	677 ± 198	619 ± 306	655 ± 211	904 ± 363
CD8[2]	989 ± 606	887 ± 494	963 ± 533	907 ± 292
Log_{10} VL	2.53 ± 1.2	2.95 ± 1.0	2.57 ± 0.86	2.21 ± 0.95

Table 2: Summary of study population characteristics. [1] In years, [2] Cells/mm^3, [3] Means ± standard deviation.

4.2 NK cells from *3DL1+B*27* carriers have a higher functional potential than those from *3DL1+Bw6*

To investigate whether NK cells from HIV-infected SPs carrying the *3DL1+B*27* genotype for an NK receptor/HLA-B ligand pair differ in their NK cell functional potential compared to *Bw6 hmz* with no ligand for 3DL1 receptors, we measured the frequency of NK cells expressing of CD107a and secreting of IFN-γ and TNF-α from K562-stimulated NK cells using eight colour multi-parametric flow cytometry. In this analysis CD107a expressing NK cells were the sum of the mono-, bi- and tri-functional functional subsets expressing CD107a. This was also the case for IFN-γ and TNF-α secreting NK cells. As shown in Figure 1A the median (range) frequency of NK cells from *3DL1+B*27* versus *3DL1+Bw6* carriers expressing CD107a was 6.92% (3.01%, 17.15%) versus 4.27% (0.74%, 13.32%), secreting IFN-γ was 8.91% (4.25%, 21.52%) versus 5.17% (0.55%, 25.92%) and secreting TNF-α was 0.92% (0.11%, 3.67%) versus 0.23% (0.01%, 3.06) ($p<0.05$ for all comparisons; Mann-Whitney test). Therefore, the frequency of NK cells with any of these functions was significantly greater when NK cells were from *3DL1+B*27* individuals than from *3DL1+Bw6*.

Since we simultaneously measured these three functions following K562 stimulation we were able to assess the frequency of seven possible NK cell functional profiles and their percent contribution to the total K562 response. Figure 1B shows the percent contribution of each NK cell functional profile in PBMC from 12 *3DL1+B*27* and 14 *3DL1+Bw6* subjects. Of the seven possible NK cell functional profiles, only the percent contribution of tri-functional NK cells to the total K562 response was significantly higher in the *3DL1+B*27* group versus *3DL1+Bw6* SPs (2.99% [0.00%, 6.43%]) and (0.52% [0.00%, 7.36%]) for *3DL1+B*27* positive and *3DL1+Bw6*, respectively, p=0.019; Mann-Whitney *U* test). Based on these results we concentrated on the tri-functional NK subset in subsequent analyses.

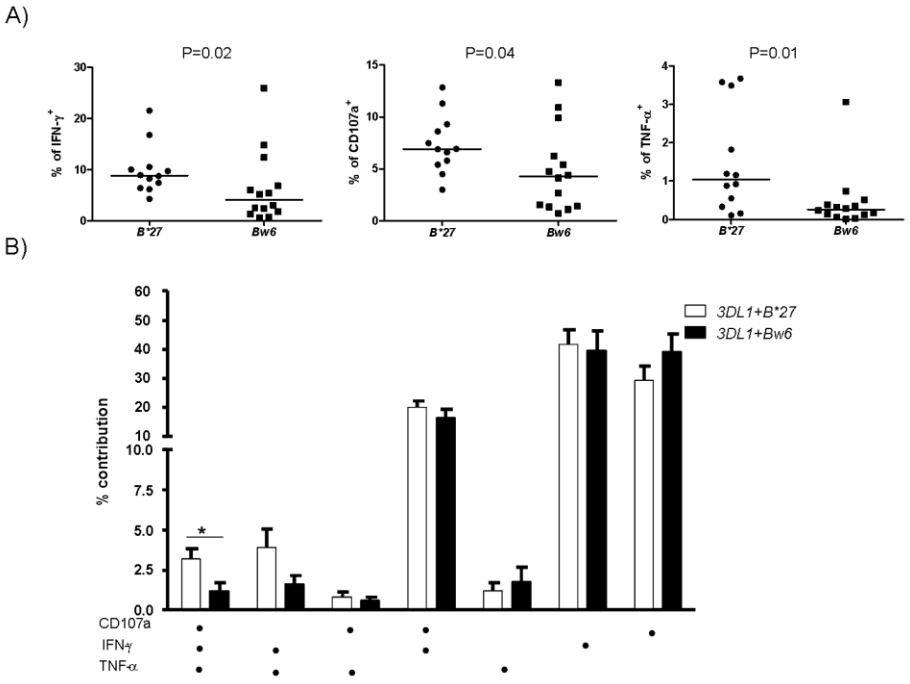

Figure 1. NK cells from individuals carrying the 3DL1+HLA B*27 NK receptor-ligand pair have an increased functional potential. The frequency of NK cells that

secrete IFN-γ (left), express CD107a (middle) or secrete TNF-α (right) in 3DL1 *hmz* individuals who carry *HLA-B*27* or *HLA-Bw6*. Each data point represents a separate individual. The bar through each scatter plot indicates the median frequency for the group. A Mann-Whitney U test was used to assess the significance of between-group comparisons (A). The percent contribution of seven different functional profiles to the total NK cell response to K562 *HLA*-devoid cells from individuals carrying *3DL1+B*27* (n=12) and *3DL1+Bw6* (n=14). Below the *x*-axis, dots refer to the presence of each functional marker (CD107a, IFN-γ and TNF-α) in that profile. The height of each bar represents the median for the group and the height of the error bar the interquartile range for that group. An asterisk (*) over the line linking two bars indicates that the contribution of that functional subset of the NK cell response was significantly different in the two study populations. A Mann-Whitney U test was used to assess the significance of between-group comparisons and $p<0.05$ was considered significant (B).

We next compared the K562 stimulated NK cells from *3DL1+B*27* individuals to that from *3DL1+Bw4*. NK cells from **h/*y+B*57* carriers have previously been shown to have superior tri-functional potential compared to *3DL1+Bw6* and *h/*y+*Bw4* subjects (17) (Kamya et al. manuscript accepted). Since HLA-B*57 is a Bw4 allele we excluded carriers of either *HLA-B*57* or *HLA-B*27* alleles from the *3DL1+Bw4* group. Although the tri-functional potential of NK cells from 13 *3DL1+Bw4* subjects was lower (1.78% [0.00%, 5.71%]) than that from

*3DL1+B*27* individuals the difference did not achieve statistical significance (p=0.2644; Mann-Whitney *U* test) (**Figure 2A**).

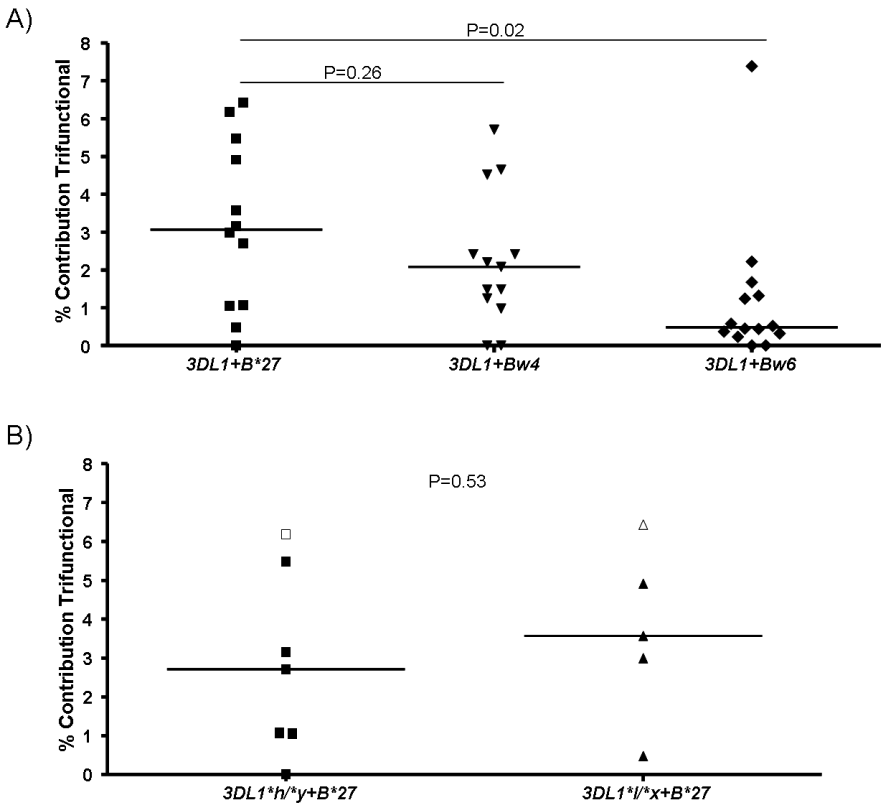

Figure 2. Comparisons of the tri-functional potential of NK cells from study subjects with defined *KIR/HLA* combinations. Scatter plots show percent contribution of tri-functional NK cells to the total K562 stimulated response in individuals who are *3DL1+B*27, 3DL1+Bw4* and *3DL1+Bw6* carriers (A), and **h/*y+B*27* and **l/*x+B*27* carriers (B). Each data point represents results from a separate individual. The data point represented by an empty square and triangle refer to individuals that carry both *B*27* and *B*57*. The bar through each scatter plot indicates the median frequency for the group. A Mann-Whitney U test was used to assess the significance of between-group differences.

3DL1 hmz genotypes can be classified as either **h/*y* or **l/*x* depending on the 3DL1 alleles expressed. Previous work showed that NK cells from **h/*y+B*57* subjects had a significantly higher tri-functional potential than those from **l/*x+B*57* subjects. We therefore questioned whether NK cells from the 7 **h/*y+B*27* and 5 **l/*x+B27* individuals differed from each other in their tri-functional potential. The median (range) NK tri-functional potential was 2.56% (0.00%, 6.18%) and 3.57% (0.47%, 6.43%) for NK cells from carriers of the **h/*y+B*27* and **l/*x+B*27* genotypes, respectively (p=0.53; Mann-Whitney test), a difference that was not statistically significant (Figure 2B). Therefore, HLA-B*27 appears to be able to interact with NK receptor alleles in either the 3DL1 *h/*y and *l/*x genotypes categories to educate NK cells for equivalent NK functional potential.

4.3 NK cells from *3DL1+B*27 and *h/*y+B*57* carriers have a similar tri-functional potential.

Next we questioned whether the level of tri-functional potential of NK cells from *3DL1+B*27* carriers was of a similar magnitude to that seen in NK cells from **h/*y+B*57* carriers. For this analysis we excluded the 2 *3DL1+B*27* individuals who also expressed a *B*57* allele and compared NK tri-functional potential in this group to that in 12 **h/*y+B*57* carriers. As seen in Figure 2C, although the tri-functional potential of NK cells from **h/*y+B*57* carriers was higher than that

from *3DL1+B*27* carriers this difference did not achieve statistical significance (p=0.09; Mann-Whitney test).

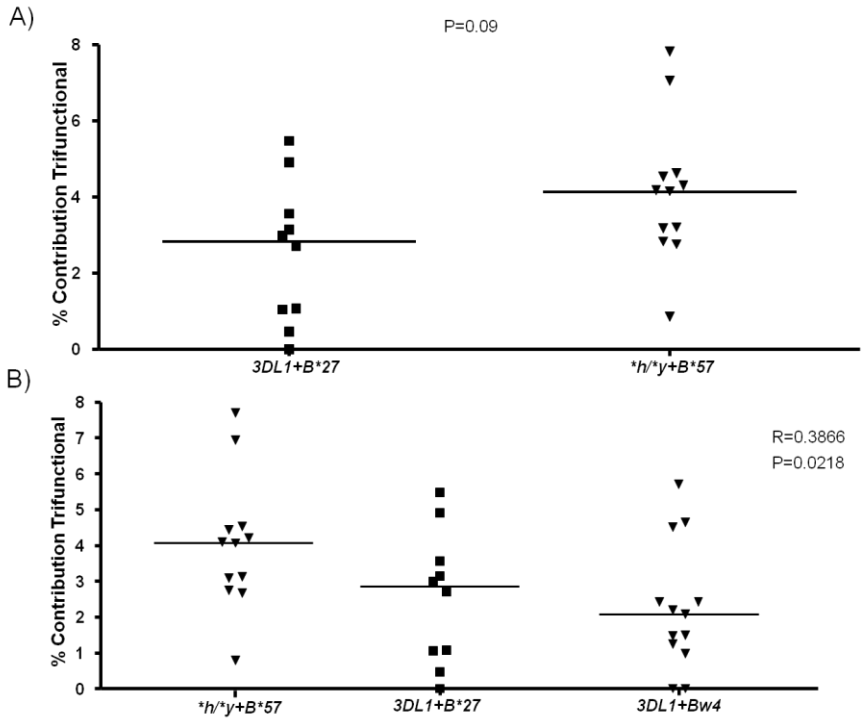

Figure 3. Comparisons of the tri-functional potential of NK cells from individuals carrying *3DL1+B*27*, **h/*y+HLA-B*57* and *3DL1+Bw4*. Scatter plots show percent contribution of tri-functional NK cells to the total K562 stimulated response in individuals who are *3DL1+B*27* and **h/*y+B*57* carriers (A) or **h/*y+B*57, 3DL1+B*27* and *3DL1+Bw4* carriers (B). Each data point represents results from a separate individual. The bar through each scatter plot indicates the median frequency for the group. A Mann-Whitney U test was used to assess the significance of between-group differences (A). A Spearman's correlation test was used to assess the significance of a trend towards decreasing functional potential in carriers of these genotype combinations (B).

Pair-wise comparisons of the tri-functional potential of NK cells from carriers of **h/*y+B*57*, *3DL1+B*27* and *3DL1+Bw4* revealed that only the comparison of **h/*y+B*57* and *3DL1+Bw4* was statistically significant. NK cells from each of these groups had higher tri-functional potential than those from the *3DL1+Bw6* group (not shown). Small group sizes and large variability within groups likely contributed to the lack of statistical significance in the tri-functional potential between the **h/*y+B*57* and *3DL1+B*27* and the *3DL1+B*27* and *3DL1+Bw4* groups. We performed another analysis testing for the significance of a trend towards declining NK functional potential among subjects with these *3DL1/HLA-B* genotypes. The rationale for this came from epidemiological studies showing that the effect of *B*57* on time to AIDS and VL control was greater in the presence of **h/*y* than **l/*x* 3DL1 genotypes and greater than that of *B*27* on these outcomes in the presence of either 3DL1 genotype (14). When the tri-functional potential of NK cells from these 3 *3DL1/HLA-B* genotypes were assessed using a test of trend we observed that this measure decreased as follows: **h/*y+B*57 > 3DL1+B*27 > 3DL1+Bw4* (r=-0.39, p=0.02; Spearman's correlation test). Together these results suggest that there is a hierarchy in the impact on NK cell education of HLA-B alleles where *B*57* is the most potent in the context of **h/*y* genotypes followed by *B*27* in the context of 3DL1 genotypes. Furthermore the impact of these alleles is superior to that of other Bw4 alleles co-expressed with 3DL1 genotypes.

5. Discussion

We have presented results showing that NK cells from carriers of the *3DL1+B*27* KIR/HLA genotype combination have tri-functional responses to missing self that are 1) significantly higher than those from *3DL1+Bw6* and 2) have a tri-functional potential that falls between that of carriers of **h/*y+B*57* and *3DL1+Bw4*.

We previously showed that B*57 is superior to most other Bw4 alleles in educating NK cells through its interaction with 3DL1 NK receptors for functional potential as measured by responses to missing self on K562 cells (Boulet et al 2010, Kamya et al manuscript accepted). These results suggested that B*57, an allele associated with slow time to AIDS and VL control, may contribute to viral control not only through its interaction with HIV epitopes recognized by $CD8^+$ T cell but also through its interaction with 3DL1 inhibitory receptors on NK cells. B*27 is another allele associated with slow time to AIDS and VL control. We therefore sought to determine whether B*27 was also able to educate NK cells for potent responses to missing self. The rationale for investigating the role of B*27 in educating NK cells for NK functional potential in HIV infected SP is that this allele is over represented among SP compared to the uninfected or HIV susceptible subjects. Among 101 SPs enrolled in the Canadian Cohort of HIV Infected SP typed to date 18 (17.8%) were B*27 positive whereas in HIV susceptible subject enrolled in a Primary HIV Infection cohort 26 of 434 (6%) expressed this allele ($p<0.001$; Fisher's Exact test), an allele frequency similar to that seen in uninfected Caucasian (www.allelefrequencies.net). The frequency of individuals expressing both an *B*27* allele and a homozygous *3DL1* genotype

would be expected to be even lower. This provided the rationale for investigating this phenomenon in SPs in whom the frequency of the *KIR/HLA* genotype under investigation was higher than in uninfected subjects. We also reasoned that SPs with either controlled viremia or long term non progression would constitute a population with limited NK dysfunction due to HIV infection.

Others have reported that HIV infection dysregulates NK cell subset distribution such that there is a reduction in the frequency of $CD56^{+}CD16^{+}$ NK subset with cytolytic activity with an associated increase the frequency of an anergic $CD56^{-}/CD16^{+}$ subset (39, 40). VL seems to play a key role in this redistribution of NK cell subsets. Even though a decrease of cytotoxic NK cells is observed in SPs compared to healthy controls it is not as pronounced as that observed in viremic HIV infected progressor subjects (41, 42). NK function may be altered by direct contact with HIV. The gp120 Envelope glycoprotein has been shown to suppress the activity, proliferation and survival of NK cells (43). Perturbations in the NK cell receptor repertoire have been reported in HIV infection, affecting both inhibitory and activating receptors (41, 44-46). Furthermore, HIV can escape NK cell recognition by restricting upregulation of activating NK cell receptor ligands such as NKp44L (47), MICA and ULBP1 and 2 (48) and by preventing downregulation of HLA-C/E (49). Results reported by Kamya et al. demonstrated a negative correlation between NK cell tri-functional potential and VL suggesting VL and HIV infection negatively impact NK function (Kamya et al. manuscript accepted). In summary, although NK function in SPs may be affected by HIV infection the effect would be expected to be limited in this population. Our results

demonstrate that NK cells from *3DL1+B*27* SPs can produce IFN-γ and TNF-α and express CD107a following K562 stimulation to a greater extent than those from *3DL1+Bw6*. This finding is unlikely to be due to difference of VL as these 2 groups had a similar VL (Table 2).

We have previously shown that NK cells from SP who carry **h/*y+B*57* have a level of tri-functional potential that is significantly higher than those from individuals carrying ether *3DL1*h/*y* or *3DL1*l/*x* genotypes with *Bw4* alleles other than *B*27* or *B*57*. The elevated tri-functional potential of NK cells from **h/*y+B*57* carriers depends on the presence of both the *3DL1*h/*y* receptor genotype and *HLA-B*57* since carriers of *3DL1*l/*x* with *HLA-B*57* also have significantly lower NK tri-functional potential (Kamya et al. manuscript accepted). In contrast, we observed no differences in tri-functional potential in NK cells from *HLA-B*27* positive SPs carrying either the *3DL1*h/*y* or **l/*x* receptor genotypes. It should be noted that a limitation in making this assertion is the small number of subject who were **h/*y+B*27* versus **l/*x+B*27* available to make this comparison. Epidemiological studies found that compared to *Bw6 hmz* the *B*57* effect on time to AIDS and VL control was enhanced in the presence of *3DL1*h/*y* compared to *3DL1*l/*x*. Overall, the effect of *B*27* on these outcomes was more moderate than that of *B*57* in the presence of *3DL1 *h/*y*. Compared to *Bw6 hmz* the *B*27-80T* allele *B*2705* was more protective in the presence of *3DL1*l/*x* than in the presence of *3DL1*h/*y* (14). All but one of the *3DL1+B*27* group of subjects in our study population expressed *B*27-80T* alleles (21). Furthermore, there is also evidence that B*2705 has a greater affinity

for one or more of the KIR3DL1*l allotypes (16). Our findings that NK cells from **h/*y+B*27* and **l/*x+B*27* carriers have similar levels of tri-functional potential that may be more modest than that of **h/*y+B*57 carriers* is in line with B*27 being able to interact with alleles in *3DL1*h/*y* and **l/*x* genotypes in *3DL1+B*27* carriers and this more effectively that B*57 interacting with alleles in *3DL1*l/*x* genotypes (Kamya et al. manuscript accepted). There is also a trend towards NK cells from *3DL1+B*27* carriers having higher function that those from *3DL1+Bw4* individuals. These results argue in favour of HLA-B*27 and B*57 being unique among HLA-Bw4 alleles in their impact on educating NK cells for subsequent activity, although the effect of B*27 is more modest than that of B*57.

According to the rheostat model of NK education, the strength of the inhibitory input received by NK cells determines the threshold of activation that is set in each NK cell. The higher the inhibitory input, the more likely the NK cell will pass the threshold required to respond to stimuli with an increased frequency of effector cells and an increased number of effector functions (25). During development, NK cells must acquire sufficient inhibitory signals to prevent autoreactivity through recognition of ligands for inhibitory NK receptors (50, 51). The larger the contribution of given receptor-ligand pairing to NK cell inhibition under homeostatic conditions the more potent a missing self response will be when the ligand is lost. This situation would be encountered in a setting of HIV infection where HIV encoded Nef downmodulates HLA-A and B alleles from the cells surface abrogating inhibitory signals mediated by 3DL1 receptors (52, 53).

In this report we have focused on comparisons of the tri-functional subset of NK cells. This was done because the percent contribution of this subset to the entire K562 stimulated response was the only functional subset that differed between carriers *3DL1+B*27* and a KIR/HLA receptor-ligand combination unable to signal through 3DL1 NK receptor alleles. NK cells able elicit 3 functions are more potent in terms of the intensity of each of their functions than corresponding mono-functional NK cells (Kamya et al manuscript accepted). This is similar to what has been reported for poly- versus mono-functional $CD8^+$ T cells (54, 55) Poly-functional HIV-specific $CD8^+$ T cells in SPs may play a role in superior anti-HIV activity (55, 56). This is still a controversial area as the low VL seen in SPs may preserve multi-functional HIV-specific immune response. Although the biological relevance of poly-functional antigen specific $CD8^+$ T cells in HIV infection is not yet clear, they do serve as an indicator of an effective response to HIV. Our experiments did not directly test the anti-viral activity of NK cells since we did not use HIV infected cells as stimuli. The role of tri-functional NK cells in inhibition of viral replication warrants further investigation.

If stimulation with HIV infected cells produces higher functionality in NK cells from *3DL1+B*27* versus *3DL1+Bw6* carriers and tri-functional NK cells are endowed with a superior capacity to suppress viral replication it would be interesting to study the ability of NK cells from *3DL1+Bw6* for other NK cells functions. Our results demonstrate that these individuals have a limited NK cell tri-functional potential upon missing self stimulation. Since these are SPs are able

to control viral replication and/or maintain CD4 counts above 400 for 7 or more years it is not unreasonable to assume that NK cells from these subjects possess other NK function. NK cells are known to mediated antibody-dependent cell-mediated cytotoxicity which has been shown to play a role in controlling viral replication (57) and may play a role in preventing infection (58). In addition, NK cells are also able to regulate antiviral immunity by modulating DC function (59, 60). In the presence of HIV replication the cross talk between NK cells and DC is impaired (61-63). It would be interesting to assess whether the interaction between NK cells and DC is maintained in SPs, particularly in *3DL1+Bw6* carriers.

6. Conclusion

We have demonstrated that NK cells from *3DL1+B*27* SPs have a higher tri-functional potential following K562 stimulation than those from *3DL1+Bw6*. A test of trend found that NK tri-functional potential declines significantly in NK isolated from carriers of the following genotypes: **h/*y+B*57 > 3DL1+B*27 > 3DL1+Bw4*. Our results suggest that although the protective effect on HIV infection conferred by HLA-B*27 is mediated in part by $CD8^+$ T cells recognizing HIV epitopes restricted by this allele, the protective effect of this alleles may also be mediated by its interaction with inhibitory 3DL1 receptors. HLA-B*27, like HLA-B*57, appears to have an impact on NK education that is superior to that of other Bw4 alleles. Although this remains to be demonstrated experimentally we hypothesize that in carriers of certain *3DL1* and *HLA-B*27* or *HLA-B*57*

genotypes, virus-infected cells that have down modulated the HLA ligand for their inhibitory 3DL1 NK receptors may be able to recruit a larger number NK cells with multiple functions, which can play a role in viral control. Such information is relevant to vaccine design by providing a rationale for modulating NK activity at the time of vaccination to favor developing protective immunity.

7. Acknowledgements

The authors wish to thank the study participants of the Canadian Cohort of HIV Infected SPs and the NIAID Cohort. We are grateful to the following physicians, who recruited and followed study subjects enrolled in the Canadian Cohort for HIV Infected SPs: Drs. Bernard Lessard, Danielle Legault, Benoit Trottier, Michel Boissonault, Serge Dufresne, Jean-Guy Baril, Danièle Longpré, Benoit Trottier, Danielle Rouleau, Howard Turner, Julian Falutz, Joseph Cox, James Allan, John MacLoed, Marina B Klein and Roger LeBlanc. We are also grateful to Ms. Stephanie Matte for Cohort coordination. We thank Mr. Benjamin Tallon, Ms. Marie-Pierre Boisvert, Ms. Tsoarello Mabanga and Mr. Saied Sharafi for the expert technical assistance with HLA and KIR allotyping. This work was supported by grants #HOP-86862 and MOP-111155 from the Canadian Institutes for Health Research (CIHR), and a grant from the Fonds de Recherche en Santé du Québec (FRSQ) AIDS and Infectious Disease Network. CMP was supported by a Ph.D. scholarship from CIHR.

8. References

1. Robertson, M.J., and Ritz, J. 1990. Biology and clinical relevance of human natural killer cells. *Blood* 76:2421-2438.
2. Bottino, C., Moretta, L., and Moretta, A. 2006. NK cell activating receptors and tumor recognition in humans. *Curr Top Microbiol Immunol* 298:175-182.
3. Bancroft, G.J. 1993. The role of natural killer cells in innate resistance to infection. *Curr Opin Immunol* 5:503-510.
4. Cooper, M.A., Fehniger, T.A., and Caligiuri, M.A. 2001. The biology of human natural killer-cell subsets. *Trends Immunol* 22:633-640.
5. Sanabria, M.X., Vargas-Inchaustegui, D.A., Xin, L., and Soong, L. 2008. Role of natural killer cells in modulating dendritic cell responses to Leishmania amazonensis infection. *Infect Immun* 76:5100-5109.
6. Smyth, M.J., Cretney, E., Kelly, J.M., Westwood, J.A., Street, S.E., Yagita, H., Takeda, K., van Dommelen, S.L., Degli-Esposti, M.A., and Hayakawa, Y. 2005. Activation of NK cell cytotoxicity. *Mol Immunol* 42:501-510.
7. Lanier, L.L. 2005. NK cell recognition. *Annu Rev Immunol* 23:225-274.
8. Kim, H.W., Bellanti, J.A., Arrobio, J.O., Mills, J., Brandt, C.D., Chanock, R.M., and Parrott, R.H. 1969. Respiratory syncytial virus neutralizing activity in nasal secretions following natural infection. *Proc Soc Exp Biol Med* 131:658-661.
9. Anfossi, N., Andre, P., Guia, S., Falk, C.S., Roetynck, S., Stewart, C.A., Breso, V., Frassati, C., Reviron, D., Middleton, D., et al. 2006. Human NK cell education by inhibitory receptors for MHC class I. *Immunity* 25:331-342.
10. Norman, P.J., Abi-Rached, L., Gendzekhadze, K., Korbel, D., Gleimer, M., Rowley, D., Bruno, D., Carrington, C.V., Chandanayingyong, D., Chang, Y.H., et al. 2007. Unusual selection on the KIR3DL1/S1 natural killer cell receptor in Africans. *Nat Genet* 39:1092-1099.
11. Yawata, M., Yawata, N., Draghi, M., Little, A.M., Partheniou, F., and Parham, P. 2006. Roles for HLA and KIR polymorphisms in natural killer cell repertoire selection and modulation of effector function. *J Exp Med* 203:633-645.
12. Gardiner, C.M., Guethlein, L.A., Shilling, H.G., Pando, M., Carr, W.H., Rajalingam, R., Vilches, C., and Parham, P. 2001. Different NK cell surface phenotypes defined by the DX9 antibody are due to KIR3DL1 gene polymorphism. *J Immunol* 166:2992-3001.
13. Pando, M.J., Gardiner, C.M., Gleimer, M., McQueen, K.L., and Parham, P. 2003. The protein made from a common allele of KIR3DL1 (3DL1*004) is poorly expressed at cell surfaces due to substitution at positions 86 in Ig domain 0 and 182 in Ig domain 1. *J Immunol* 171:6640-6649.
14. Martin, M.P., Qi, Y., Gao, X., Yamada, E., Martin, J.N., Pereyra, F., Colombo, S., Brown, E.E., Shupert, W.L., Phair, J., et al. 2007. Innate partnership of HLA-B and KIR3DL1 subtypes against HIV-1. *Nat Genet* 39:733-740.
15. Cella, M., Longo, A., Ferrara, G.B., Strominger, J.L., and Colonna, M. 1994. NK3-specific natural killer cells are selectively inhibited by Bw4-positive HLA alleles with isoleucine 80. *J Exp Med* 180:1235-1242.
16. Luque, I., Solana, R., Galiani, M.D., Gonzalez, R., Garcia, F., Lopez de Castro, J.A., and Pena, J. 1996. Threonine 80 on HLA-B27 confers protection against lysis by a group of natural killer clones. *Eur J Immunol* 26:1974-1977.
17. Boulet, S., Song, R., Kamya, P., Bruneau, J., Shoukry, N.H., Tsoukas, C.M., and Bernard, N.F. 2010. HIV protective KIR3DL1 and HLA-B genotypes influence NK

cell function following stimulation with HLA-devoid cells. *J Immunol* 184:2057-2064.
18. Kaslow, R.A., Dorak, T., and Tang, J.J. 2005. Influence of host genetic variation on susceptibility to HIV type 1 infection. *J Infect Dis* 191 Suppl 1:S68-77.
19. Altfeld, M., Addo, M.M., Rosenberg, E.S., Hecht, F.M., Lee, P.K., Vogel, M., Yu, X.G., Draenert, R., Johnston, M.N., Strick, D., et al. 2003. Influence of HLA-B57 on clinical presentation and viral control during acute HIV-1 infection. *AIDS* 17:2581-2591.
20. Leslie, A.J., Pfafferott, K.J., Chetty, P., Draenert, R., Addo, M.M., Feeney, M., Tang, Y., Holmes, E.C., Allen, T., Prado, J.G., et al. 2004. HIV evolution: CTL escape mutation and reversion after transmission. *Nat Med* 10:282-289.
21. Carrington, M., Martin, M.P., and van Bergen, J. 2008. KIR-HLA intercourse in HIV disease. *Trends Microbiol* 16:620-627.
22. Martin, M.P., Gao, X., Lee, J.H., Nelson, G.W., Detels, R., Goedert, J.J., Buchbinder, S., Hoots, K., Vlahov, D., Trowsdale, J., et al. 2002. Epistatic interaction between KIR3DS1 and HLA-B delays the progression to AIDS. *Nat Genet* 31:429-434.
23. Miura, T., Brockman, M.A., Schneidewind, A., Lobritz, M., Pereyra, F., Rathod, A., Block, B.L., Brumme, Z.L., Brumme, C.J., Baker, B., et al. 2009. HLA-B57/B*5801 human immunodeficiency virus type 1 elite controllers select for rare gag variants associated with reduced viral replication capacity and strong cytotoxic T-lymphocyte [corrected] recognition. *J Virol* 83:2743-2755.
24. Leslie, A., Kavanagh, D., Honeyborne, I., Pfafferott, K., Edwards, C., Pillay, T., Hilton, L., Thobakgale, C., Ramduth, D., Draenert, R., et al. 2005. Transmission and accumulation of CTL escape variants drive negative associations between HIV polymorphisms and HLA. *J Exp Med* 201:891-902.
25. Brodin, P., Karre, K., and Hoglund, P. 2009. NK cell education: not an on-off switch but a tunable rheostat. *Trends Immunol* 30:143-149.
26. Kaslow, R.A., Carrington, M., Apple, R., Park, L., Munoz, A., Saah, A.J., Goedert, J.J., Winkler, C., O'Brien, S.J., Rinaldo, C., et al. 1996. Influence of combinations of human major histocompatibility complex genes on the course of HIV-1 infection. *Nat Med* 2:405-411.
27. Carrington, M., and Bontrop, R.E. 2002. Effects of MHC class I on HIV/SIV disease in primates. *AIDS* 16 Suppl 4:S105-114.
28. Goulder, P.J., Edwards, A., Phillips, R.E., and McMichael, A.J. 1997. Identification of a novel HLA-B*2705-restricted cytotoxic T-lymphocyte epitope within a conserved region of HIV-1 Nef. *AIDS* 11:536-538.
29. Trachtenberg, E., Korber, B., Sollars, C., Kepler, T.B., Hraber, P.T., Hayes, E., Funkhouser, R., Fugate, M., Theiler, J., Hsu, Y.S., et al. 2003. Advantage of rare HLA supertype in HIV disease progression. *Nat Med* 9:928-935.
30. Schneidewind, A., Brumme, Z.L., Brumme, C.J., Power, K.A., Reyor, L.L., O'Sullivan, K., Gladden, A., Hempel, U., Kuntzen, T., Wang, Y.E., et al. 2009. Transmission and long-term stability of compensated CD8 escape mutations. *J Virol* 83:3993-3997.
31. Goulder, P.J., Phillips, R.E., Colbert, R.A., McAdam, S., Ogg, G., Nowak, M.A., Giangrande, P., Luzzi, G., Morgan, B., Edwards, A., et al. 1997. Late escape from an immunodominant cytotoxic T-lymphocyte response associated with progression to AIDS. *Nat Med* 3:212-217.

32. den Uyl, D., van der Horst-Bruinsma, I.E., and van Agtmael, M. 2004. Progression of HIV to AIDS: a protective role for HLA-B27? *AIDS Rev* 6:89-96.
33. Goulder, P.J., Brander, C., Tang, Y., Tremblay, C., Colbert, R.A., Addo, M.M., Rosenberg, E.S., Nguyen, T., Allen, R., Trocha, A., et al. 2001. Evolution and transmission of stable CTL escape mutations in HIV infection. *Nature* 412:334-338.
34. Madec, Y., Boufassa, F., Porter, K., and Meyer, L. 2005. Spontaneous control of viral load and CD4 cell count progression among HIV-1 seroconverters. *AIDS* 19:2001-2007.
35. Deeks, S.G., and Walker, B.D. 2007. Human immunodeficiency virus controllers: mechanisms of durable virus control in the absence of antiretroviral therapy. *Immunity* 27:406-416.
36. Migueles, S.A., Osborne, C.M., Royce, C., Compton, A.A., Joshi, R.P., Weeks, K.A., Rood, J.E., Berkley, A.M., Sacha, J.B., Cogliano-Shutta, N.A., et al. 2008. Lytic granule loading of CD8+ T cells is required for HIV-infected cell elimination associated with immune control. *Immunity* 29:1009-1021.
37. Boulet, S., Sharafi, S., Simic, N., Bruneau, J., Routy, J.P., Tsoukas, C.M., and Bernard, N.F. 2008. Increased proportion of KIR3DS1 homozygotes in HIV-exposed uninfected individuals. *AIDS* 22:595-599.
38. Boulassel, M.R., Spurll, G., Rouleau, D., Tremblay, C., Edwardes, M., Sekaly, R.P., Lalonde, R., and Routy, J.P. 2003. Changes in immunological and virological parameters in HIV-1 infected subjects following leukapheresis. *J Clin Apher* 18:55-60.
39. Mavilio, D., Lombardo, G., Benjamin, J., Kim, D., Follman, D., Marcenaro, E., O'Shea, M.A., Kinter, A., Kovacs, C., Moretta, A., et al. 2005. Characterization of CD56-/CD16+ natural killer (NK) cells: a highly dysfunctional NK subset expanded in HIV-infected viremic individuals. *Proc Natl Acad Sci U S A* 102:2886-2891.
40. Tarazona, R., Casado, J.G., Delarosa, O., Torre-Cisneros, J., Villanueva, J.L., Sanchez, B., Galiani, M.D., Gonzalez, R., Solana, R., and Pena, J. 2002. Selective depletion of CD56(dim) NK cell subsets and maintenance of CD56(bright) NK cells in treatment-naive HIV-1-seropositive individuals. *J Clin Immunol* 22:176-183.
41. O'Connor, G.M., Holmes, A., Mulcahy, F., and Gardiner, C.M. 2007. Natural Killer cells from long-term non-progressor HIV patients are characterized by altered phenotype and function. *Clin Immunol* 124:277-283.
42. Barker, E., Martinson, J., Brooks, C., Landay, A., and Deeks, S. 2007. Dysfunctional natural killer cells, in vivo, are governed by HIV viremia regardless of whether the infected individual is on antiretroviral therapy. *AIDS* 21:2363-2365.
43. Kottilil, S., Shin, K., Jackson, J.O., Reitano, K.N., O'Shea, M.A., Yang, J., Hallahan, C.W., Lempicki, R., Arthos, J., and Fauci, A.S. 2006. Innate immune dysfunction in HIV infection: effect of HIV envelope-NK cell interactions. *J Immunol* 176:1107-1114.
44. Kottilil, S., Shin, K., Planta, M., McLaughlin, M., Hallahan, C.W., Ghany, M., Chun, T.W., Sneller, M.C., and Fauci, A.S. 2004. Expression of chemokine and inhibitory receptors on natural killer cells: effect of immune activation and HIV viremia. *J Infect Dis* 189:1193-1198.

45. Mavilio, D., Benjamin, J., Daucher, M., Lombardo, G., Kottilil, S., Planta, M.A., Marcenaro, E., Bottino, C., Moretta, L., Moretta, A., et al. 2003. Natural killer cells in HIV-1 infection: dichotomous effects of viremia on inhibitory and activating receptors and their functional correlates. *Proc Natl Acad Sci U S A* 100:15011-15016.
46. De Maria, A., Fogli, M., Costa, P., Murdaca, G., Puppo, F., Mavilio, D., Moretta, A., and Moretta, L. 2003. The impaired NK cell cytolytic function in viremic HIV-1 infection is associated with a reduced surface expression of natural cytotoxicity receptors (NKp46, NKp30 and NKp44). *Eur J Immunol* 33:2410-2418.
47. Fausther-Bovendo, H., Sol-Foulon, N., Candotti, D., Agut, H., Schwartz, O., Debre, P., and Vieillard, V. 2009. HIV escape from natural killer cytotoxicity: nef inhibits NKp44L expression on CD4+ T cells. *AIDS* 23:1077-1087.
48. Cerboni, C., Neri, F., Casartelli, N., Zingoni, A., Cosman, D., Rossi, P., Santoni, A., and Doria, M. 2007. Human immunodeficiency virus 1 Nef protein downmodulates the ligands of the activating receptor NKG2D and inhibits natural killer cell-mediated cytotoxicity. *J Gen Virol* 88:242-250.
49. Bonaparte, M.I., and Barker, E. 2004. Killing of human immunodeficiency virus-infected primary T-cell blasts by autologous natural killer cells is dependent on the ability of the virus to alter the expression of major histocompatibility complex class I molecules. *Blood* 104:2087-2094.
50. Valiante, N.M., Uhrberg, M., Shilling, H.G., Lienert-Weidenbach, K., Arnett, K.L., D'Andrea, A., Phillips, J.H., Lanier, L.L., and Parham, P. 1997. Functionally and structurally distinct NK cell receptor repertoires in the peripheral blood of two human donors. *Immunity* 7:739-751.
51. Hoglund, P., Sundback, J., Olsson-Alheim, M.Y., Johansson, M., Salcedo, M., Ohlen, C., Ljunggren, H.G., Sentman, C.L., and Karre, K. 1997. Host MHC class I gene control of NK-cell specificity in the mouse. *Immunol Rev* 155:11-28.
52. Collins, K.L., Chen, B.K., Kalams, S.A., Walker, B.D., and Baltimore, D. 1998. HIV-1 Nef protein protects infected primary cells against killing by cytotoxic T lymphocytes. *Nature* 391:397-401.
53. Cohen, G.B., Gandhi, R.T., Davis, D.M., Mandelboim, O., Chen, B.K., Strominger, J.L., and Baltimore, D. 1999. The selective downregulation of class I major histocompatibility complex proteins by HIV-1 protects HIV-infected cells from NK cells. *Immunity* 10:661-671.
54. Darrah, P.A., Patel, D.T., De Luca, P.M., Lindsay, R.W., Davey, D.F., Flynn, B.J., Hoff, S.T., Andersen, P., Reed, S.G., Morris, S.L., et al. 2007. Multifunctional TH1 cells define a correlate of vaccine-mediated protection against Leishmania major. *Nat Med* 13:843-850.
55. Betts, M.R., Nason, M.C., West, S.M., De Rosa, S.C., Migueles, S.A., Abraham, J., Lederman, M.M., Benito, J.M., Goepfert, P.A., Connors, M., et al. 2006. HIV nonprogressors preferentially maintain highly functional HIV-specific CD8+ T cells. *Blood* 107:4781-4789.
56. Makedonas, G., and Betts, M.R. 2011. Living in a house of cards: re-evaluating CD8+ T-cell immune correlates against HIV. *Immunological reviews* 239:109-124.
57. Forthal, D.N., Landucci, G., and Daar, E.S. 2001. Antibody from patients with acute human immunodeficiency virus (HIV) infection inhibits primary strains of HIV type 1 in the presence of natural-killer effector cells. *J Virol* 75:6953-6961.

58. Rerks-Ngarm, S., Pitisuttithum, P., Nitayaphan, S., Kaewkungwal, J., Chiu, J., Paris, R., Premsri, N., Namwat, C., de Souza, M., Adams, E., et al. 2009. Vaccination with ALVAC and AIDSVAX to prevent HIV-1 infection in Thailand. *N Engl J Med* 361:2209-2220.
59. Gerosa, F., Baldani-Guerra, B., Nisii, C., Marchesini, V., Carra, G., and Trinchieri, G. 2002. Reciprocal activating interaction between natural killer cells and dendritic cells. *J Exp Med* 195:327-333.
60. O'Leary, J.G., Goodarzi, M., Drayton, D.L., and von Andrian, U.H. 2006. T cell- and B cell-independent adaptive immunity mediated by natural killer cells. *Nat Immunol* 7:507-516.
61. Mavilio, D., Lombardo, G., Kinter, A., Fogli, M., La Sala, A., Ortolano, S., Farschi, A., Follmann, D., Gregg, R., Kovacs, C., et al. 2006. Characterization of the defective interaction between a subset of natural killer cells and dendritic cells in HIV-1 infection. *J Exp Med* 203:2339-2350.
62. Melki, M.T., Saidi, H., Dufour, A., Olivo-Marin, J.C., and Gougeon, M.L. 2010. Escape of HIV-1-infected dendritic cells from TRAIL-mediated NK cell cytotoxicity during NK-DC cross-talk--a pivotal role of HMGB1. *PLoS Pathog* 6:e1000862.
63. Alter, G., Kavanagh, D., Rihn, S., Luteijn, R., Brooks, D., Oldstone, M., van Lunzen, J., and Altfeld, M. 2010. IL-10 induces aberrant deletion of dendritic cells by natural killer cells in the context of HIV infection. *J Clin Invest* 120:1905-1913.

Annex II: Conference Abstracts

Proteomic Fingerprinting in HCV mono- and HIV-1/HCV Co-infection reveals plasma Biomarkers prognostic of fibrosis.

C. E. Melendez-Pena, C. Santamaria, B. Conway, C. Cooper, B. Segatto, B. Ward, M. Ndao, M. Klein[1].

Atlanta, United States, CROI, March 3rd-6th 2013. *Poster*

Background: Reliable biomarkers that can distinguish fibrosis states are essential for studying the natural history and for clinical management of HCV and HCV/HIV co-infection as serial liver biopsies are impractical on a population scale. We evaluated plasma proteome profiles in HCV mono and HIV/HCV co-infected patients using Surface-enhanced laser desorption (SELDI)-time-of-flight (TOF) mass spectrometry (MS), to identify novel plasma biomarkers capable of identifying different stages of fibrosis.

Methods: 151 individuals were prospectively recruited (68 HCV mono-infected and 84 co-infected). Fibrosis stage (Batt and Ludwig 0-1, 2, 3, 4) was determined by liver biopsy and only plasma collected within one year of biopsy were profiled. Plasma were fractionated, randomly applied to protein chip arrays (IMAC, CM10 and H50) and spectra were generated at low and high laser intensities.

Results:. The majority of individuals were Caucasian men between the ages of 20 to 62 years old. For HIV co- infected, the median CD4 cell count was 640 (136-900) cell/mm^3, HIV RNA was 49 (24-29 973) copies/ml and 89.7 % were receiving antiretroviral therapy. There was no statistically significant difference between the HCV mono and HIV/HCV co-infected groups in regards to their age, duration of HCV infection, alcohol use or smoking. After manual peak re-labeling, 14 biomarkers achieved a p-value <0.01 (ROC values >0.75 or <0.25) predictive of fibrosis status (stage 0-1 vs. 3&4) in co-infected individuals and 17 in mono-infected subjects. Only 5 of these candidates contributed in both mono- and co-infected subjects. These five biomarkers showed significant correlation between each other (Spearman's correlation test $p<0.05$). None of the biomarkers identified in co-infection correlated with HIV viral load or CD4 counts ($p>0.05$). MS/MS MALDI-TOF and immunologic methods were used to profile 9 of these biomarker peaks. Thus far Serotransferin, Ig Heavy Chain, Haptoglobin, Apolipoprotein A1 (Apo-A1) have been identified by MALDI. The 18.4 truncation of Apo-A1 was confirm by Western-Blot. We are in the process to try to identify the remaining biomarkers.

Conclusion: We obtained several potential biomarkers peaks useful for staging liver fibrosis in HIV-HCV co-infected persons. Identification of such protein biomarkers may reduce the need for liver biopsy, facilitate follow-up and the timing of HCV treatment, and help in the understanding of the impact of HIV and its treatment on liver disease in the setting of HCV infection.

Serum Biomarkers Predictive of Fibrosis by Proteomic Fingerprinting in HIV-1/HCV Co-infection.

Melendez-Pena C, Mazen H, Saeed S,Ward B., Ndao M, Klein M.

Montréal, Canada, CAHR, April 19th-22nd 2012. *Oral*

Background: Hepatic complications of HCV, including fibrosis and cirrhosis are accelerated in HIV-infected individuals. Liver biopsy remains the gold standard for staging HCV-associated liver disease but is invasive and has major limitations such as serious complications and sampling error. These problems have prompted a search for non-invasive methods for liver fibrosis staging. To this end, we compared serum proteome profiles at different stages of fibrosis in HCV mono and HIV-1/HCV co-infected patients using SELDI-TOF MS.

Methods: A panel of 76 sera was used, including 36 HCV mono infected and 40 HIV/HCV co-infected subjects where in both group 10 were in each 4 stages of fibrosis (0-1, 2, 3,4) except for stage 4 mono-infection where there was 6 subjects. Fibrosis stage was assessed by liver biopsy and only sera collected within a year of biopsy were profiled. Sera were fractionated, randomly applied to protein chip arrays (IMAC, CM10 and H50) and spectra were generated at low and high laser intensities. Each sample was analyzed using three pH fractions (F1, F3 and F6).

Results: The 76 sera studied yield a total of 1368 spectra. More than 100 peaks of interest were found by automated peak detection. After manual peak relabeling, 24 biomarkers achieved a p value <0.01 (ROC values >0.75 or <0.25) predictive of fibrosis status in co-infected individuals and 27 in mono infected subjects. Only 5 of these candidate biomarkers contributed in both mono and co-infected subjects. Using biomarker pattern software to generate candidate diagnostic algorithms, 4 biomarker peaks with good discriminatory power were identified exclusively in co-infection.

Conclusion: These preliminary data suggest that SELDI mass spectrometric profiling can identify diagnostic serum biomarkers for fibrosis not only in HCV mono infected individuals but also in HIV/HCV co-infected individuals. The 4 most promising biomarkers are currently being identified and validated.

Although the combined inhibitory NK receptor-HLA-B genotype homozygous KIR3DL1 with HLA-B*27 is associated with slower time to AIDS it is not associated with a lower risk of HIV infection.

C.E. Melendez-Pena, B. Tallon, T. Mabanga, J.-P. Routy, C. Tsoukas, J. Bruneau, N. Bernard.

Rome, Italy, IAS, July 17th-20th 2011. *poster*

Background: Work by others has shown that carriage of combined genotypes of Killer Immunoglobulin-like receptor (KIR) KIR3DL1 and HLA-B alleles such as KIR3DL1*h/*y with HLA-B*57 and KIR3DL1*l/*x with HLA-B*27 is associated with slower time to AIDS and lower viral load (VL). We have previously shown that NK cells from individuals carrying both these KIR/HLA genotypes have elevated functional potential compared to those from Bw6 homozygotes (hmz) with no ligands for KIR3DL1. Since KIR3DL1*h/*y+B*57 carriage is associated with protection from HIV infection we questioned whether carriage of KIR3DL1hmz+HLA-B*27 also reduced the risk of HIV infection.

Methods: We compared months to outome (seroconversion or censoring) of 19 carriers of KIR3DL1hmz+HLA-B*27 and 57 Bw6 hmz. HIV exposed individuals. All had a known start date for exposure to HIV. Censoring was done at the date of the last documented HIV exposure while still seronegative. A log rank test was used to test the significance of between-group differences in time to infection. In an alternate analysis we compared the frequency of KIR3DL1hmz+HLA-B*27 carriers in 86 HIV exposed seronegative (HESN) and 409 recently infected (PI) subjects.

Results: There were no significant differences in time to seroconversion in carriers of 3DL1hmz+HLA-B*27 versus Bw6hmz (HR 1.57, p=0.40, log rank test) and 6/86 (6.9%) of HESN versus 22/409 (5.4%) of PI subjects carried the KIR3DL1hmz+HLA-B*27 genotype. (p=0.6062, Fisher's exact test).

Conclusion: Although carriage of KIR3DL1 adds to the protective effect of being HLA-B*27 on time to AIDS and VL, this Natural Killer cells receptors HLA-ligand combination does not appear to confer protection against HIV infection. This contrasts with observation that the KIR3DL1*h/*y+B*57 genotype is associated with protection both at the level of disease progression and infection.

The protective KIR3DL1 and HLA-B genotype, influence NK cell function in HIV infected slow progressors.

Melendez-Pena C, Kamya P, Potte M, Kovac C, Baril JG, Tsoukas C, Tremblay C, Bernard N.

Toronto, Canada, CAHR, Apr14th-17th 2011. *oral*

Background: The KIR3DL1 gene encodes inhibitory Natural Killer (NK) receptors that recognize HLA-Bw4 alleles as ligands. NK cells that carry KIR3DL1 to self HLA ligands should be licensed for elevated function upon encountering targets that have down-modulated ligand such as occurs HIV infection. HLA-B*57/B*27 are Bw4 alleles frequently expressed by HIV-infected slow progressors (SP). We questioned whether NK cells from SP carrying KIR3DL1 homozygotes (hmz) genotype and an HLA-Bw4 ligand had KIR3DL1^{+} NK cells with higher functional potential than KIR3DL1^{-} NK cells and whether the functionality of these NK subsets would differ in Bw6 hmz with no ligands for KIR3DL1, in whom KIR3DL1 could not participate in NK licensing.

Methods: The functional potential of NK cells from SP was investigated by stimulating PBMC with HLA-devoid K562. 45 KIR3DL1hmz/Bw4 and 7 Bw6hmz SP were studied. Multi-parametric flow cytometry was used to assess functional potential defined as the percent contribution of KIR3DL1^{+} and KIR3DL1^{-} NK cells expressing CD107a or secreting IFN-γ or TNF-α to the entire KIR3DL1^{+} or KIR3DL1^{-} subsets, respectively.

Results: KIR3DL1^{+} NK had a higher CD107a, IFN-γ or TNF-α functional potential than KIR3DL1^{-} NK cells when from KIR3DL1hmz/Bw4 carriers ($p<0.001$, Wilcoxon test). The functional potential of the KIR3DL1^{+} and KIR3DL1^{-} subsets from Bw6hmz did not differ from each other for any function tested. KIR3DL1^{+} NK cells from KIR3DL1*h/*y/B*27 or B*57 carriers had higher functional potential than those from KIR3DL1*h/*y/Bw4 (not B*27/B*57) carriers and Bw6hmz.

Conclusion: KIR3DL1 and HLA-Bw4 interact to confer potent educational signals that translate into high functional potential upon encountering targets expressing aberrant ligand levels due to virus-infection. HLA-B*27 and B*57 may be superior to other Bw4 alleles in this capacity. If so, the protection these alleles confer in HIV-infection may be mediated not only through CD8^{+} T cells but also through NK cells.

NK Cells From HIV Infected Slow Progressors Who Are KIR3DL1 Homozygotes (Hmz) and Positive For a Potective HLA-B*27 Allele Have Higher Tri-Functional Potential Than Those From Bw6 Hmz.

C. E. Melendez-Pena, P Kamya, S Boulet, R Song, C Tremblay and N Bernard.

Boston, United-States, CROI, Feb 27th –Mar2nd 2011. *Poster*

Background: The carriage of certain combined genotypes of the Killer Immunoglobulin-like Receptor (KIR) KIR3DL1 locus and the HLA-B locus is associated with slower time to AIDS and lower viral load. Previous work from our group showed that NK cells from individuals carrying KIR/HLA genotypes for receptor-ligand pairs such as KIR3DL1*h/*y-HLA-B*57 have an elevated functional potential compared to those from Bw6 hmz with no ligands for KIR3DL1 (3DL1). HLA-B*27 like HLA-B*57 is an HLA Bw4 alleles considered protective for HIV disease progression. We questioned whether HLA-B*27 had a higher impact on educating NK cells for functional potential than most other Bw4 or Bw6 alleles, as was shown for HLA-B*57.

Methods: The functional potential of NK cells from HIV infected slow progressors was investigated by stimulating PBMC with HLA-devoid K562 cells. Study groups included those carrying 3DL1*h/*y/B*27 (n=8), 3DL1*h/*y/Bw4 alleles other than B*27 or B*57 (n=8) and Bw6 hmz (n=6). Multi-parametric flow cytometry was used to detect NK cells with 7 functional profiles representing all permutations of CD107a expression, IFN-γ and TNF-α secretion. Between-group difference for each functional subset was assessed using non parametric-tests (Mann-Whitney or Kruskal-Wallis), as appropriate.

Results: We assessed the contribution of tri-functional cells to the total K562-stimulated response. NK cells from 3DL1*h/*y/B*27+ subjects had higher tri-functional responses with a median (range) of 2.92% (0-6.18) than those from Bw6 hmz (0.48% [0-1.68] p=<0.05) and tended to be higher than those from 3DL1*h/*y with other Bw4 alleles (1.36% [0-1.68] p=0.1). The levels of NK cell tri-functional response in those 3DL1*h/*y/B*27+ was similar to that seen in 3DL1*h/*y/B*57 subjects (3.21% [0.86%-4.31%]).

Conclusion: Although the protective effect on HIV infection conferred by HLA-B*27 is mediated in part by $CD8^+$ T cells recognizing HIV epitopes restricted by this allele, our results suggest that its protective effect may also be mediated by its interaction with 3DL1 receptors. Interactions between inhibitory 3DL1 and HLA-B*27 alleles may confer potent educational signals that translate into high functional potential upon encountering virus-infected or tumor cells that have down modulated the HLA ligand for these receptors. Such information is relevant to vaccine design by providing a rationale for modulating NK activity at the time of vaccination to favor developing protective immunity.